Supporting Information

Tunable Low-LUMO Boron-Doped Polycyclic Aromatic Hydrocarbons by General One-Pot C-H Borylations

Jeffrey M. Farrell, Carina Mützel, David Bialas, Maximilian Rudolf, Kaan Menekse, Ana-Maria Krause, Matthias Stolte, Frank Würthner*

Institut für Organische Chemie, Universität Würzburg, Am Hubland, 97074 Würzburg, Germany
Center for Nanosystems Chemistry, Universität Würzburg, Theodor-Boveri-Weg, 97074 Würzburg, Germany

Table of Contents

1. Materials and Methods

General considerations. Where indicated, glovebox synthetic manipulations were carried out in an atmosphere of dry, O_2-free N_2 in an MBraun glovebox using oven-dried glassware. 1,3-diisopropylimidazol-2-ylidene borane was prepared according to a literature procedure.[S1] Bis(trifluoromethylsulfonyl)imide was obtained from Merck or TCI and used without further purification. 2,2,6,6-Tetramethylpiperidine-1-oxyl free radical (TEMPO radical) was obtained from TCI and used without further purification. Anhydrous chlorobenzene and 1,2-dichorobenzene were obtained from Sigma Aldrich and dried over 4Å molecular sieves before use. THF was purified with a Grubbs-type column system manufactured by Innovative Technology. Deuterated solvents were obtained from commercial sources and used without further purification. Anhydrous hexane was obtained from Sigma Aldrich and used without further purification. All other solvents for spectroscopic measurements were spectroscopic grade and used without further purification. Column chromatography was performed with commercial glass columns using silica gel 60M (particle size 0.04-0.063 mm). 1-styrylnaphthalene, 1,4-distyrylnaphthalene, 1,5-distyrylnaphthalene and 1,6-distyrylpyrene were prepared as described herein and were spectroscopically identical to literature reports. [S2-5] All other reagents and solvents were obtained from commercial sources and used without further purification.

UV-Vis absorption spectra were recorded on a Jasco V-670 or Jasco V-770 spectrophotometer for solution phase measurements or a Perkin Elmer Lambda 950 UV/Vis/NIR spectrometer equipped with an integrating sphere for thin-film measurements. Thin films of **1**-**3** and **6**-**10** for UV-Vis spectroscopy were prepared by spin coating filtered (PTFE, 0.45µm pore size) 1 x 10^{-2} M solutions in $CHCl_3$ (**1**, **6**-**10**) or THF/$CHCl_3$ 1:3 (**2**, **3**) onto quartz substrates at 700 rpm (1000 rpm s^{-1}, 60 s, **1**, **6**) or at 2000 rpm (3000 rpm s^{-1}, 180 s, **7**-**10**) using an SPIN150 spin coater (SPS Europe). Thin films of **4a**, **4b**, and **5** for UV-Vis spectroscopy were prepared by dip coating quartz substrates with filtered (PTFE, 0.45µm pore size) 1 x 10^{-2} M solutions in THF/$CHCl_3$ 1:1.

Fluorescence spectra were recorded on an Edinburgh Instruments FLS980 fluorescence spectrometer. Relative fluorescence quantum yields were determined using the comparative method at four excitation wavelengths with respect to standards: perylene in cyclohexane,[S6] *N*,*N*'-bis(2,6-diisopropylphenyl)-3,4:9,10-perylenebis(dicarboximide) in $CHCl_3$,[S7] *N*,*N*'-bis(2,6-diisopropylphenyl)-1,6,7,12-tetraphenoxy-3,4:9,10-perylenebis(dicarboximide) in $CHCl_3$,[S7] or rhodamine 101 in EtOH.[S8] Time-resolved measurements were performed with Edinburgh

Instruments picosecond pulsed laser diodes and a TCSPC detection unit. Solid-state absolute fluorescence quantum yields were determined on a Hamamatsu Absolute PL Quantum Yield Measurement System C9920-02.

NMR spectra were recorded on Bruker Avance III HD 400 or Bruker Avance III HD 600 spectrometers. Chemical shifts are listed in parts per million and are given relative to $SiMe_4$ and referenced to a residual solvent signal (^1H, ^{13}C) or relative to an external standard (^{11}B: 15% $(Et_2O)BF_3$; ^{19}F: 15% $(Et_2O)BF_3$. Coupling constants (*J*) are quoted in Hertz (Hz). In some cases ^{11}B signals for boron-containing compounds could not be observed due to broadening and/or poor solubility.

High resolution mass spectrometry was carried out on a Bruker Daltonics micrOTOF focus or a Thermo Scientific Exactive Plus Orbitrap instrument.

Cyclic voltammetry was carried out using a standard commercial electrochemical analyzer (EC epsilon; BAS Instruments, UK) with a three-electrode single-compartment cell. The supporting electrolyte tetrabutylammonium hexafluorophosphate (*n*-Bu_4NPF_6) was prepared according to the literature,[S9] and recrystallized from ethanol/water. The measurements were carried out using ferrocene (Fc) as an internal standard for the calibration of the potential. Potentials of irreversible redox events were determined by square wave voltammetry experiments. An Ag/AgCl reference electrode was used. A Pt disc and a Pt wire were used as working and auxiliary electrodes, respectively.

Single crystal X-ray diffraction data were collected at 100 K on a Bruker D8 Quest Kappa diffractometer with a Photon100 CMOS detector and multi-layered mirror monochromated CuK_α radiation. The structures were solved using direct methods, expanded with Fourier techniques and refined with the Shelx software package.[S10] All non-hydrogen atoms were refined anisotropically. Hydrogen atoms were included in the structure factor calculation on geometrically idealized positions. Crystallographic data have been deposited with the Cambridge Crystallographic Data Centre as supplementary publication no. CCDC 1878998 (**2**), CCDC 1878996 (**4**), CCDC 1879000 (**5**), CCDC 1878999 (**8**), and CCDC 1878997 (9,10-bis(2,3,4,5,6-pentafluorostyryl)anthracene). These data can be obtained free of charge from The Cambridge Crystallographic Data Centre via www.ccdc.ac.uk/data.request/cif.

Computational details. Geometry optimizations were performed at the level of density functional theory (DFT) employing B3LYP as functional[S11-13] and 6-31++G** as basis set[S14-16] as implemented in the Gaussian 09 program package.[S17] The geometries were optimized

followed by frequency calculations to confirm the existence of minima. The electron affinities of compounds **2**, **4a** and **5** were calculated from the energy difference between the geometry-optimized structure of the neutral molecule and the geometry-optimized structure of the anion.[S18] Time-dependent density functional theory (TDDFT) calculations were performed on the geometry-optimized structures employing the same basis set and functional as for the geometry optimizations. The absorption spectra were simulated with the help of the GaussView 5 visualization software package.[S19]

Organic thin film transistor fabrication and characterization. Before fabrication, *n*-tetradecylphosphonic acid (TPA) modified Si/SiO_2 (100 nm)/AlO_x (8 nm) substrates (1.7 nm TPA monolayer; capacitance C_i = 32.4 nF cm^{-2}) were successively cleaned with toluene (p.a. grade, VWR chemicals), acetone and *i*-propanol (both semiconductor grade VLSI PURANAL™, Aldrich® Chemistry). Afterwards, 30 nm thin films were vacuum-deposited in an OPTIvap-XL (CreaPhys GmbH) vacuum deposition system at a pressure below 10^{-6} mbar. During the deposition of the molecule, a growth rate of 0.2-1.0 nm min^{-1} was adjusted by monitoring the film growth with a quartz crystal microbalance. Furthermore, the substrate temperature (T_{sub}) was kept constant at 60 °C. Subsequently, 30 nm gold were evaporated through steel shadow masks onto the thin films to form the source and drain electrodes yielding bottom-gate, top-contact devices with a channel length L and width W of 100 µm and 200 µm, respectively. Devices were characterized under inert conditions (M.Braun Inertgas Systeme GmbH, UNIlab Pro, $c(O_2)$ < 1 ppm, $c(H_2O)$ < 1 ppm) by measuring the transfer (saturation regime, V_{DS} = −50 V) and output characteristics with an Agilent 4055C parameter analyzer and a Cascade EPS150 probe station. Prior to the characterization, the semiconducting film around the device was scratched with a needle of the used micromanipulator to electrically isolate the device. Atomic force microscopy for the investigation of film morphology was carried out with a Bruker AXS MultiMode™ Nanoscope IV instrument in the tapping mode. Silicon cantilevers (OMCL-AC160TS, Olympus) with a spring constant of 42 N m^{-1} and a resonance frequency of ~300 kHz were used.

Solar cell fabrication and measurement. Patterned ITO-glass substrates (Soluxx GmbH) were used as the cathode in the solar cells. The ITO coated glass substrates were cleaned by sonication in an aqueous detergent solution (mucasol®), rinsed with deionized water, acetone, and isopropyl alcohol and dried in a nitrogen stream. Sol-gel-derived ZnO films were prepared using zinc

acetate dihydrate in 2-methoxyethanol:2-aminoethanol as a precursor solution and spin-coating onto the ITO substrate followed by thermal treatment at 200 °C for 60 min according to literature.[S20] The substrates were then transferred into a nitrogen-filled glove box. Compound **8** was blended with donor polymers PCE10 or PBDB-T (1-Material Inc) and dissolved in chlorobenzene (CB) with the addition of a small amount of 1,8-diiodooctane (CB:DIO = 97:3, v/v). The blended ratio of polymer:**8** was 1:1 by weight. The solutions were then spin-coated onto the ITO/ZnO at 1000 rpm. The thicknesses of the active layers were approximately 80 nm. Subsequently, 10 nm of MoO_3 and 100 nm of Al were deposited through a shadow mask (defined active area of 7.2 mm^2) onto the photoactive layer in an OPTIvap-XL (CreaPhys GmbH) vacuum deposition system at a pressure below 10^{-6} mbar. All device fabrication processes were carried out under inert conditions (M.Braun Inertgas Systeme GmbH, UNIlab Pro, $c(O_2) < 1$ ppm, $c(H_2O) < 1$ ppm). PCEs were measured under an AM1.5G Oriel Sol3ATM Class AAA solar simulator (Newport®). The power of the sun simulation was calibrated before the testing using a standard silicon solar cell, giving a value of 100 mW cm^{-2}. The current density-voltage (*J*-*V*) characteristics were recorded with a parameter analyzer (Botest Systems GmbH). Spectrally resolved EQE measurements were performed with a Quantum Efficiency/IPCE Measurement Kit (Newport®). A 300 W Xe lamp was taken as light source. Monochromatic light was generated by a Cornerstone monochromator. A Merlin Lock-In Amplifier was utilized for detection of the measurement signal at a chopping frequency of 30 Hz. As reference a calibrated Si-detector was used.

2. Synthetic Procedures

Synthesis of 1-hydroxy-2-phenyl-1-boraphenalene (1)

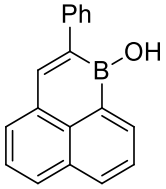

In an inert atmosphere in a glovebox, 1,3-diisopropylimidazol-2-ylidene borane (100. mg, 0.600 mmol, 1.2 equiv.) was dissolved in 3.5 mL dry chlorobenzene in a 50 mL Schlenk tube with a magnetic stirbar. Bis(trifluoromethylsulfonyl)imide (172 mg, 0.610 mmol, 1.22 equiv.) was added to the solution and hydrogen gas evolved. The solution was stirred for 90 minutes after

which 1-styrylnaphthalene (115 mg, 0.500 mmol, 1 equiv.) was added with an additional 2.5 mL chlorobenzene. A 50 mL dropping funnel containing 2.5 mL 0.46 M TEMPO radical solution (1.15 mmol, 2.3 equiv.) in chlorobenzene was affixed to the Schlenk tube. The apparatus was sealed and removed from the glovebox. The reaction mixture was stirred at 110 °C for 5 h and then cooled to 80 °C. The TEMPO solution was added and the reaction was stirred for 36 h at 80 °C, cooled to room temperature and concentrated *in vacuo*. The residue was purified by column chromatography (toluene/CH_2Cl_2, 7:3). Following solvent removal *in vacuo*, pure 1-hydroxy-2-phenyl-1-boraphenalene **1** was isolated as a yellow solid (63.0 mg, 0.246 mmol, 49% yield). **^{1}H NMR** (400 MHz, DMSO-d_6, 298 K): δ 9.84 (s, 1H, B-O*H*), 8.68 (dd, 1H, $^3J_{HH}$ = 6.9 Hz, $^4J_{HH}$ = 1.2 Hz), 8.25 (dd, 1H, $^3J_{HH}$ = 8.1 Hz, ^4J = 1.0 Hz), 8.04 (dd, 1H, $^3J_{HH}$ = 8.3 Hz, $^4J_{HH}$ = 1.0 Hz), 7.92 (s, 1H), 7.86 (dd, 1H, $^3J_{HH}$ = 7.1 Hz, $^4J_{HH}$ = 1.0 Hz), 7.79 (dd, 1H, $^3J_{HH}$ = 8.0 Hz, $^3J_{HH}$ = 8.0 Hz), 7.69 (m, 2H), 7.63 (dd, 1H, $^3J_{HH}$ = 8.1 Hz, $^3J_{HH}$ = 8.1 Hz), 7.41 (t, 2H, $^3J_{HH}$ = 7.7 Hz), 7.29 (tt, 1H, $^3J_{HH}$ = 7.4 Hz, $^4J_{HH}$ = 1.9 Hz). **^{13}C{^{1}H} NMR** (100 MHz, DMSO-d_6, 298 K, partial): δ 146.3 (C), 142.5 (C, br, B-*C*), 142.4 (C), 135.2 (C), 133.1 (C), 132.4 (C), 131.7 (C), 131.3 (C), 131.1 (C), 130.4 (C), 128.1 (2C), 127.9 (2C), 126.4 (C), 126.1 (C), 126.1 (C), one B-*C* peak not resolved. **^{11}B NMR** (128 MHz, $CDCl_3$, 298 K): δ 40.33. **MP**: 78 °C. **HR-MS** (ASAP, negative mode) *m/z*: $[M]^-$ Calc'd for $C_{18}H_{13}BO$ 256.1060; Found 256.1064. **CV** (1 x 10^{-3} M, 0.1 M *n*-Bu_4NPF_6 in DMSO, vs. $Fc^{+/0}$, 298 K): $E_{1/2\ red\ 1}$ = –1.98 V. **UV-Vis** Solution: (3.99 x 10^{-5} M in $CHCl_3$, 298 K): λ_{max} (ε_{max}) = 374 nm (8800), 348 nm (9600). Thin Film: λ_{max} = 388 nm, 353 nm. **Fluorescence** Solution: (1.6 x 10^{-5} M in $CHCl_3$, 298 K): λ_{max} = 489 nm (Φ = 0.27). Thin Film: λ_{em} = 530 nm (Φ = 0.10).

Synthesis of 1,6-dihydroxy-2,7-diphenyl-1,6-diborapyrene (2)

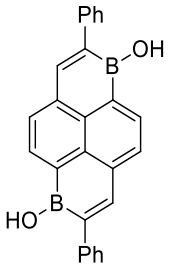

In an inert atmosphere in a glovebox, 1,3-diisopropylimidazol-2-ylidene borane (200. mg, 1.20 mmol, 2.4 equiv.) was dissolved in 7 mL dry chlorobenzene in a 100 mL Schlenk tube with a magnetic stirbar. Bis(trifluoromethylsulfonyl)imide (343 mg, 1.22 mmol, 2.44 equiv.) was added

and the reaction was stirred for 90 minutes over which time hydrogen gas evolved. 1,5-distyrylnaphthalene (166 mg, 0.500 mmol, 1 equiv.) was added to the solution with an additional 5 mL chlorobenzene. A 50 mL dropping funnel with a 5 mL 0.46 M TEMPO radical solution (2.30 mmol, 4.6 equiv.) in chlorobenzene was affixed to the Schlenk tube. The apparatus was sealed and removed from the glovebox. The reaction mixture was stirred at 110 °C for 5 h over which time the solution turned orange. The mixture was then cooled to 80 °C and the TEMPO solution was added. The reaction was stirred for a subsequent 36 h at 80 °C, cooled to room temperature and concentrated *in vacuo*. The residue was purified by column chromatography (gradient elution, toluene/CH_2Cl_2 2:3 to pure CH_2Cl_2). Pure 1,6-dihydroxy-2,7-diphenyl-1,6-diborapyrene **2** was isolated as an orange solid following solvent removal by rotary evaporation and drying under high vacuum (74.1 mg, 0.193 mmol, 39% yield). Single crystals suitable for X-ray crystallography could be obtained from a concentrated DMSO solution of **2** upon exposure to atmospheric moisture. **^{1}H NMR** (400 MHz, DMSO-d_6, 298 K): δ 10.04 (s, 2H, B-O*H*), 8.56 (d, 2H, $^3J_{HH}$ = 7.1 Hz), 7.88 (d, 2H, $^3J_{HH}$ = 7.5 Hz), 7.80 (s, 2H), 7.69 (m, 4H), 7.42 (t, 4H, $^3J_{HH}$ = 7.3 Hz), 7.32 (tt, 2H, $^3J_{HH}$ = 7.3 Hz, $^4J_{HH}$ = 1.9 Hz). **^{13}C{^{1}H} NMR** (100 MHz, DMSO-d_6, 298 K): δ 146.8 (2C), 145.2 (2C, br, B-*C*), 142.4 (2C), 137.4 (2C), 135.5 (2C), 133.2 (2C, br, B-*C*), 131.3 (2C), 130.8 (2C), 128.6 (4C), 128.3 (4C), 127.6 (2C). **^{11}B NMR** (128 MHz, DMSO-d_6, 298 K): not observed. **MP**: 300 °C (decomp.). **HR-MS** (ASAP, negative mode) *m/z*: $[M]^-$ Calc'd for $C_{26}H_{18}B_2O_2$ 384.1498; Found 384.1500. **CV** (9 x 10^{-4} M, 0.1 M *n*-Bu_4NPF_6 in DMSO, vs. $Fc^{+/0}$, 298 K): $E_{1/2\ red\ 1}$ = −1.47 V. $E_{1/2\ red\ 2}$ = −1.84 V. **UV-Vis** Solution: (2.64 x 10^{-5} M in $CHCl_3$, 298 K): λ_{max} (ε_{max}) = 425 nm (17500), 383 nm (12700). Thin Film: λ_{max} = 416 nm. **Fluorescence** Solution: (7.0 x 10^{-6} M in $CHCl_3$, 298 K): λ_{max} = 561 nm (Φ = 0.44). Thin Film: λ_{em} = 566 nm (Φ = 0.05).

Synthesis of 1,8-dihydroxy-2,7-diphenyl-1,8-diborapyrene (3)

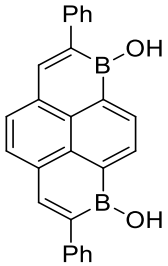

In an inert atmosphere in a glovebox, 1,3-diisopropylimidazol-2-ylidene borane (200. mg, 1.20 mmol, 2.4 equiv.) was dissolved in 7 mL dry chlorobenzene in a 100 mL Schlenk tube with a magnetic stirbar. Bis(trifluoromethylsulfonyl)imide (343 mg, 1.22 mmol, 2.44 equiv.) was added and stirred for 90 minutes over which time hydrogen gas evolved. 1,4-distyrylnaphthalene (166 mg, 0.500 mmol, 1 equiv.) was added to the solution with an additional 5 mL chlorobenzene. A 50 mL dropping funnel with a 5 mL 0.46 M TEMPO radical solution (2.30 mmol, 4.6 equiv.) in chlorobenzene was affixed to the Schlenk tube. The apparatus was sealed and removed from the glovebox. The reaction mixture was stirred at 110 °C for 5 h over which time the solution turned deep red. The mixture was then cooled to 80 °C and the TEMPO solution was added. The reaction was stirred for 36 h at 80 °C, cooled to room temperature and concentrated *in vacuo*. The residue was purified by column chromatography (gradient elution, CH_2Cl_2 to CH_2Cl_2/EtOAc 5:1). Pure 1,8-dihydroxy-2,7-diphenyl-1,8-diborapyrene **3** was isolated as a red solid following solvent removal *in vacuo* (59.3 mg, 0.154 mmol, 31% yield). **^{1}H NMR** (400 MHz, $CDCl_3$, 298 K): δ 10.09 (s, 2H, B-O*H*), 8.68 (s, 2H), 7.78 (s, 2H), 7.75 (s, 2H), 7.69 (d, 4H, $^3J_{HH}$ = 7.4 Hz), 7.42 (t, 4H, $^3J_{HH}$ = 7.5 Hz), 7.30 (t, 2H, $^3J_{HH}$ = 7.3 Hz). **^{13}C{^{1}H} NMR** (100 MHz, DMSO-d_6, 298 K): δ 146.6 (2C), 143.2 (2C, br, B-*C*), 142.2 (2C), 135.8 (2C, br, B-*C*), 134.9 (2C), 133.9 (2C), 131.4 (2C), 131.2 (2C), 128.3 (4C), 128.0 (4C), 126.8 (2C). **^{11}B NMR** (128 MHz, DMSO-d_6, 298 K): not observed. **MP**: 140 °C (decomp.). **HR-MS** (ASAP, negative mode) *m/z*: $[M]^-$ Calc'd for $C_{26}H_{18}B_2O_2$ 384.1498; Found 384.1506. **CV** (3 x 10^{-5} M, 0.1 M *n*-Bu_4NPF_6 in DMSO, vs. $Fc^{+/0}$, 298 K): $E_{1/2\ red\ 1}$ = −1.46 V. $E_{1/2\ red\ 2}$ = −1.82 V. **UV-Vis** Solution: (2.13 x 10^{-5} M in $CHCl_3$, 298 K): λ_{max} (ε_{max}) = 466 nm (11600), 358 nm (6800). Thin Film: λ_{max} = 478 nm, 368 nm. **Fluorescence** Solution: (8.8 x 10^{-6} M in $CHCl_3$, 298 K): λ_{max} = 586 nm (Φ = 0.51). Thin Film: λ_{em} = 643 nm (Φ = 0.03).

Synthesis of 3,9-dihydroxy-2,8-bis(pentafluorophenyl)-3,9-diboraperylene (4)

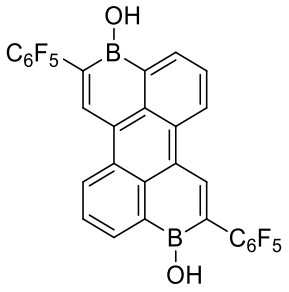

In an inert atmosphere in a glovebox, 1,3-diisopropylimidazol-2-ylidene borane (200. mg, 1.20 mmol, 2.4 equiv.) was dissolved in 5 mL dry 1,2-dichlorobenzene in a 50 mL Schlenk tube with a magnetic stirbar. Bis(trifluoromethylsulfonyl)imide (343 mg, 1.22 mmol, 2.4 equiv.) was added and the reaction stirred for 90 minutes over which time hydrogen gas evolved. 9,10-bis(2,3,4,5,6-pentafluorophenyl)anthracene (281 mg, 0.500 mmol, 1 equiv.) was then added to the solution. A 50 mL dropping funnel with a 5 mL 0.46 M TEMPO radical solution (2.30 mmol, 4.6 equiv.) in 1,2-dichlorobenzene was affixed to the Schlenk tube. The apparatus was sealed and removed from the glovebox. The reaction mixture was stirred at 160 °C for 24 h over which time the solution turned deep red. The reaction mixture was then cooled to 80 °C and the TEMPO solution was added. The reaction was stirred for 36 h at 80 °C, cooled to room temperature and diluted in 2 L EtOAc. In a separatory funnel, the organic layer was washed twice with an aqueous layer containing 100 mL 0.5 M HCl and 50 mL brine. The organic layer was concentrated *in vacuo* and suspended in water. The residue was sonicated and then filtered. The collected solid was washed with water and with 1:1 water/MeOH before being dried under flow of air and washed with dichloromethane. The collected solid was again suspended in water, sonicated, separated via centrifugation and the water decanted. This centrifugation process was repeated with methanol and with dichloromethane. The resulting red solid was collected and dried *in vacuo* to give 3,9-dihydroxy-2,8-bis(pentafluorophenyl)-3,9-diboraperylene **4** (36 mg, 0.059 mmol, 12% yield). Single crystals suitable for X-ray crystallography could be obtained from a concentrated DMSO solution of **4** upon exposure to atmospheric moisture. **^{1}H NMR** (400 MHz, DMSO-d_6, 298 K): δ 9.95 (s, 2H, B-O*H*), 9.25 (s, 2H), 9.25 (d, 2H, $^{3}J_{HH}$ = 9.3 Hz), 8.80 (d, 2H, $^{3}J_{HH}$ = 6.6 Hz), 7.99 (dd, 2H, $^{3}J_{HH}$ = 6.6 Hz, $^{3}J_{HH}$ = 9.0 Hz). **^{13}C{^{1}H} NMR** (151 MHz, DMSO-d_6, 298 K): δ 146.3 (2C), 143.7 (br, d, $^{1}J_{CF}$ = 242 Hz, 4C), 138.9 (br, d, $^{1}J_{CF}$ = 248 Hz, 2C), 137.1 (br, dt, $^{1}J_{CF}$ = 248 Hz, $^{2}J_{CF}$ = 15 Hz, 4C), 137.7 (2C), 131.6 (2C), 130.7 (2C), 130.3 (2C), 129.5 (2C), 129.3 (2C), 129.2 (2C), 127.6 (2C), 117.3 (br, t, $^{2}J_{CF}$ = 20 Hz, 2C). **^{11}B NMR** (128 MHz, DMSO-d_6, 298 K): not observed. **^{19}F NMR** (376 MHz, DMSO-d_6, 298 K): δ −140.8 (m, 4F), −158.7 (t, $^{3}J_{FF}$ = 22 Hz, 2F), −164.8 (m, 4F). **MP**: 245 ºC (decomp.). **HR-MS** (ASAP, negative mode) *m/z*: $[M]^-$ Calc'd for $C_{30}H_{10}B_2F_{10}O_2$ 614.0713; Found 614.0732. **CV** (7 x 10^{-4} M, 0.1 M *n*-Bu_4NPF_6 in DMSO, vs. $Fc^{+/0}$, 298 K): $E_{1/2\ red\ 1}$ = −1.13 V. $E_{1/2\ red\ 2}$ = −1.47 V. **UV-Vis** Solution: (2.25 x 10^{-5} M in $CHCl_3$, 298 K): λ_{max} (ε_{max}) = 540 nm (26800), 504 nm (19300), 473 (8400). Thin Film: λ_{max} = 490 nm. **Fluorescence** (5.5 x 10^{-6} M in $CHCl_3$, 298 K): λ_{max} = 563 nm (Φ = 0.95).

Synthesis of 1,7-dihydroxy-2,8-diphenyl-1,7-diboraanthanthrene (5)

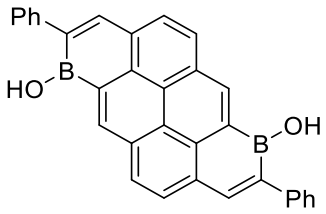

In an inert atmosphere in a glovebox, 1,3-diisopropylimidazol-2-ylidene borane (200. mg, 1.20 mmol, 2.4 equiv.) was dissolved in 5 mL dry chlorobenzene in a 100 mL Schlenk tube with a magnetic stirbar. Bis(trifluoromethylsulfonyl)imide (343 mg, 1.22 mmol, 2.4 equiv.) was added and the reaction was stirred for 90 minutes over which time hydrogen gas evolved. 1,6-distyrylpyrene (203 mg, 0.50 mmol, 1 equiv.) was then added to the solution with an additional 20 mL chlorobenzene. A 50 mL dropping funnel containing 5 mL 0.46 M TEMPO radical (2.30 mmol, 4.6 equiv.) solution in chlorobenzene was affixed to the Schlenk tube. The apparatus was sealed and removed from the glovebox. The reaction mixture was stirred at 110 °C for 4 h. The reaction mixture was then cooled to 80 °C and the TEMPO solution was added. The reaction was stirred for 24 h at 80 °C, cooled to room temperature and concentrated *in vacuo*. The residue was purified by column chromatography (degassed toluene/CH_2Cl_2, 1:3). Pure 1,7-dihydroxy-2,8-diphenyl-1,7-diboraanthanthrene **5** (50. mg, 0.11 mmol, 22% yield) was isolated as a purple solid following solvent removal by rotary evaporation and high vacuum. Single crystals suitable for X-ray crystallography could be obtained by slow evaporation of a concentrated dioxane solution of **5.** **^{1}H NMR** (400 MHz, DMSO, 298 K): δ 10.23 (s, 2H, B-O*H*), 9.40 (s, 2H), 8.47 (d, 2H, $^{3}J_{HH}$ = 8.0 Hz), 8.33 (d, 2H, $^{3}J_{HH}$ = 8.1 Hz), 8.14 (s, 2H), 7.79 (d, 4H, $^{3}J_{HH}$ = 8.3 Hz,) 7.47 (t, 4H, $^{3}J_{HH}$ = 7.6 Hz), 7.35 (tt, 2H, $^{3}J_{HH}$ = 7.3 Hz, $^{4}J_{HH}$ = 1.2 Hz). **^{13}C{^{1}H} NMR** (100 MHz, DMSO, 298 K): δ 147.0 (2C), 144.5 (2C, br, B-*C*), 142.3 (2C), 139.1 (2C), 133.1 (2C), 130.3 (2C, br, B-C), 130.2 (2C), 129.9 (2C), 128.2 (4C), 128.1 (2C), 128.0 (2C), 127.9 (4C), 126.7 (2C), 123.8 (2C). **^{11}B NMR** (128 MHz, DMSO-d_6, 298 K): not observed. **MP:** 285 °C (decomp.). **HR-MS** (ASAP, negative mode) *m/z*: $[M]^-$ Calc'd for $C_{32}H_{20}B_2O_2$ 458.1650; Found 458.1672. **CV** (3 x 10^{-4} M, 0.1 M *n*-Bu_4NPF_6 in DMSO, vs. $Fc^{+/0}$, 298 K): $E_{1/2\ red\ 1}$ = −1.39 V. $E_{1/2\ red\ 2}$ = −1.70 V. **UV-Vis** Solution: (5.84 x 10^{-6} M in CH_2Cl_2, 298 K): λ_{max} (ε_{max}) = 525 nm (32600), 491 nm (26400), 433 nm (12400). Thin Film: λ_{max} = 491 nm. **Fluorescence**: (6.88 x 10^{-7} M in CH_2Cl_2, 298 K): λ_{max} = 548 nm, 586 nm (Φ = 0.35).

Synthesis of 11-*tert*-butyl-2,8-dihydroxy-3,7-diphenyl-2,8-diboratriangulene (6)

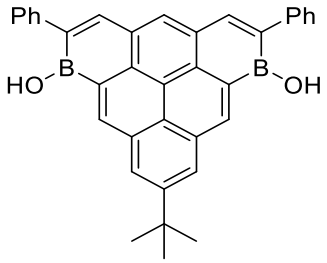

In an inert atmosphere glovebox, 1,3-diisopropylimidazol-2-ylidene borane (200. mg, 1.20 mmol, 2.4 equiv.) was dissolved in 5 mL dry chlorobenzene in a 100 mL Schlenk tube with a magnetic stirbar. Bis(trifluoromethylsulfonyl)imide (343 mg, 1.22 mmol, 2.4 equiv.) was added and stirred for 90 minutes over which time hydrogen gas evolved. 7-(*tert*-butyl)-1,3-distyrylpyrene (231 mg, 0.500 mmol, 1 equiv.) was then added to the solution with an additional 5 mL chlorobenzene. A 50 mL dropping funnel with a 5 mL 0.46 M TEMPO solution (2.30 mmol, 4.6 equiv.) in chlorobenzene was affixed to the Schlenk tube. The apparatus was sealed and removed from the glovebox. The reaction mixture was stirred at 110 °C for 4 h, cooled to 80 °C and the TEMPO solution was added. The reaction was stirred for 24 h at 80 °C, cooled to room temperature and concentrated *in vacuo*. The residue was purified by column chromatography (degassed toluene/CH_2Cl_2, 1:3). Pure 11-*tert*-butyl-2,8-dihydroxy-3,7-diphenyl-2,8-diboratriangulene **6** (39 mg, 0.076 mmol, 15% yield) was isolated as a red-brown solid following solvent removal by rotary evaporation and high vacuum. **^{1}H NMR** (400 MHz, CD_2Cl_2, 298 K): δ 9.32 (s, 2H), 8.78 (s, 2H), 8.34 (s, 1H), 8.19 (s, 2H), 7.64 (d, 4H, $^3J_{HH}$ = 8.3 Hz), 7.55 (t, 4H, $^3J_{HH}$ = 7.8 Hz), 7.41 (tt, 2H, $^3J_{HH}$ = 7.4 Hz, $^4J_{HH}$ = 1.3 Hz), 5.99 (s, 2H, B-O*H*), 1.67 (s, 9H). **^{13}C{^{1}H} NMR** (100 MHz, $CDCl_3$, 298 K): δ 150.0 (1C), 148.7 (2C), 142.4 (2C), 141.4 (2C, br, C-*B*), 139.0 (2C), 133.0 (2C), 130.4 (2C, br, B-*C*), 129.9 (3C), 129.6 (2C), 129.5 (4C), 129.1 (2C), 127.5 (4C), 127.1 (2C), 124.2 (1C), 122.5 (1C), 35.5 (1C), 32.0 (3C). **^{11}B NMR** (128 MHz, DMSO-d_6, 298 K): not observed. **MP:** 217 °C (decomp.). **HR-MS** (ESI-TOF, positive mode) *m/z*: $[M+1]^+$ Calc'd for $C_{36}H_{29}B_2O_2$ 515.2348; Found 515.2367. **CV** (3 x 10^{-4} M, 0.1 M *n*-Bu_4NPF_6 in DMSO, vs. $Fc^{+/0}$, 298 K): $E_{1/2\ red\ 1}$ = −1.53 V. **UV-Vis** Solution: (4.91 x 10^{-6} M in CH_2Cl_2, 298 K): λ_{max} (ε_{max}) = 547 nm (5900), 509 nm (8800), 479 nm (9300), 450 nm (7800), 377 nm (24100). Thin Film: λ_{max} = 372 nm. **Fluorescence**: (1.2 x 10^{-7} M in CH_2Cl_2, 298 K): λ_{max} = 573 nm, 619 nm (Φ = 0.42).

Synthesis of 1,6-dimesityl-2,7-diphenyl-1,6-diborapyrene (7)

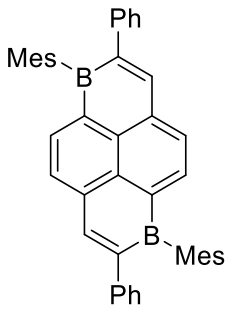

In an inert atmosphere glovebox, 1,6-dihydroxy-2,7-diphenyl-1,6-diborapyrene (50.0 mg, 0.130 mmol, 1 equiv.) was dissolved in CH_2Cl_2 (5 mL) in a Schlenk flask. The vessel was sealed, removed from the glovebox and BBr_3 (0.063 mL, 0.65 mmol, 5 equiv.) was added to the solution via injection under nitrogen. The mixture was stirred at room temperature for 5 h and then all volatiles were removed under reduced pressure. The remaining solid was dissolved in dry toluene (5 mL) and mesitylmagnesium bromide (0.91 mL 1.0 M in THF, 0.91 mmol, 7 equiv.) was added under nitrogen. The solution was stirred at room temperature for 16 h and then concentrated *in vacuo*. The crude product was purified by column chromatography (hexane/CH_2Cl_2, 10:1) to yield 1,6-dimesityl-2,7-diphenyl-1,6-diborapyrene **7** as a red solid (22 mg, 0.037 mmol, 29% yield). **^{1}H NMR** (400 MHz, CD_2Cl_2, 298 K): δ 7.90 (d, 2H, $^3J_{HH}$ = 7.0 Hz), 7.78 (d, 2H, $^3J_{HH}$ = 7.5 Hz), 7.76 (s, 2H), 7.28-7.20 (m, 10H), 6.83 (s, 4H), 2.32 (s, 6H), 2.00 (s, 12H). **^{13}C{^{1}H} NMR** (100 MHz, CD_2Cl_2, 298 K): δ 148.7 (2C), 144.4 (2C), 143.1 (2C), 140.5 (2C), 138.2 (4C), 137.4 (2C), 133.5 (2C), 130.3 (2C), 128.2 (4C), 127.6 (4C), 127.3 (4C), 127.1 (2C), 23.1 (4C), 21.4 (2C). Due to poor solubility peaks corresponding to B-*C* (6C) could not be resolved. **^{11}B NMR** (128 MHz, CD_2Cl_2, 298 K): δ 64.59 (br). **MP**: 254 °C. **HR-MS** (ASAP, positive mode) *m/z*: $[M+1]^+$ Calc'd for $C_{44}H_{39}B_2$ 589.3232; Found 589.3230. **CV** (3 x 10^{-4} M, 0.1 M *n*-Bu_4NPF_6 in CH_2Cl_2, vs. $Fc^{+/0}$, 298 K): $E_{1/2\ red\ 1}$ = −1.15 V. $E_{1/2\ red\ 2}$ = −1.62 V. **UV-Vis** Solution: (6.50 x 10^{-6} M in CH_2Cl_2, 298 K): λ_{max} (ε_{max}) = 467 nm (14100), 411 nm (14600). Thin Film: λ_{max} = 474 nm, 416 nm. **Fluorescence** Solution: (1.57 x 10^{-4} M in CH_2Cl_2, 298 K): λ_{max} = 635 nm (Φ < 0.01). Thin Film: λ_{em} = 670 nm (Φ = 0.03).

Synthesis of 3,9-dimesityl-2,8-diphenyl-3,9-diboraperylene (8)

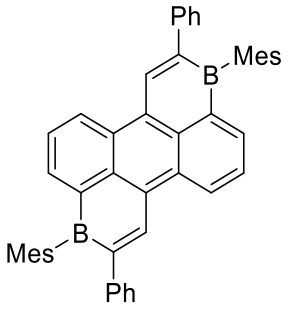

In an inert atmosphere glovebox, 3,9-dihydroxy-2,8-diphenyl-3,9-diboraperylene (102. mg, 0.235 mmol, 1 equiv.) was dissolved in CH_2Cl_2 (15 mL) in a Schlenk flask. The vessel was sealed, removed from the glovebox and BBr_3 (0.11 mL, 1.1 mmol, 5 equiv.) was added to the solution under nitrogen via injection. The mixture was stirred at room temperature for 26 h and then all volatiles were removed under reduced pressure. The remaining solid was dissolved in dry toluene (5 mL) and mesitylmagnesium bromide (1.64 mL 1.0 M in THF, 1.64 mmol, 7 equiv.) was added under nitrogen. The solution was stirred at room temperature for 16 h and then poured into water (50 mL). The aqueous mixture was extracted with toluene (20 mL) and the organic phase was concentrated *in vacuo*. The crude product was purified by column chromatography (hexane/ CH_2Cl_2, 4:1) to yield 3,9-dimesityl-2,8-diphenyl-3,9-diboraperylene **8** as a blue solid (32 mg, 0.050 mmol, 21% yield). Single crystals suitable for X-ray crystallography could be obtained by slow evaporation of a solution of **8** in hexanes/CH_2Cl_2 1:1. **^{1}H NMR** (400.1 MHz, CD_2Cl_2, 298 K): δ 9.44 (d, 2H, $^3J_{HH}$ = 9.4 Hz), 9.32 (s, 2H), 8.37 (d, 2H, $^3J_{HH}$ = 6.6 Hz), 7.96 (dd, 2H, $^3J_{HH}$ = 8.7 Hz, $^3J_{HH}$ = 8.7 Hz), 7.47-7.44 (m, 4H), 7.33-7.27 (m, 6H), 6.88 (s, 4H), 2.36 (s, 6H), 2.01 (s, 12H). **^{13}C{^{1}H} NMR** (100 MHz, CD_2Cl_2, 298 K): δ 150.9 (2C, br, B-*C*), 146.5 (2C), 145.8 (2C), 142.1 (2C), 141.5 (2C, br, B-*C*), 138.7 (4C), 137.5 (2C, br, B-*C*), 137.2 (2C), 132.4 (2C), 131.9 (2C), 131.7 (2C), 128.7 (2C), 128.4 (4C), 128.2 (2C), 128.1 (4C), 127.3 (4C), 127.0 (2C), 23.5 (4C), 21.4 (2C). **^{11}B NMR** (128 MHz, CD_2Cl_2, 298 K): δ 61.51 (br). **MP**: 272 °C. **HR-MS** (ASAP, negative mode) *m/z*: $[M]^-$ Calc'd for $C_{48}H_{40}B_2$ 638.3322; Found 638.3333. **CV** (3 x 10^{-4} M, 0.1 M *n*-Bu_4NPF_6 in CH_2Cl_2, vs. $Fc^{+/0}$, 298 K): $E_{1/2\ red\ 1}$ = −1.07 V. $E_{1/2\ red\ 2}$ = −1.41 V. **UV-Vis** Solution: (8.90 x 10^{-6} M in CH_2Cl_2, 298 K): λ_{max} (ε_{max}) = 611 nm (31900), 417 nm (10100). Thin Film: λ_{max} = 628 nm, 421 nm. **Fluorescence**: (1.32 x 10^{-6} M in CH_2Cl_2, 298 K): λ_{max} = 668 nm (Φ = 0.74).

Synthesis of 1,7-dimesityl-2,8-diphenyl-1,7-diboraanthanthrene (9)

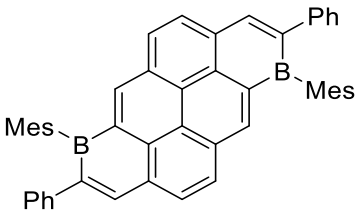

In an inert atmosphere glovebox, 1,7-dihydroxy-2,8-diphenyl-1,7-diboraanthanthrene **5** (20.0 mg, 0.0437 mmol, 1 equiv.) was dissolved in CH_2Cl_2 (7 mL) in a Schlenk flask. The vessel was sealed, removed from the glovebox and BBr_3 (0.021 mL, 0.22 mmol, 5 equiv.) was added to the solution under nitrogen via injection. The mixture was stirred at room temperature for 26 h and then all volatiles were removed under reduced pressure. The remaining solid was dissolved in dry toluene and mesitylmagnesium bromide (0.31 mL 1.0 M in THF, 0.31 mmol, 7 equiv.) was added under nitrogen at 0 °C. The solution was warmed to room temperature and stirred for 20 h. The solvent was removed under reduced pressure. The crude product was purified by column chromatography (hexane/CH_2Cl_2, 4:1) to yield 1,7-dimesityl-2,8-diphenyl-1,7-diboraanthanthrene (**9**) as a red solid (6.0 mg, 0.0091 mmol, 21% yield). **^{1}H NMR** (400.1 MHz, CD_2Cl2, 298 K): δ 8.77 (s, 2H), 8.38 (d, 2H, $^3J_{HH}$ = 8.0 Hz), 8.27 (d, 2H, $^3J_{HH}$ = 8.3 Hz), 8.17 (s, 2H), 7.37-7.35 (m, 4H), 7.28-7.22 (m, 6H), 6.90 (s, 4H), 2.38 (s, 6H), 2.06 (s, 12H). **^{13}C{^{1}H} NMR** (100 MHz, CD_2Cl_2, 298 K): δ 150.8 (2C, br, B-*C*), 149.4 (2C), 149.0 (2C), 145.1 (2C), 141.1 (2C, br, B-*C*), 138.7 (4C), 137.3 (2C), 135.9 (2C), 135.9 (2C, br, B-*C*), 132.1 (2C), 131.4 (2C), 130.5 (2C), 128.3 (4C), 128.2 (2C), 127.8 (4C), 127.4 (4C), 126.9 (2C), 125.7 (2C), 23.4 (4C), 21.4 (2C). **^{11}B NMR** (128 MHz, CD_2Cl_2, 298 K): not observed. **MP**: 264 °C **HR-MS** (ASAP, negative mode) *m/z*: $[M]^-$ Calc'd for $C_{50}H_{40}B_2$ 662.3322; Found: 662.3327. **CV** (3 x 10^{-4} M, 0.1 M *n*-Bu_4NPF_6 in CH_2Cl_2, vs. $Fc^{+/0}$, 298 K): $E_{1/2\ red\ 1}$ = −1.17 V. $E_{1/2\ red\ 2}$ = −1.51 V. **UV-Vis** Solution: (1.22 x 10^{-5} M in CH_2Cl_2, 298 K): λ_{max} (ε_{max}) = 575 nm (34700), 541 nm (28800), 455 nmm (19600). Thin Film: λ_{max} = 590 nm, 551 nm, 460 nm. **Fluorescence**: (1.43 x 10^{-6} M in CH_2Cl_2, 298 K): λ_{max} = 622 nm (Φ = 0.28).

Synthesis of 11-*tert*-butyl-2,8-dimesityl-3,7-diphenyl-2,8-diboratriangulene (10)

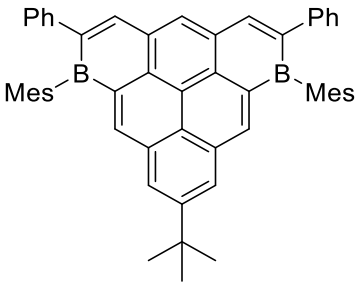

In an inert atmosphere glovebox 11-*tert*-butyl-2,8-dihydroxy-3,7-diphenyl-2,8-diboratriangulene **6** (62.5 mg, 0.122 mmol, 1 equiv.) was dissolved in CH_2Cl_2 (7 mL) in a Schlenk flask. The vessel was sealed, removed from the glovebox and BBr_3 (0.058 mL, 0.61 mmol, 5 equiv.) was added to the solution under nitrogen via injection. The mixture was stirred at room temperature for 26 h and then all volatiles were removed under reduced pressure. The remaining solid was dissolved in dry toluene and mesitylmagnesium bromide (0.85 mL 1.0 M in THF, 0.85 mmol, 7 equiv.) was added. The solution was stirred at room temperature for 20 h. The solvent was removed under reduced pressure. The crude product was purified by column chromatography (hexane/CH_2Cl_2, 4:1) to yield 11-*tert*-butyl-2,8-dimesityl-3,7-diphenyl-2,8-diboratriangulene **10** as a brown solid (18 mg, 0.025 mmol, 21% yield). **^{1}H NMR** (400 MHz, CD_2Cl_2, 298 K): δ 9.05 (s, 2H), 8.81 (s, 3H), 8.56 (s, 2H), 7.45-7.42 (m, 4 H), 7.32-7.22 (m, 6H), 6.93 (s, 4H), 2.40 (s, 6H), 2.07 (s, 12H), 1.58 (s, 9H). **^{13}C{^{1}H} NMR** (100 MHz, CD_2Cl_2, 298 K) δ 151.1 (1C), 150.1 (2C), 148.8 (2C), 148.3 (2C, br, B-*C*), 145.6 (2C), 141.6 (2C, br, B-*C*), 138.8 (4C), 137.1 (2C), 136.2 (2C), 136.0 (2C, br, B-*C*), 134.0 (2C), 130.6 (2C), 130.2 (2C), 129.2 (1C), 128.3 (4C), 128.1 (4C), 127.4 (4C), 126.5 (2C), 125.0 (1C), 122.5 (1C), 35.8 (1C), 31.8 (3C), 23.5 (4C), 21.5 (2C). **^{11}B NMR** (128 MHz, CD_2Cl_2, 298 K): δ 61.13 (br). **MP**: 168 °C **HR-MS** (ASAP, negative mode) *m/z*: $[M]^-$ Calc'd for $C_{54}H_{48}B_2$ 718.3948; Found: 718.3960. **CV** (3 x 10^{-4} M, 0.1 M *n*-Bu_4NPF_6 in CH_2Cl_2, vs. $Fc^{+/0}$, 298 K): $E_{1/2\ red}$ = −1.34 V. **UV-Vis** Solution: (6.69 x 10^{-6} M in CH_2Cl_2, 298 K): λ_{max} (ε_{max}) = 591 nm (5100), 550 nm (7200), 434 nm (22600), 404 nm (37200). Thin Film: λ_{max} = 602 nm, 511 nm, 440 nm, 406 nm. **Fluorescence**: (1.45 x 10^{-6} M in CH_2Cl_2, 298 K): λ_{max} = 633 nm, 684 nm (Φ = 0.34).

Synthesis of 1-styrylnaphthalene

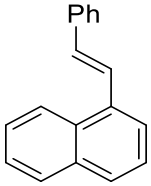

$Pd(OAc)_2$ (66.5 mg, 0.296 mmol) and tri(*o*-tolyl)phosphine (450. mg, 1.48 mmol) were placed into a 50 mL Schlenk flask fitted with a magnetic stirbar and sealed with a rubber septum. The Schlenk flask was evacuated and backfilled with nitrogen. Dry DMF (25 mL) and NEt_3 (10 mL) were added via syringe. Subsequently, 1-bromonaphthalene (2.08 mL, 14.9 mmol, 1 equiv.) and styrene (2.04 mL, 17.9 mmol, 1.2 equiv.) were added via syringe. The reaction mixture was stirred for 5 h at 90 °C then cooled to room temperature and stirred for a further 12 h. 0.5 M aq. HCl (150 mL) and 2 M aq. HCl (150 mL) were successively added to the reaction mixture. The mixture was extracted with Et_2O (5 x 100 mL) and the organic phase was washed with brine (3x 100 mL) and distilled water (2 x 100 mL). The organic layer was dried with $MgSO_4$, filtered and concentrated *in vacuo* to give an oil from which colorless crystals formed over five days. The remaining liquid was decanted from the crystals, which were further purified by silica gel column chromatography (15:1 *n*-hexane/EtOAc) to afford 1-styrylnaphthalene as a white solid (2.57 g, 11.2 mmol, 75% yield) that was spectroscopically identical to a literature account.[S2] **^{1}H NMR** (400 MHz, $CDCl_3$, 298 K): δ 8.24 (d, $^3J_{HH}$ = 8.17 Hz, 1H), 7.88 (m, 2H), 7.80 (d, $^3J_{HH}$ = 8.1 Hz, 1H), 7.75 (d, $^3J_{HH}$ = 7.3 Hz, 1H), 7.61 (d, $^3J_{HH}$ = 7.74 Hz, 2H), 7.51 (m, 3H), 7.41 (t, $^3J_{HH}$ = 7.8 Hz, 2H), 7.31 (t, $^3J_{HH}$ = 7.4 Hz, 1H), 7.16 (d, $^3J_{HH}$ = 16.1 Hz, 1H). **HR-MS** (MALDI-TOF, positive mode) *m/z*: $[M]^+$ Calc'd for $C_{18}H_{14}$ 230.1090; Found 230.10864.

Synthesis of 1,5-distyrylnaphthalene

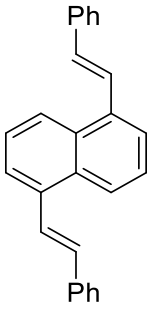

1,5-Dibromonapthalene (0.95 g, 3.3 mmol, 1 equiv.), $Pd(OAc)_2$ (31.2 mg, 0.141 mmol) and tri(*o*-tolyl)phosphine (211 mg, 0.704 mmol) were added to a Schlenk flask fitted with a magnetic stirbar and sealed with a rubber septum. The Schlenk flask was then evacuated and backfilled with nitrogen. Dry DMF (10 mL), NEt_3 (2.4 mL) and styrene (0.95 mL, 8.3 mmol, 2.5 equiv.) were added via syringe. The reaction mixture was stirred at 90 °C for 16 hours. The reaction mixture was cooled to -20 ºC and crystals formed. The solvent was decanted from the crystals, which were subsequently washed with DMF (10 mL), 2 N aq. HCl (200 mL), distilled water (500 mL), and MeOH (100 mL). The crystalline product was further purified by chromatography on a short silica gel column (1:19 EtOAc/pentane) to afford 1,5-di(styryl)naphthalene (561 mg, 1.69 mmol, 51% yield) as an off-white solid that was spectroscopically identical to a literature account.[S3] **^{1}H NMR** (400 MHz, $CDCl_3$, 298 K): δ 8.19 (d, 2H, ^3J = 8.6 Hz), 7.90 (d, 2H, ^3J = 16.0 Hz), 7.77 (d, 2H, ^3J = 7.0 Hz), 7.62 (d, 4H, ^3J = 7.2 Hz), 7.55 (t, 2H, ^3J = 7.8 Hz), 7.42 (t, 4H, ^3J = 7.3 Hz), 7.31 (tt, 2H, ^3J = 7.3 Hz, ^4J = 1.9 Hz), 7.15 (d, 2H, ^3J = 16.0 Hz). **HR-MS** (MALDI-TOF, positive mode) *m/z*: $[M]^+$ Calc'd for $C_{26}H_{20}$ 332.1560; Found 332.15697.

Synthesis of 1,4-distyrylnaphthalene

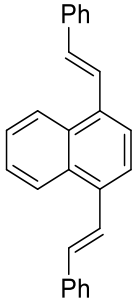

1,4-Dibromonapthalene (2.00 g, 7.00 mmol, 1 equiv.), $Pd(OAc)_2$ (62.4 mg, 0.282 mmol) and tri(*o*-tolyl)phosphine (422 mg, 1.41 mmol) were added to a Schlenk flask fitted with a magnetic stirbar and sealed with a rubber septum. The Schlenk flask was then evacuated and backfilled with nitrogen. Dry DMF (20 mL), NEt_3 (4.8 mL) and styrene (1.90 mL, 16.7 mmol, 2.4 equiv.) were added via syringe. The reaction mixture was stirred at 90 °C for 16 hours. The reaction mixture was cooled to -20 ºC and crystals formed. The solvent was decanted from the crystals, which were subsequently washed with DMF (20 mL), 2 N aq. HCl (400 mL), distilled water (1 L), and MeOH (200 mL). The crystalline product was further purified by chromatography on a short silica gel column (1:19 EtOAc/pentane) to afford 1,4-di(styryl)naphthalene (1.29 g, 3.89 mmol, 55% yield) as a yellow crystalline solid that was spectroscopically identical to a literature

account.[S4] **^{1}H NMR** (400 MHz, $CDCl_3$, 298 K): δ 8.28 (dd, 2H ^3J = 6.6 Hz, ^4J = 3.4 Hz), 7.92 (d, 2H, ^3J = 16.0 Hz), 7.78 (s, 2H), 7.66-7.61 (m, 4H), 7.58 (dd, 2H ^3J = 6.6 Hz, ^4J = 3.3 Hz), 7.42 (t, 4H, ^3J = 7.3 Hz), 7.31 (tt, 2H, ^3J = 7.4 Hz, ^4J = 1.8 Hz), 7.19 (d, 2H, ^3J = 16.0 Hz). **HR-MS** (MALDI-TOF, positive mode) *m/z*: $[M]^+$ Calc'd for $C_{26}H_{20}$ 332.1560; Found 332.15498.

Synthesis of 9,10-bis(2,3,4,5,6-pentafluorostyryl)anthracene

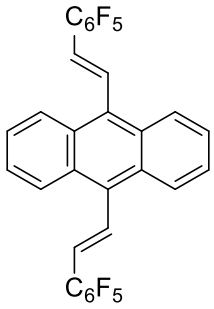

9,10-Dibromoanthracene (5.00 g, 14.9 mmol, 1 equiv.), tri(*o*-tolyl)phosphine (900. mg, 3.00 mmol), 25 mL dry DMF and 10 mL NEt_3 were added to a Schlenk flask fitted with a magnetic stirbar. The mixture was purged with bubbling argon for ten minutes, after which $Pd(OAc)_2$ (133 mg, 0.600 mmol) was added and the vessel was sealed with a rubber septum. Pentafluorostyrene (4.9 mL, 6.9 g, 36 mmol, 2.4 equiv.) was added via injection. The reaction mixture was stirred at 110 °C for 68 hours. The reaction mixture was cooled to room temperature and poured into 300 mL 2 N HCl. The yellow precipitate was collected by filtration and washed with 2 N aq. HCl (200 mL) and deionized water (500 mL). The product was further purified by recrystallization from hot chloroform solution and dried *in vacuo* to afford 9,10-bis(2,3,4,5,6-pentafluorostyryl)anthracene as a yellow crystalline solid (3.48 g , 6.19 mmol, 42% yield). From the crystallization, crystals suitable for X-ray crystallography could be obtained. **^{1}H NMR** (400 MHz, $CDCl_3$, 298 K): δ 8.34 (dd, 4H ^3J = 6.7 Hz, ^4J = 3.4 Hz), 8.25 (d, 2H, ^3J = 17.0 Hz), 7.55 (dd, 4H ^3J = 6.7 Hz, ^4J = 3.4 Hz), 6.85 (d, 2H, ^3J = 17.0 Hz). **^{13}C{^{1}H} NMR** (100 MHz, $CDCl_3$, 298 K, partial): δ 145.1 (br, d, $^1J_{CF}$ = 242 Hz, 4C), 138.0 (br, d, $^1J_{CF}$ = 240 Hz, 4C), 134.9 (m, 2C), 132.7 (2C), 129.2 (4C), 126.2 (4C), 126.1 (4C), 122.0 (d, $^4J_{CF}$ = 2.5 Hz, 2C), 112.3 (br, m, 2C). Due to poor solubility, peaks corresponding to *o*-*C*-F (2C) could not be resolved. **^{19}F NMR** (376 MHz, $CDCl_3$, 298 K): δ= −142.4 (m, 4F), −155.4 (t, $^3J_{FF}$ = 21 Hz, 2F), −162.4 (m, 4F). **MP**: 265 °C **HR-MS** (ESI-TOF, positive mode) *m/z*: $[M]^+$ Calc'd for $C_{30}H_{12}F_{10}$ 562.07738; Found 562.07753.

Synthesis of 1,6-distyrylpyrene

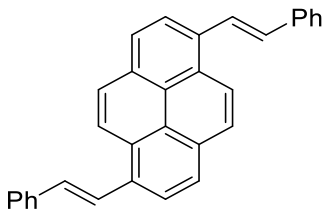

A Schlenk flask was charged with 1,6-dibromopyrene (1.00 g, 2.78 mmol 1 equiv.), tri-*o*-tolylphosphine (169 mg, 0.56 mmol), triethylamine (6 ml) and dry DMF (30 ml). The mixture was flushed with nitrogen for 10 min after which styrene (723 mg, 6.94 mmol, 2.5 equiv.) and palladium (II) acetate (60.0 mg, 0.267 mmol) were added. The reaction mixture was stirred under nitrogen at 110 °C for 17 h, cooled to room temperature, and then quenched with 2N HCl (80 ml). The precipitate was collected by filtration and thoroughly washed with water. The solid was dissolved in hot toluene and triturated with methanol to give pure 1,6-distyrylpyrene (810 mg, 2.00 mmol, 72% yield) as a yellow-green solid spectroscopically identical to a literature account.[S5] **^{1}H-NMR** (400.1 MHz, $CDCl_3$, 298 K): δ 8.49 (d, 2H, $^3J_{HH}$ = 9.3 Hz), 8.33 (d, 2H, $^3J_{HH}$ = 8.0 Hz), 8.21 (d, 2H, $^3J_{HH}$ = 16.0 Hz), 8.19 (d, 2H, $^3J_{HH}$ = 8.0 Hz), 8.13 (d, 2H, $^3J_{HH}$ = 9.3 Hz), 7.71-7.69 (m, 4 H), 7.45-7.43 (m, 4H), 7.36 (d, 2H, $^3J_{HH}$ = 16.0 Hz), 7.34 (tt, 2H, $^3J_{HH}$ = 7.4 Hz, $^4J_{HH}$ = 1.2 Hz). **HR-MS** (ESI-TOF, positive mode) *m/z*: $[M]^+$ Calc'd for $C_{32}H_{22}$: 406.1716; Found 406.1708.

Synthesis of 7-(*tert*-butyl)-1,3-distyrylpyrene

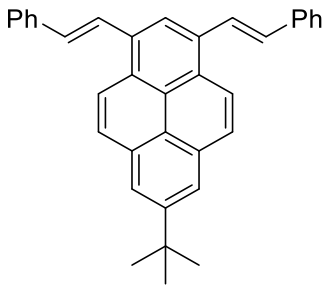

1,3-dibromo-7-*tert*-butylpyrene (1.23 g, 2.96 mmol) and tri-*o*-tolylphosphine (180 mg, 591 μmol) were dissolved in dry DMF (10 ml) and triethylamine (2.5 ml) in a round bottom flask and degassed by bubbling nitrogen through the solution for 10 min. Palladium(II)acetate (26.6 mg, 119 μmol) and styrene (771 mg, 7.41 mmol) were added and the reaction mixture was stirred

under nitrogen for 13 h at 110 °C. The reaction was cooled to room temperature and 2 N HCl (60 ml) was added. The precipitate was filtered off and dried under reduced pressure. Recrystallization from chloroform yielded pure 7-(*tert*-butyl)-1,3-distyryl-pyrene as a yellow solid (827 mg, 1.79 mmol, 60% yield). **^{1}H-NMR** (400.1 MHz, $CDCl_3$, 298 K): δ 8.56 (s, 1H), 8.45 (d, 2H, $^{3}J_{HH}$ = 9.2 Hz), 8.22 (s, 2H), 8.20 (d, 2H, $^{3}J_{HH}$ = 14.8 Hz), 8.10 (d, 2H, $^{3}J_{HH}$ = 9.2 Hz), 7.73 (d, 4H, $^{3}J_{HH}$ = 8.4 Hz), 7.46 (t, 4H, $^{3}J_{HH}$ = 7.8 Hz), 7.42 (d, 2H, $^{3}J_{HH}$ = 16.8 Hz), 7.34 (tt, 2H, $^{3}J_{HH}$ = 7.4 Hz, $^{4}J_{HH}$ = 1.2 Hz), 1.59 (s, 9H). **^{13}C{^{1}H} NMR** (100 MHz, $CDCl_3$, 298 K): δ 149.3 (1C), 137.9 (2C), 132.1 (2C), 131.9 (2C), 131.3 (2C), 129.0 (4C), 128.3 (2C), 128.0 (2C), 127.8 (2C), 126.9 (4C), 126.1 (2C), 125.6 (1C), 123.6 (1C), 123.1 (2C), 122.8 (2C), 121.4 (1C), 35.3 (1C), 32.0 (3C). **MP:** 222 °C. **HR-MS** (ESI-TOF, positive mode) *m/z*: $[M]^+$ Calc'd for $C_{36}H_{30}$ 462.2342; Found 462.2326.

3. NMR Spectra

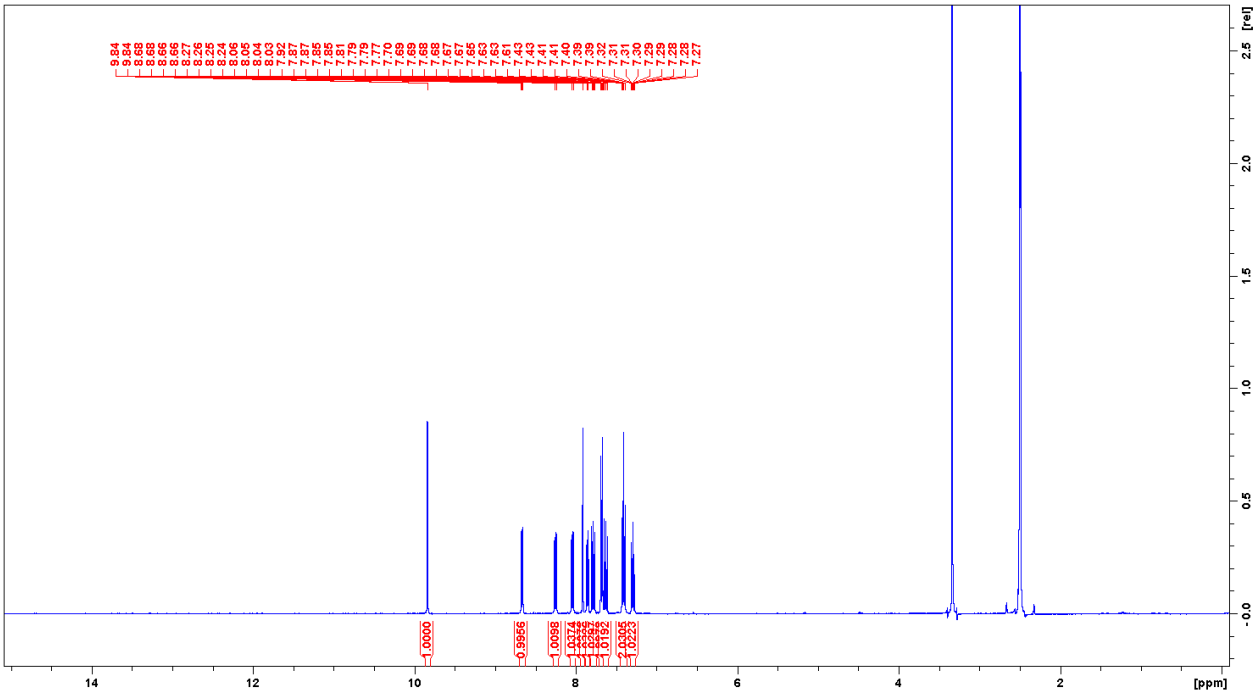

Figure S1. ^{1}H NMR spectrum of 1-hydroxy-2-phenyl-1-boraphenalene (**1**) (400 MHz, DMSO-d_6, 298 K).

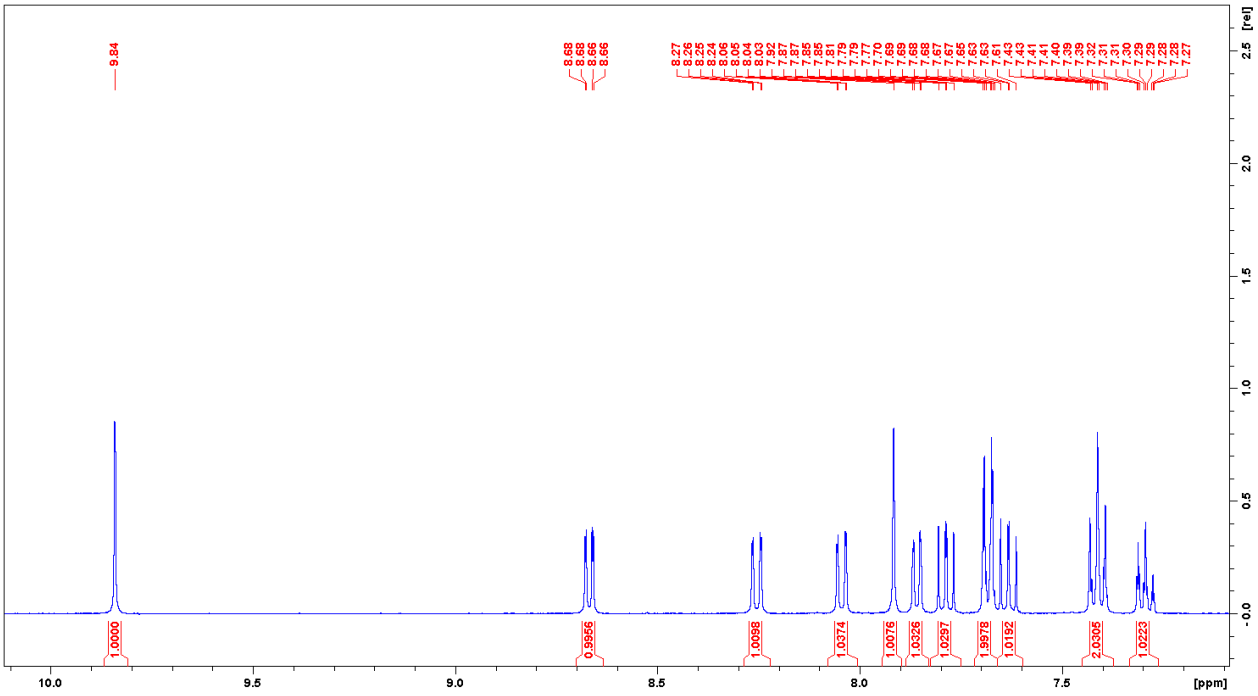

Figure S2. Magnified aromatic region of the ^{1}H NMR spectrum of 1-hydroxy-2-phenyl-1-boraphenalene (**1**) (400 MHz, DMSO-d$_6$, 298 K).

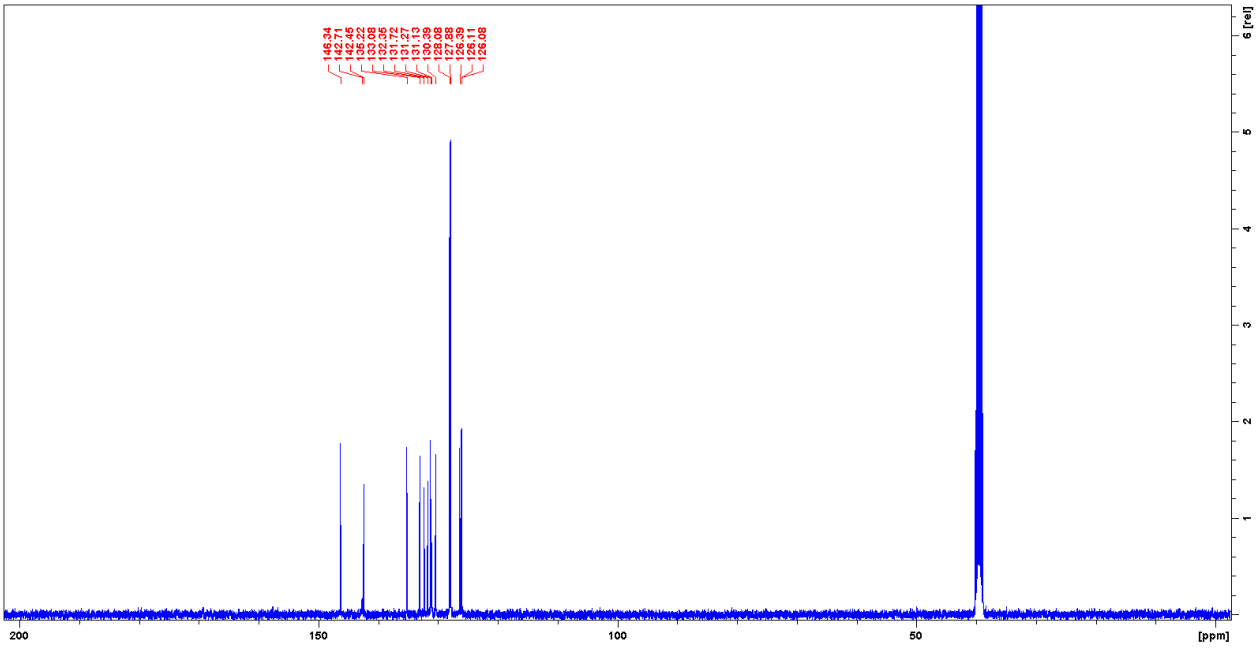

Figure S3. ^{13}C{^{1}H} NMR spectrum of 1-hydroxy-2-phenyl-1-boraphenalene (**1**) (100 MHz, DMSO-d$_6$, 298 K).

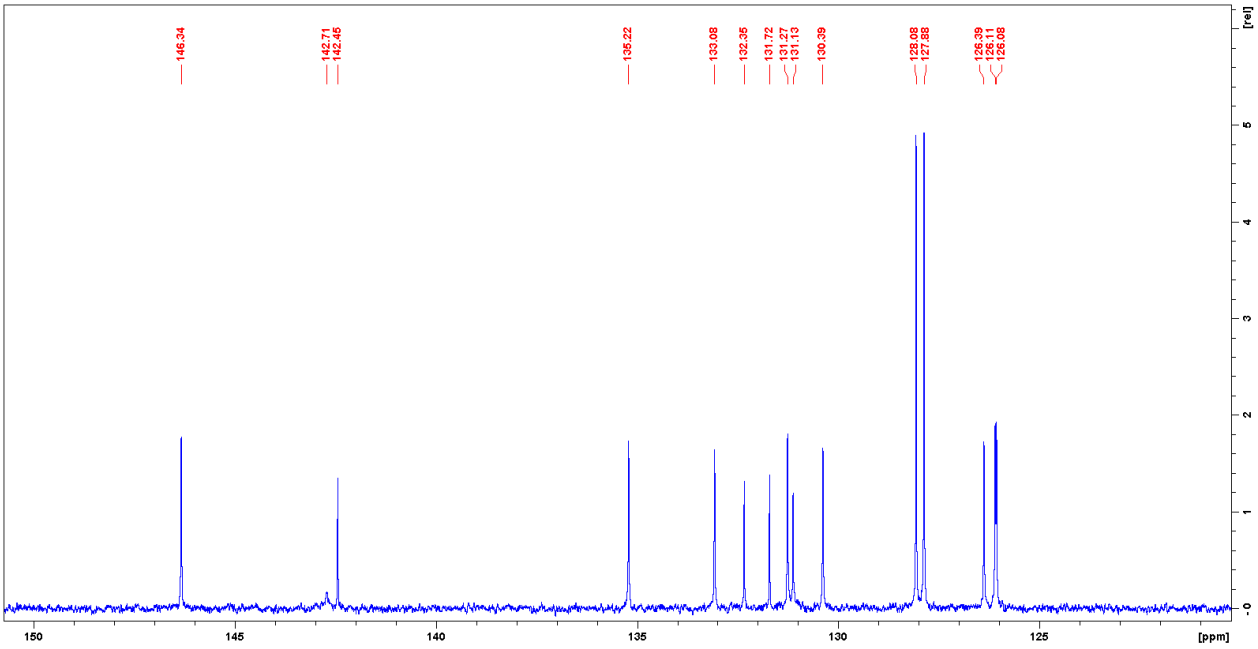

Figure S4. Magnified aromatic region of the $^{13}C\{^{1}H\}$ NMR spectrum of 1-hydroxy-2-phenyl-1-boraphenalene (**1**) (100 MHz, DMSO-d_6, 298 K).

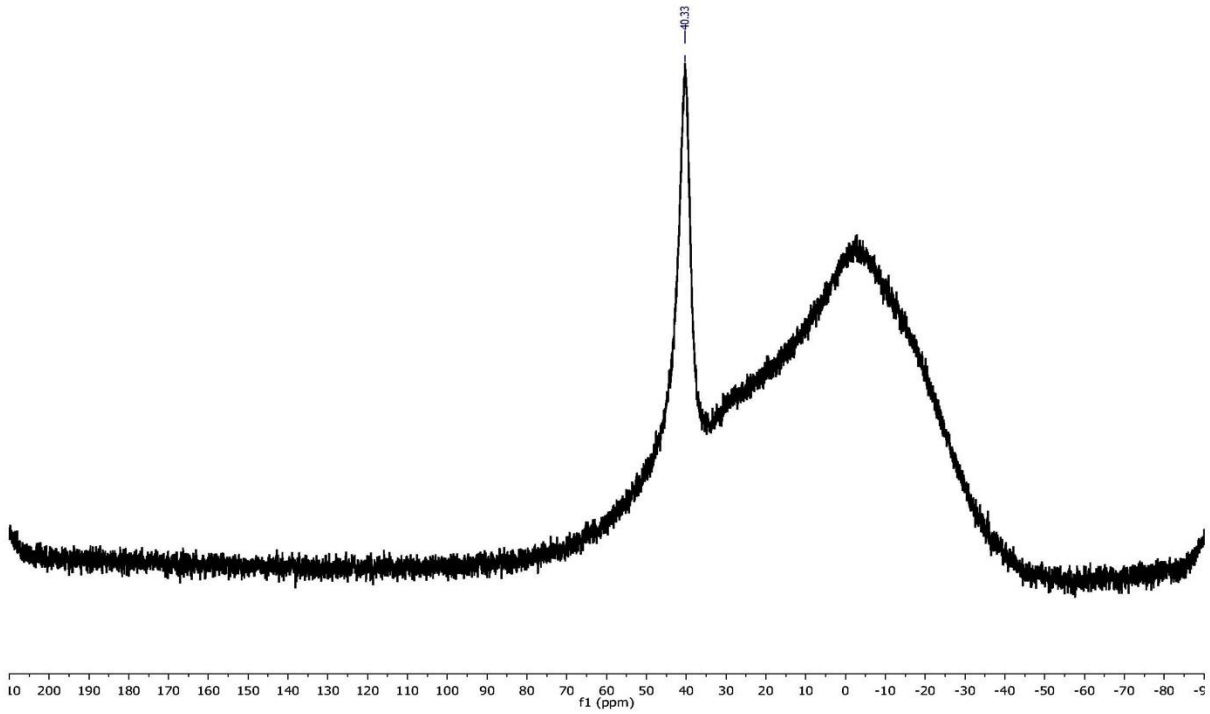

Figure S5. ^{11}B NMR spectrum of 1-hydroxy-2-phenyl-1-boraphenalene (**1**) (128 MHz, $CDCl_3$, 298 K).

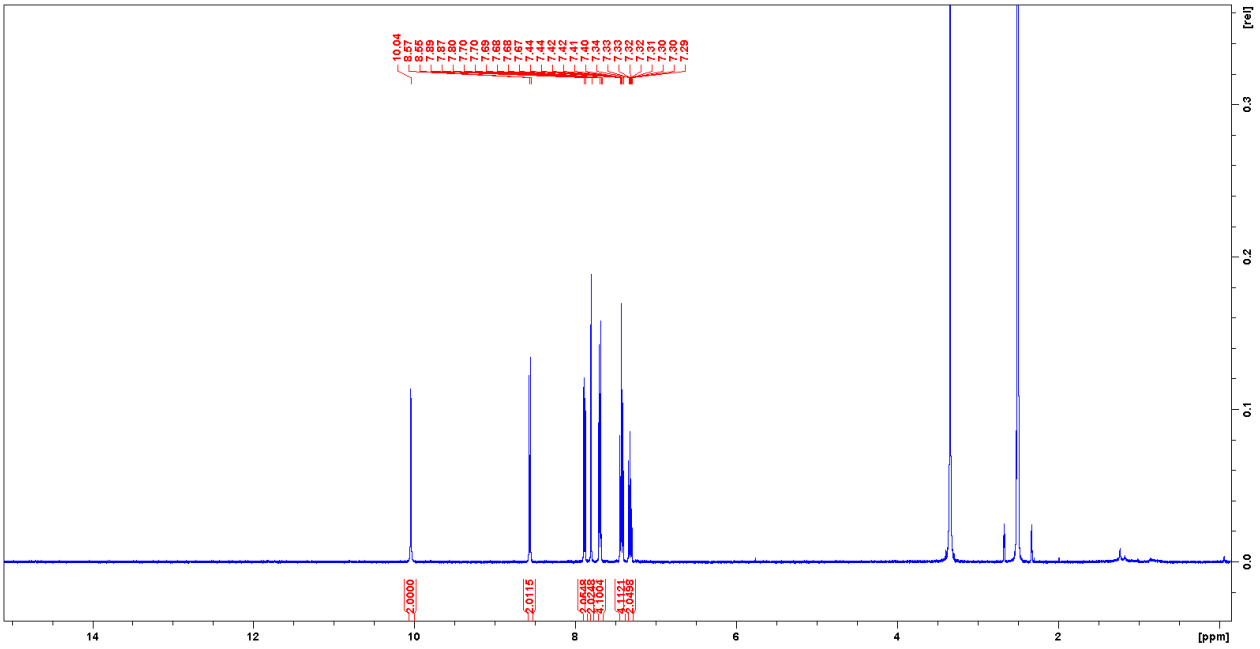

Figure S6. ^{1}H NMR spectrum of 1,6-dihydroxy-2,7-diphenyl-1,6-diborapyrene (**2**) (400 MHz, DMSO-d_6, 298 K).

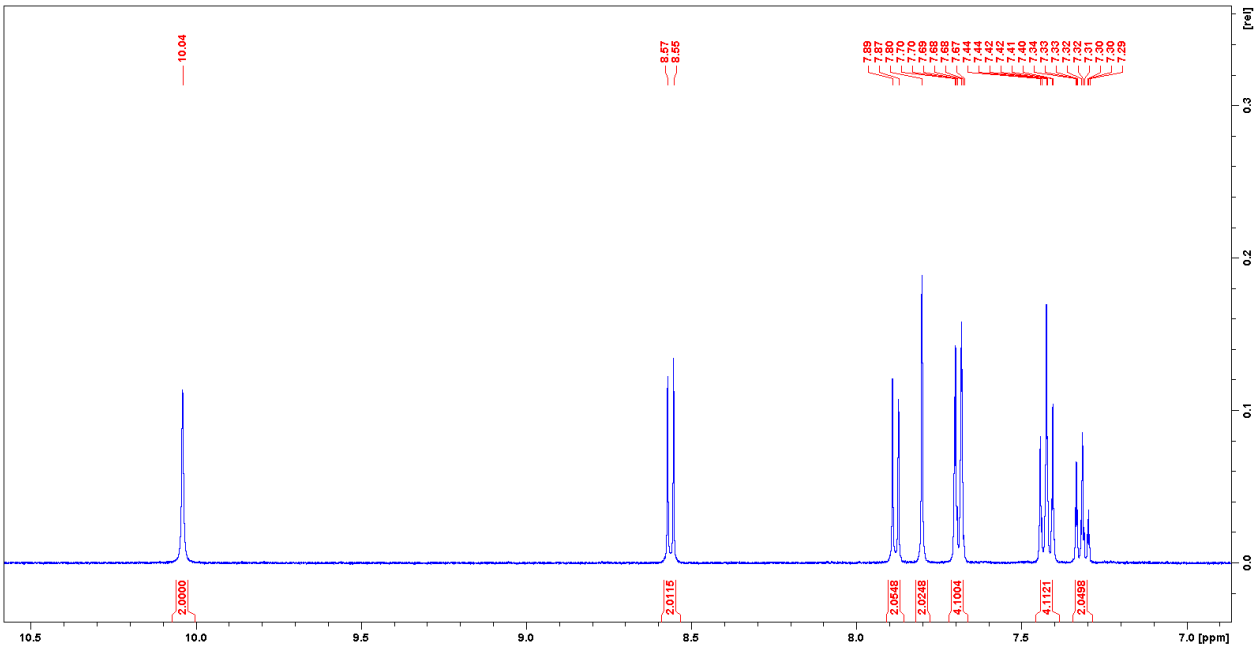

Figure S7. Magnified aromatic region of the ^{1}H NMR spectrum 1,6-dihydroxy-2,7-diphenyl-1,6-diborapyrene (**2**) (400 MHz, DMSO-d_6, 298 K).

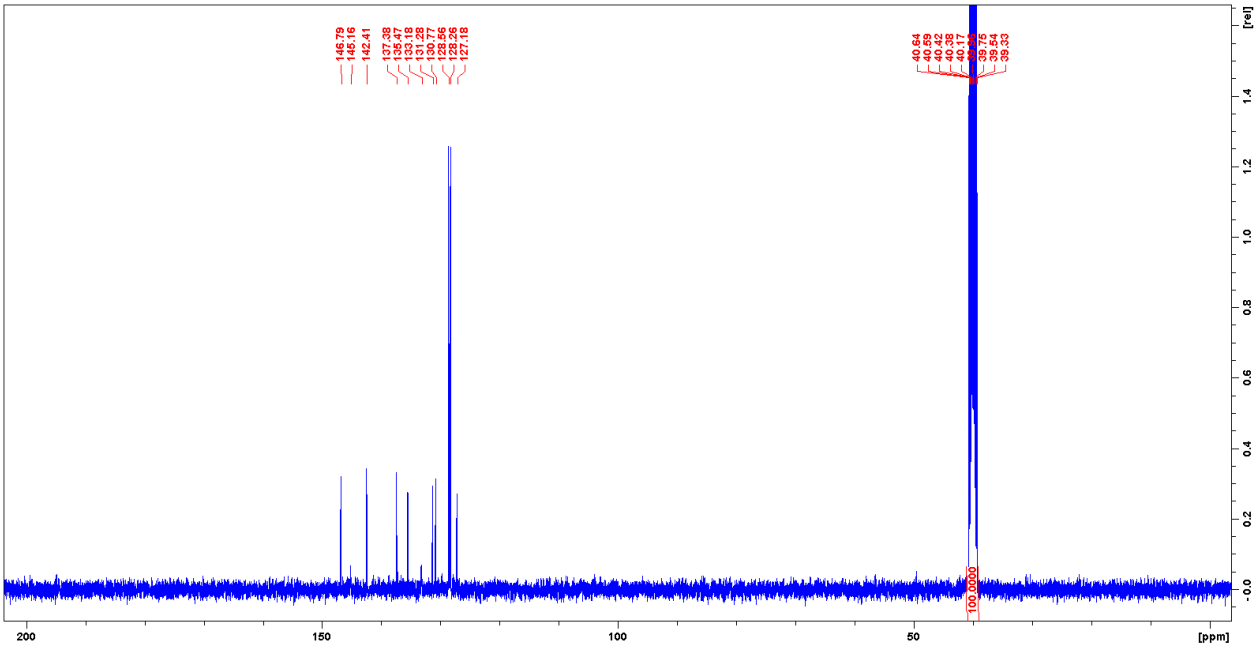

Figure S8. $^{13}C\{^{1}H\}$ NMR spectrum of 1,6-dihydroxy-2,7-diphenyl-1,6-diborapyrene (**2**) (100 MHz, DMSO-d_6, 298 K).

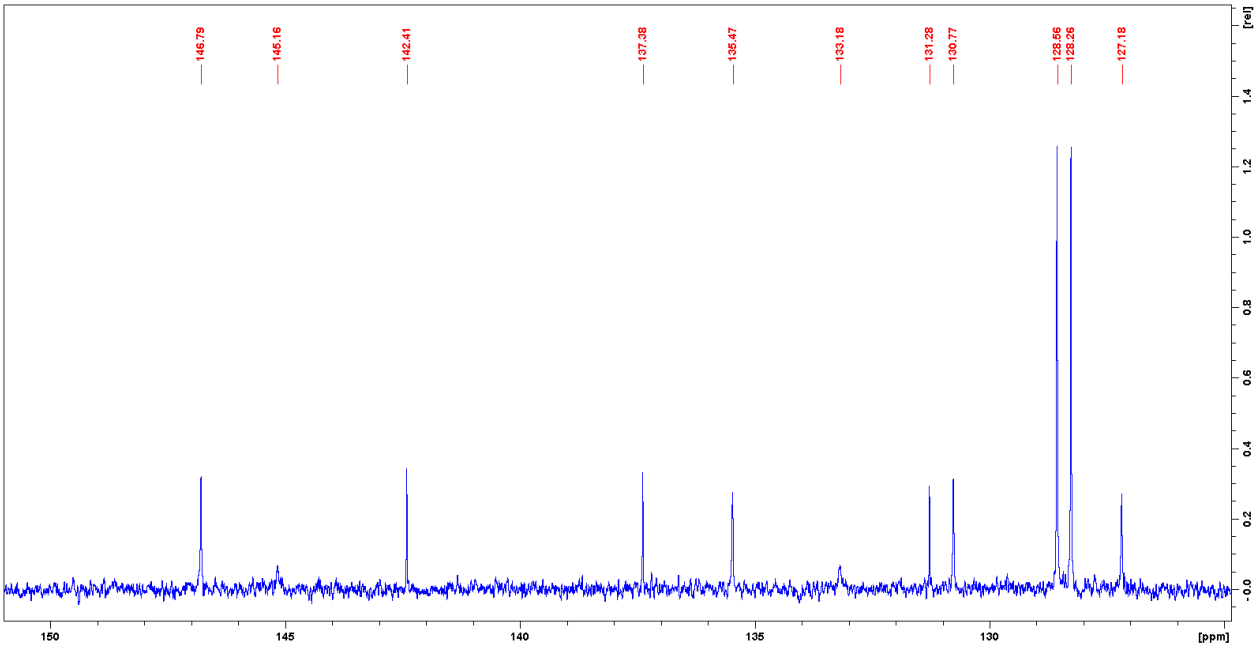

Figure S9. Magnified aromatic region of the $^{13}C\{^{1}H\}$ NMR spectrum 1,6-dihydroxy-2,7-diphenyl-1,6-diborapyrene (**2**) (100 MHz, DMSO-d_6, 298 K).

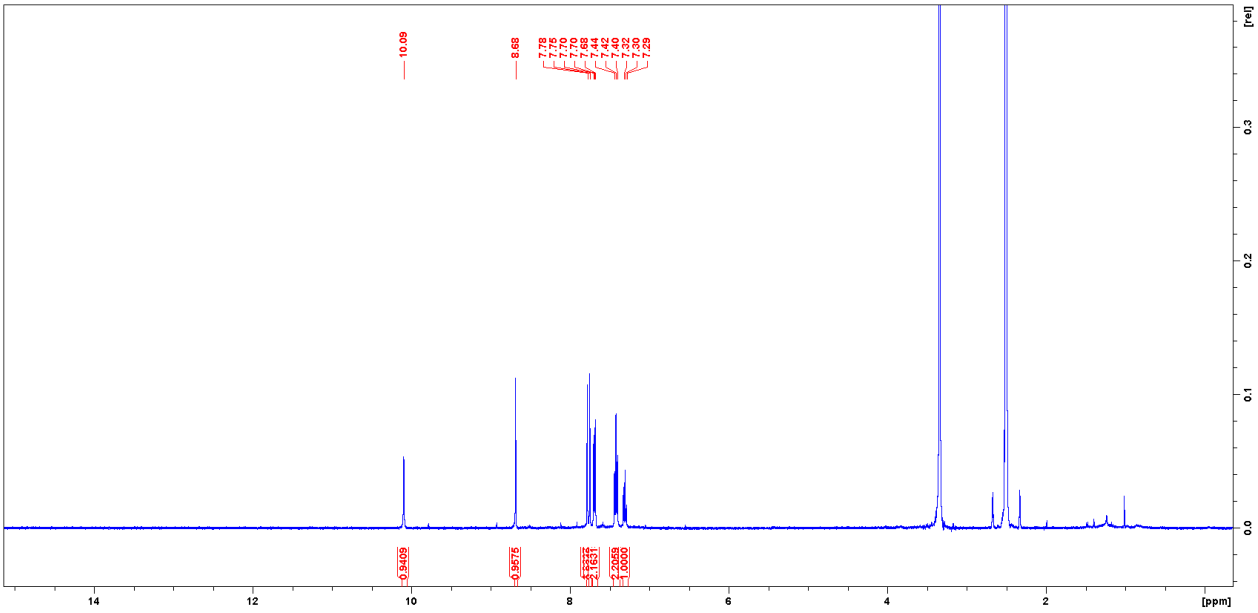

Figure S10. ^{1}H NMR spectrum 1,8-dihydroxy-2,7-diphenyl-1,8-diborapyrene (**3**) (400 MHz, DMSO-d_6, 298 K).

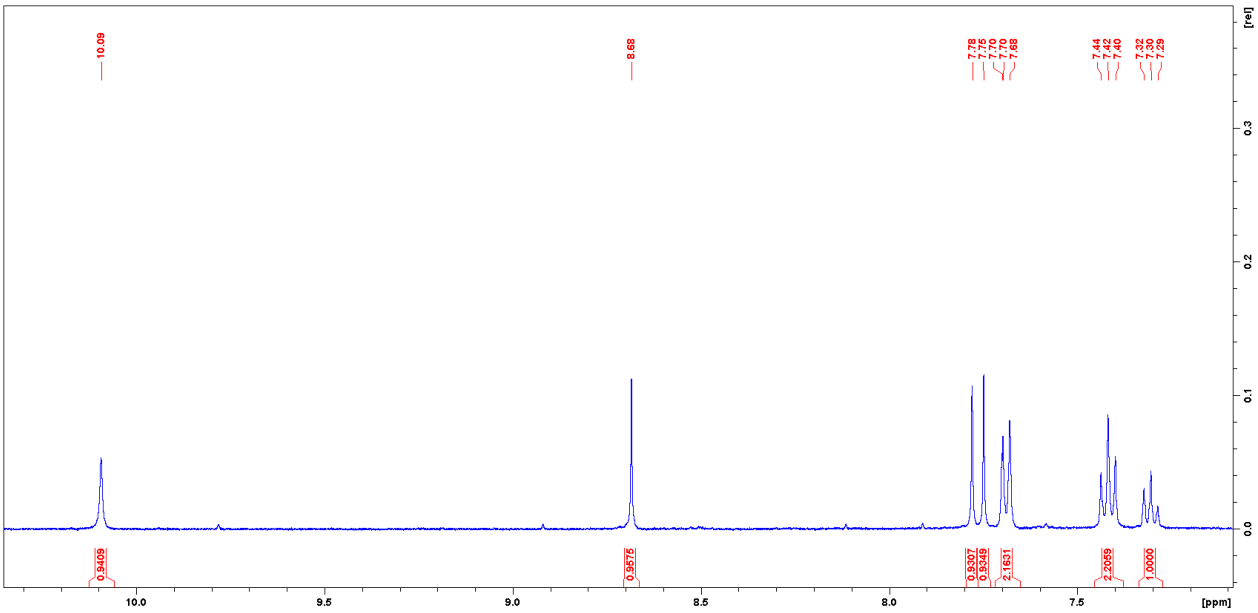

Figure S11. Magnified aromatic region of the ^{1}H NMR spectrum 1,8-dihydroxy-2,7-diphenyl-1,8-diborapyrene (**3**) (400 MHz, DMSO-d_6, 298 K).

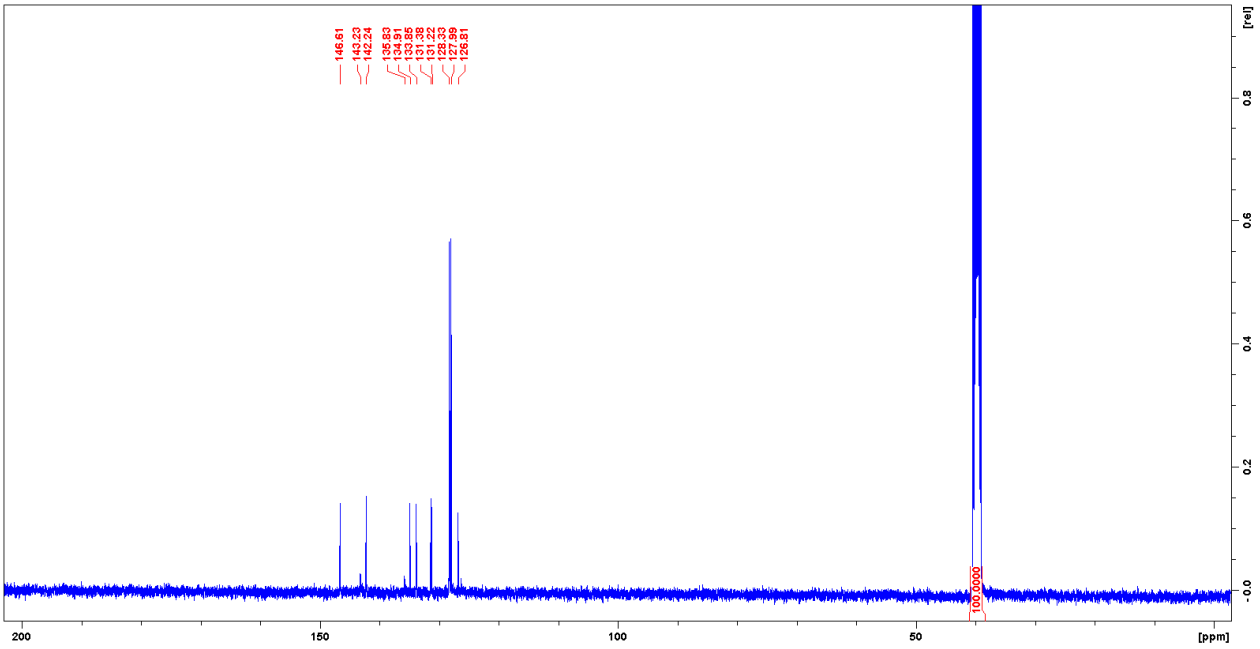

Figure S12. $^{13}C\{^{1}H\}$ NMR spectrum 1,8-dihydroxy-2,7-diphenyl-1,8-diborapyrene (**3**) (100 MHz, DMSO-d_6, 298 K).

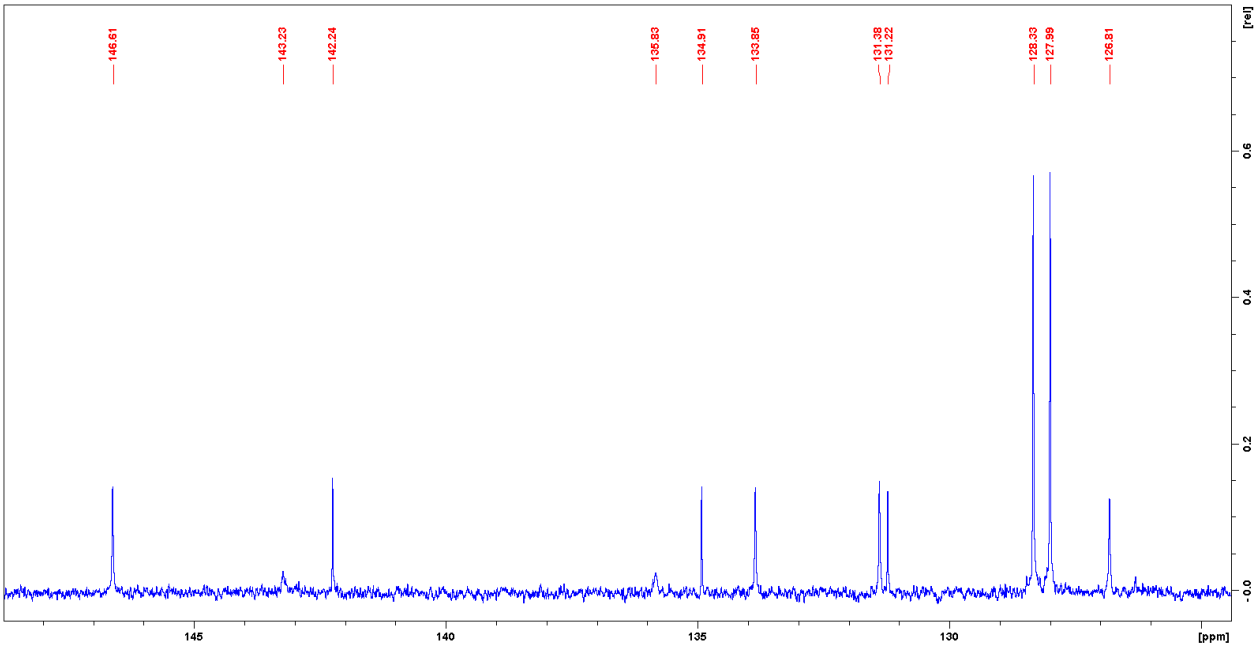

Figure S13. Magnified aromatic region of the $^{13}C\{^{1}H\}$ NMR spectrum 1,8-dihydroxy-2,7-diphenyl-1,8-diborapyrene (**3**) (100 MHz, DMSO-d_6, 298 K).

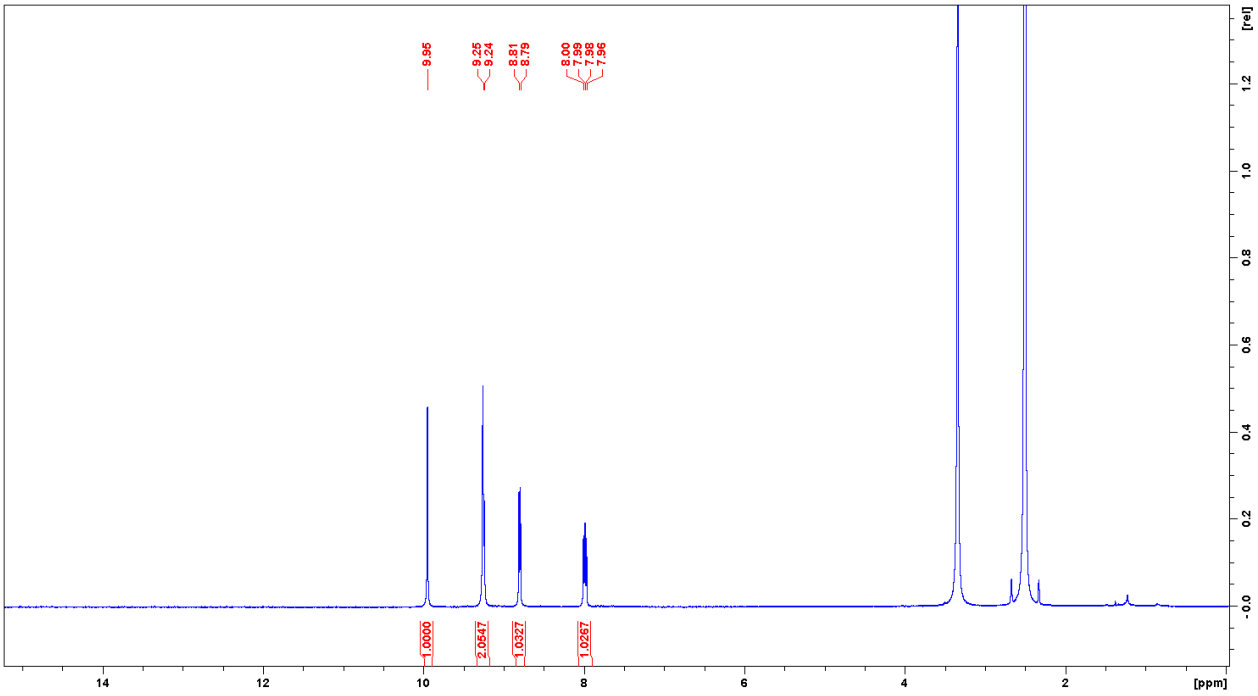

Figure S14. ^{1}H NMR spectrum of 3,9-dihydroxy-2,8-bis(pentafluorophenyl)-3,9-diboraperylene (**4b**) (600 MHz, DMSO-d_6, 298 K).

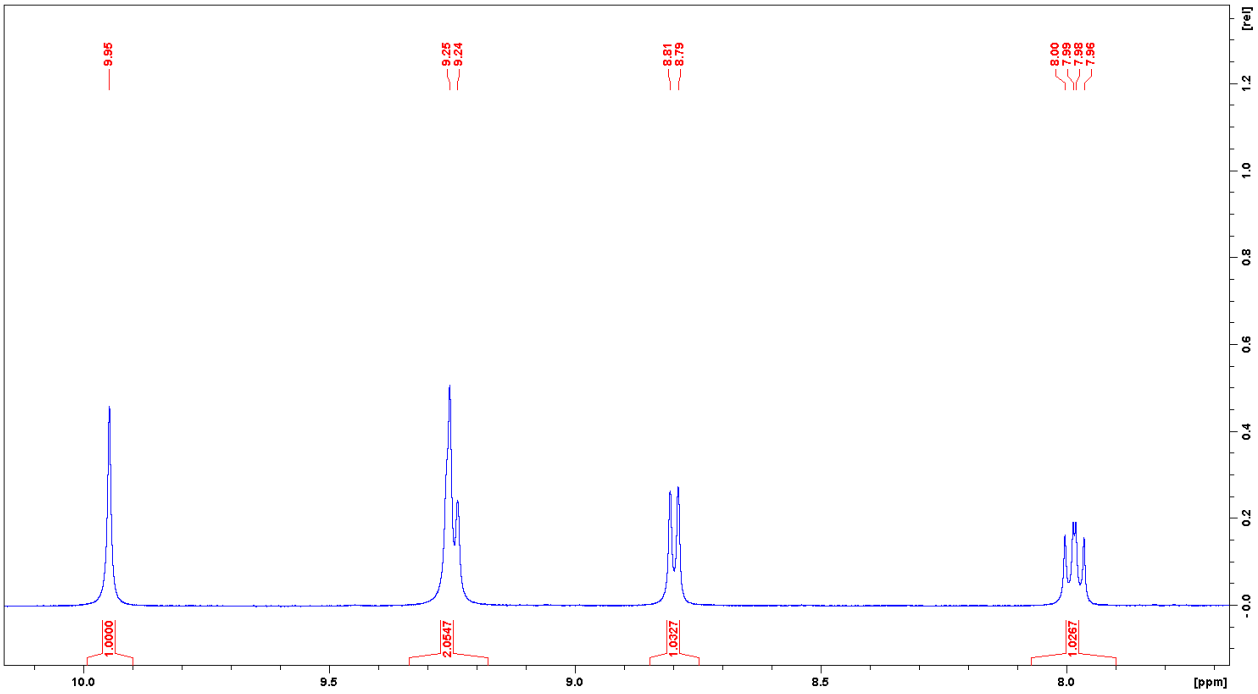

Figure S15. Magnified aromatic region of the ^{1}H NMR spectrum of 3,9-dihydroxy-2,8-bis(pentafluorophenyl)-3,9-diboraperylene (**4b**) (600 MHz, DMSO-d_6, 298 K).

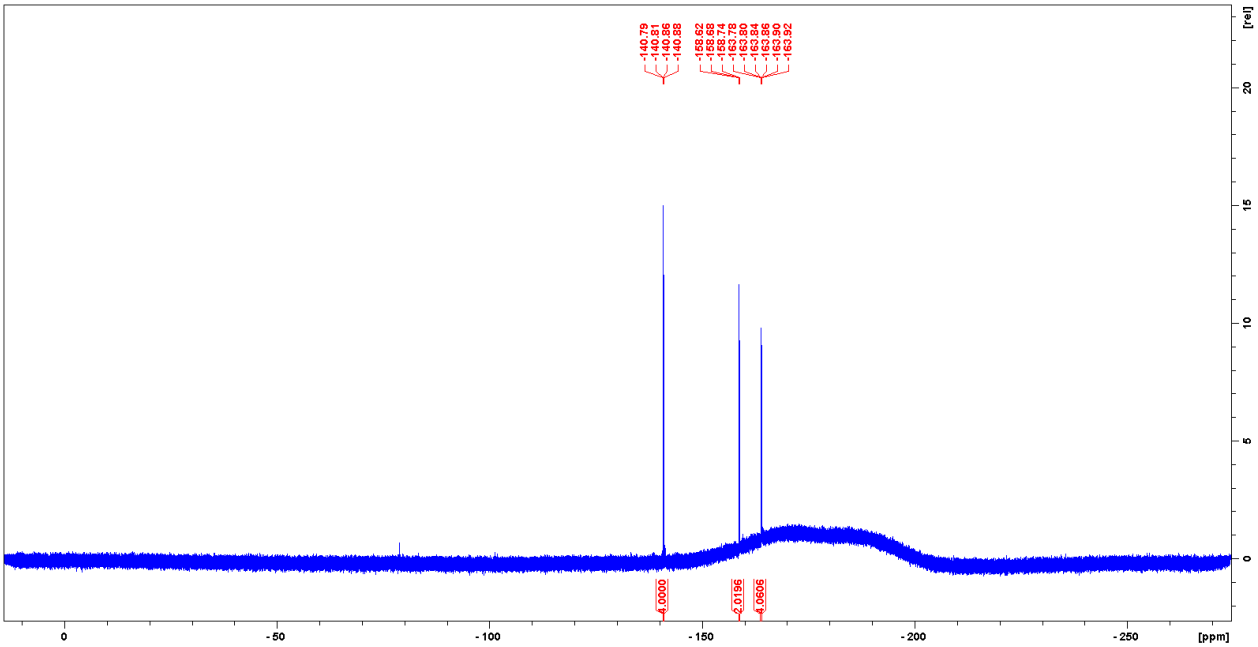

Figure S16. ^{19}F NMR spectrum of 3,9-dihydroxy-2,8-bis(pentafluorophenyl)-3,9-diboraperylene (**4b**) (376 MHz, DMSO-d_6, 298 K).

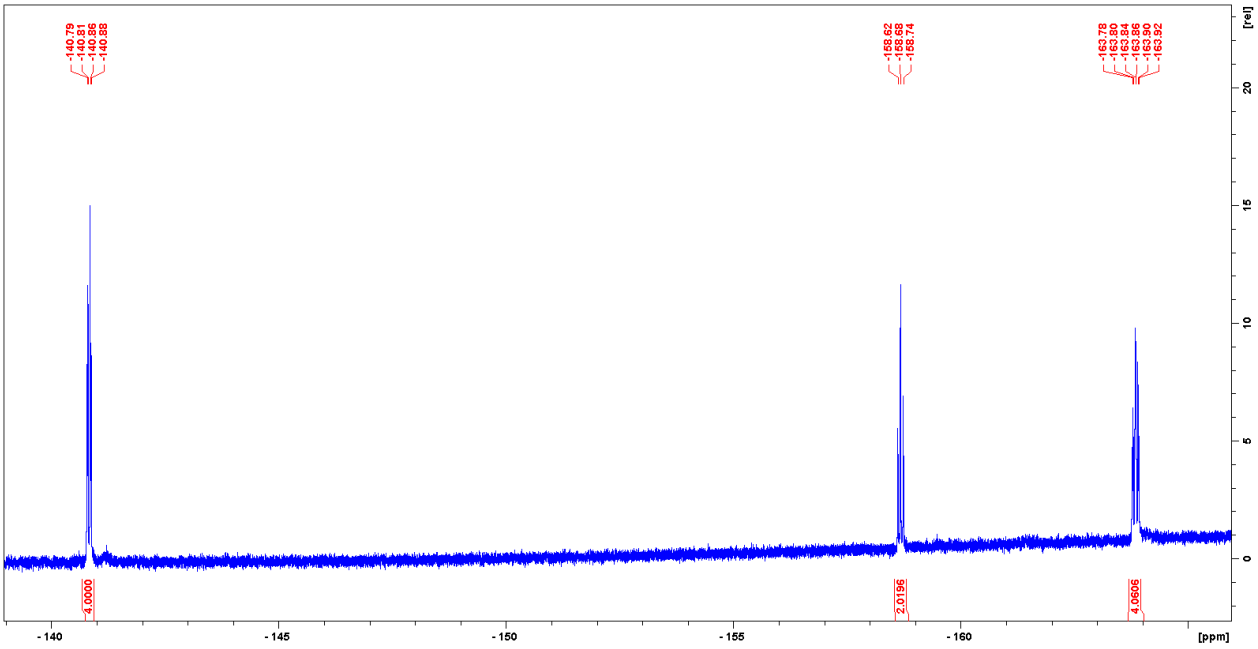

Figure S17. Expansion of the ^{19}F NMR spectrum of 3,9-dihydroxy-2,8-bis(pentafluorophenyl)-3,9-diboraperylene (**4b**) (376 MHz, DMSO-d_6, 298 K).

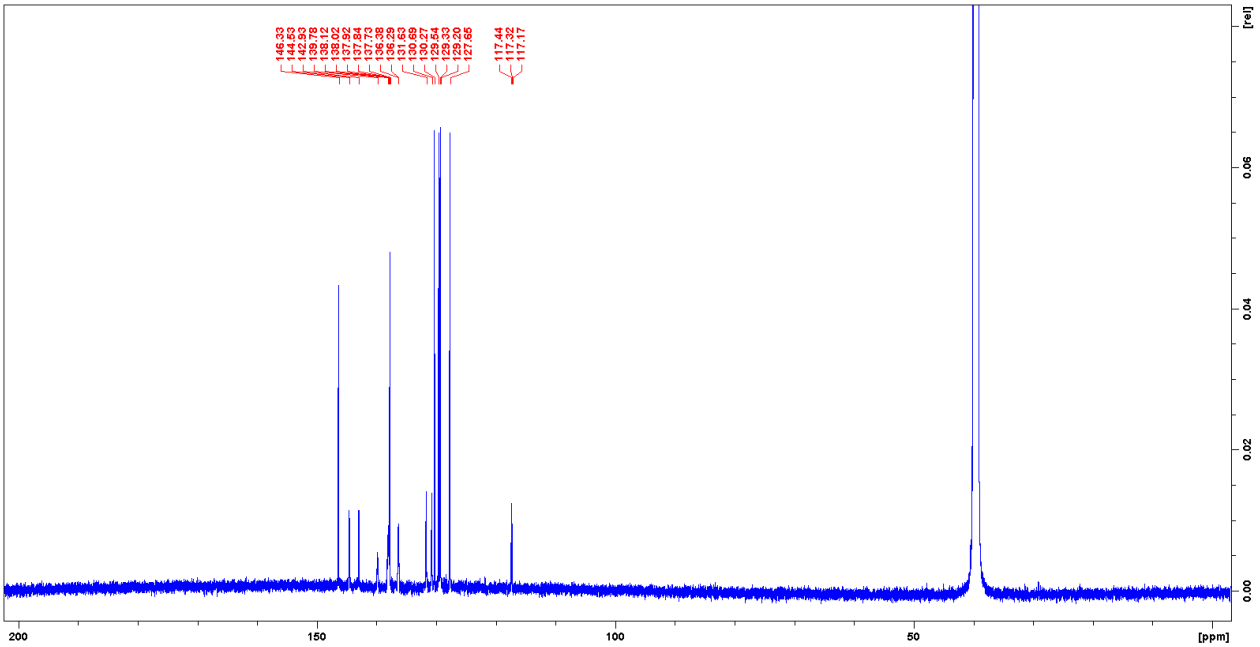

Figure S18. $^{13}C\{^{1}H\}$ NMR spectrum of 3,9-dihydroxy-2,8-bis(pentafluorophenyl)-3,9-diboraperylene (**4b**) (151 MHz, DMSO-d_6, 298 K).

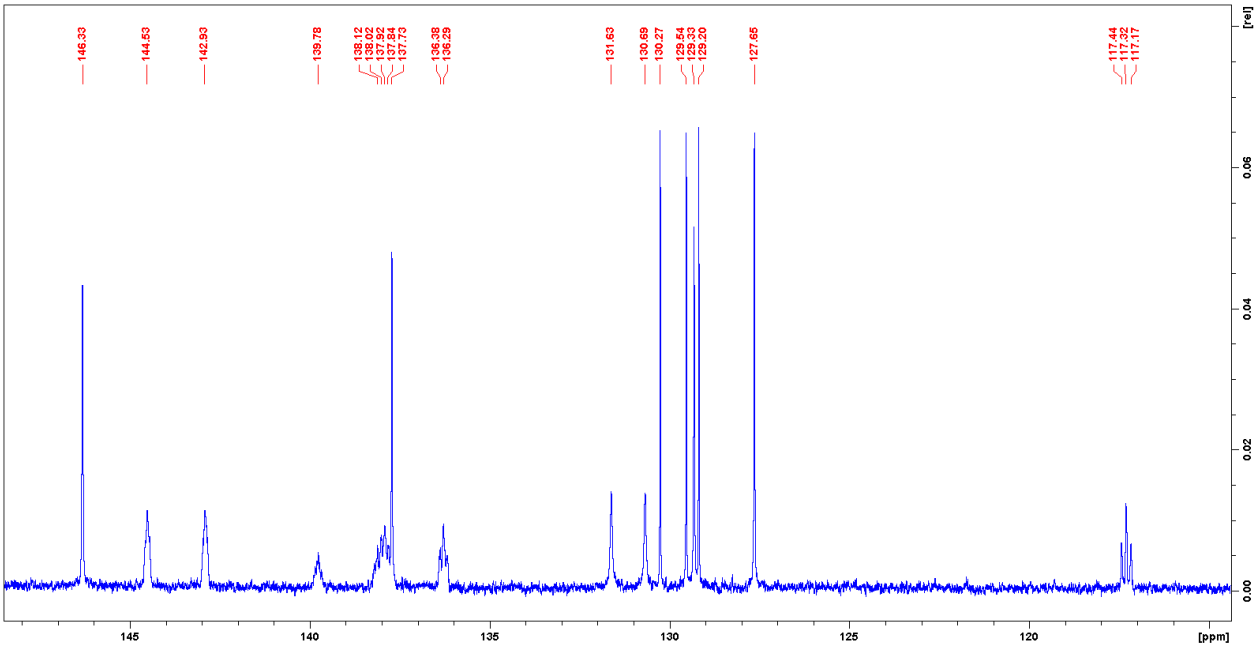

Figure S19. Magnified aromatic region of the $^{13}C\{^{1}H\}$ NMR spectrum of 3,9-dihydroxy-2,8-bis(pentafluorophenyl)-3,9-diboraperylene (**4b**) (151 MHz, DMSO-d_6, 298 K).

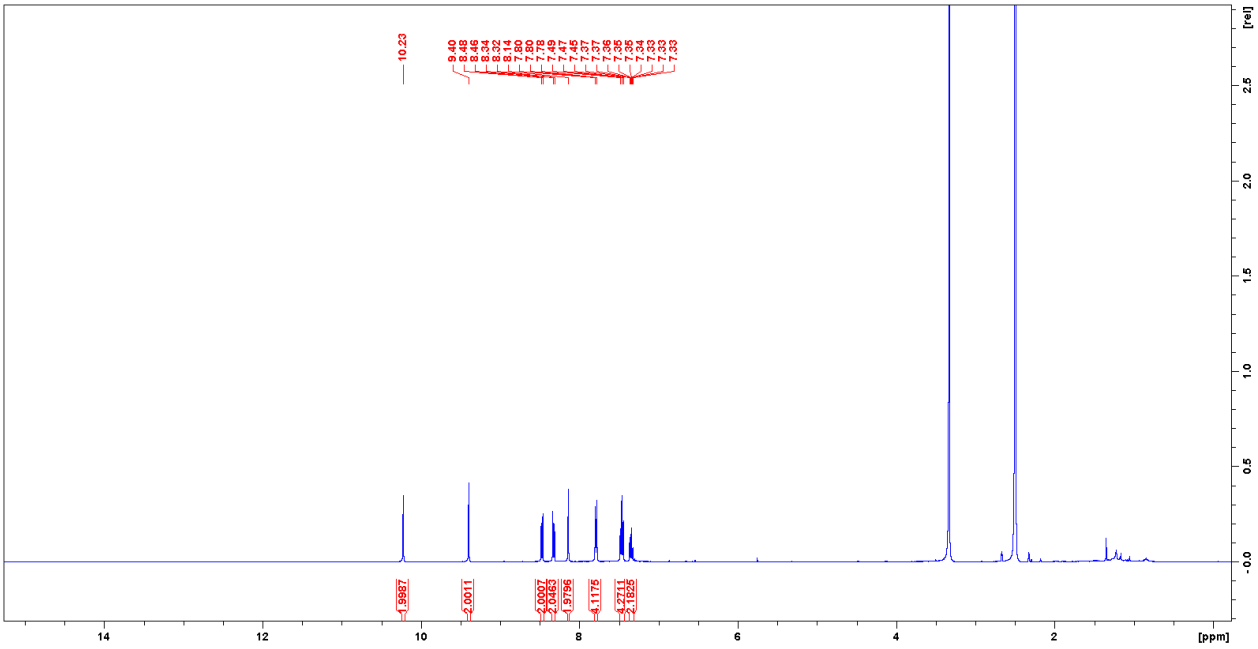

Figure S20. ^{1}H NMR spectrum of 1,7-dihydroxy-2,8-diphenyl-1,7-diboraanthanthrene (**5**) (400 MHz, DMSO-d_6, 298 K).

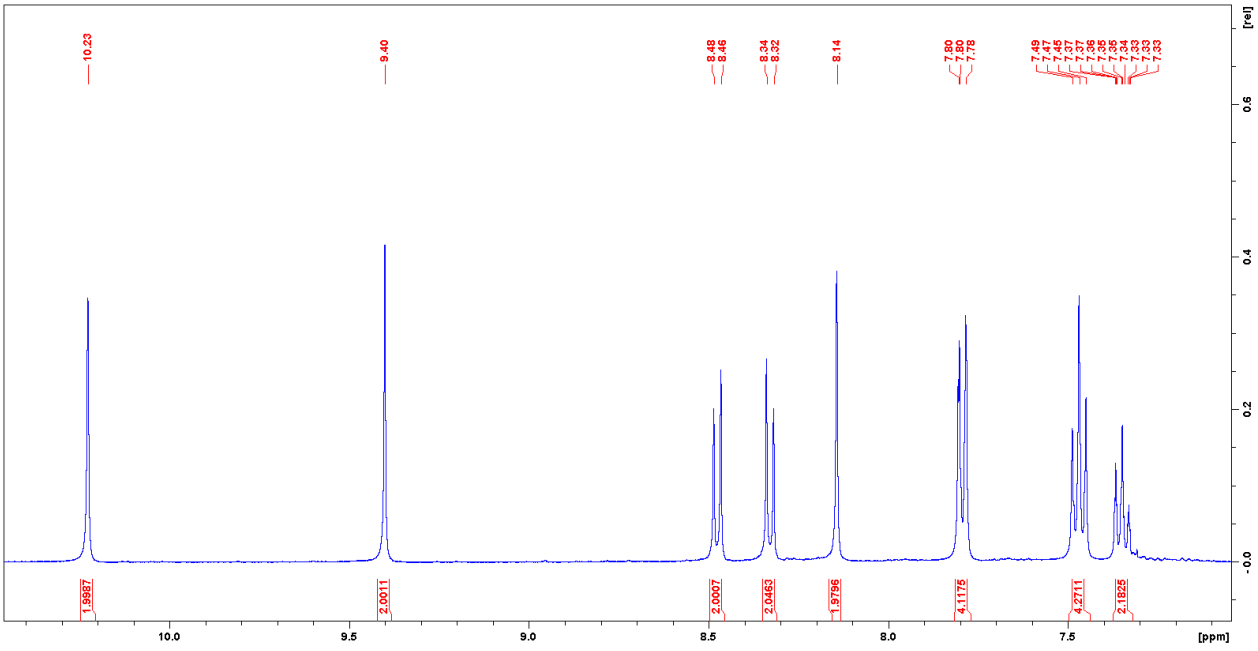

Figure S21. Magnified aromatic region of the ^{1}H NMR spectrum 1,7-dihydroxy-2,8-diphenyl-1,7-diboraanthanthrene (**5**) (400 MHz, DMSO-d_6, 298 K).

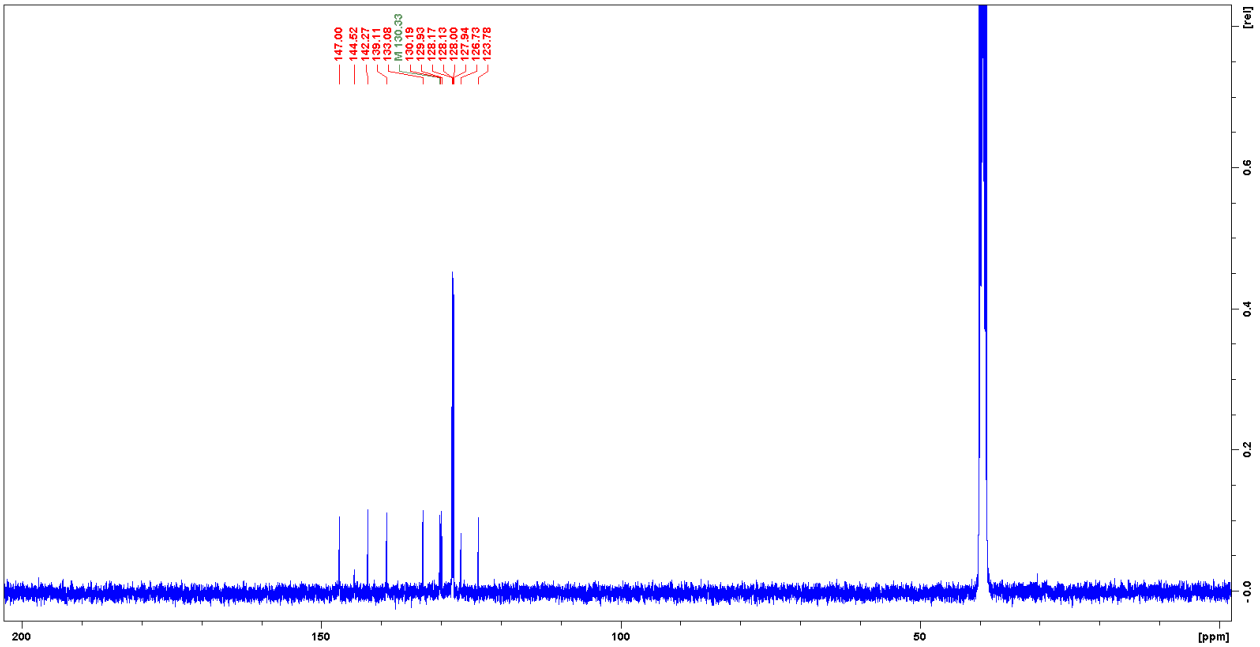

Figure S22. $^{13}C\{^{1}H\}$ NMR spectrum of 1,7-dihydroxy-2,8-diphenyl-1,7-diboraanthanthrene (**5**) (151 MHz, DMSO-d_6, 298 K).

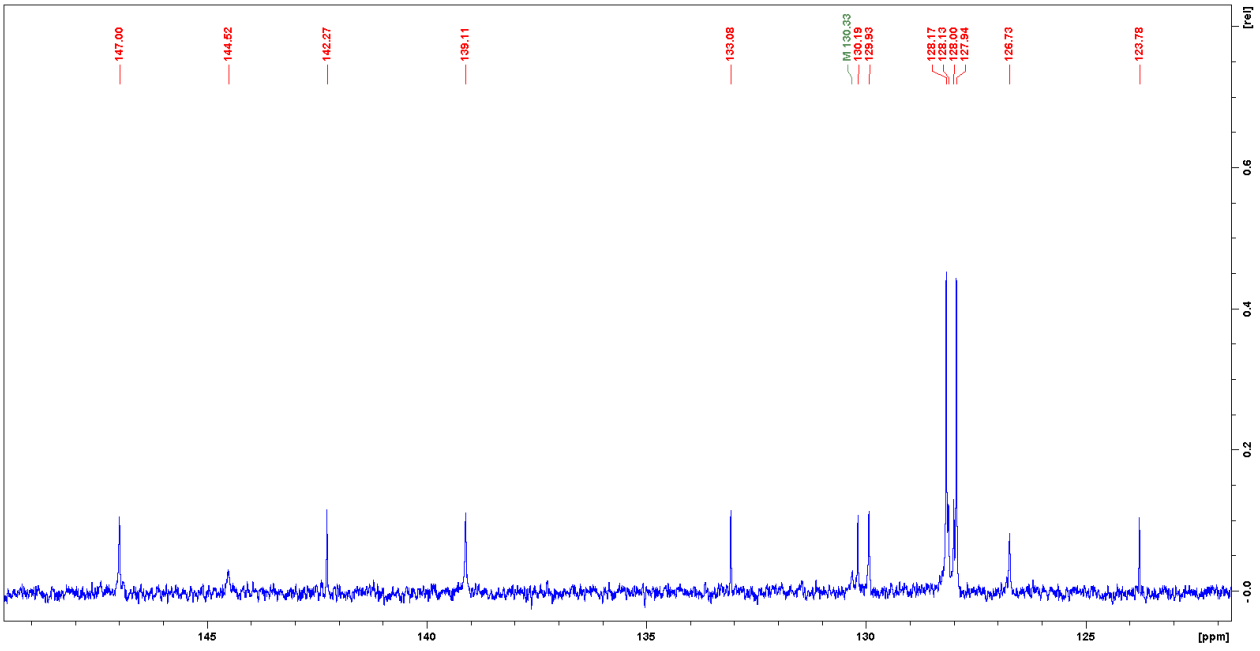

Figure S23. Magnified aromatic region of the $^{13}C\{^{1}H\}$ NMR spectrum of 1,7-dihydroxy-2,8-diphenyl-1,7-diboraanthanthrene (**5**) (151 MHz, DMSO-d_6, 298 K).

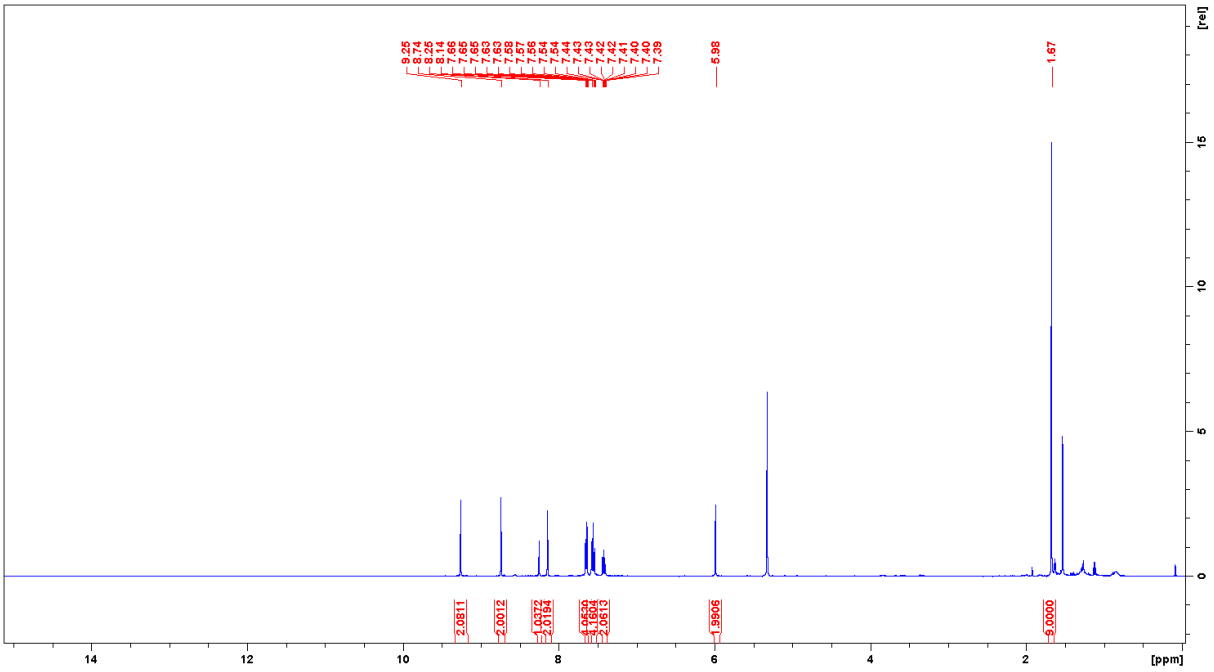

Figure S24. ^{1}H NMR spectrum of 11-*tert*-butyl-2,8-dihydroxy-3,7-diphenyl-2,8-diboratriangulene (**6**) (400 MHz, CD_2Cl_2, 298 K).

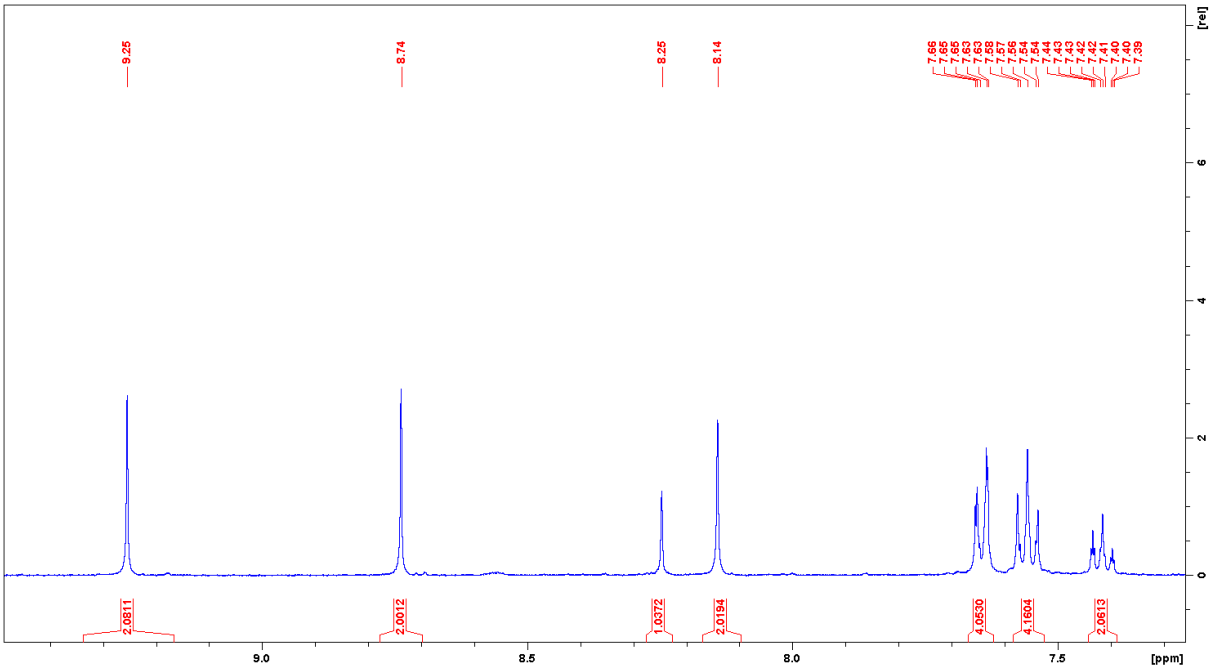

Figure S25. Magnified aromatic region of the ^{1}H NMR spectrum of 11-*tert*-butyl-2,8-dihydroxy-3,7-diphenyl-2,8-diboratriangulene (**6**) (400 MHz, CD_2Cl_2, 298 K).

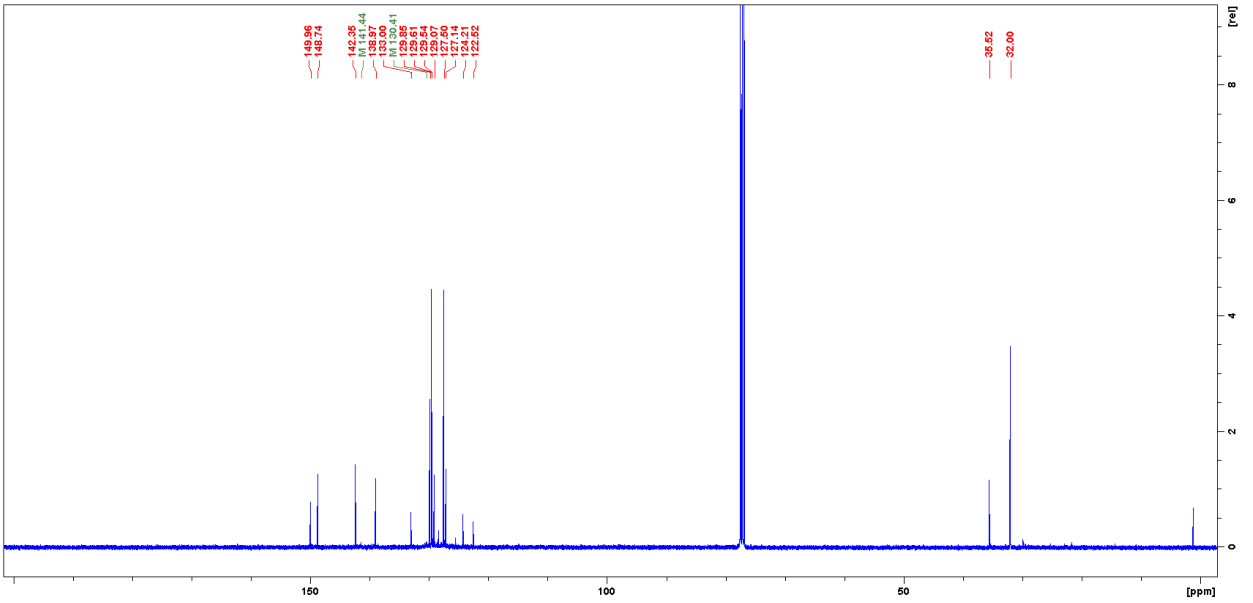

Figure S26. $^{13}C\{^{1}H\}$ NMR spectrum of 11-*tert*-butyl-2,8-dihydroxy-3,7-diphenyl-2,8-diboratriangulene (**6**) (100 MHz, $CDCl_3$, 298 K).

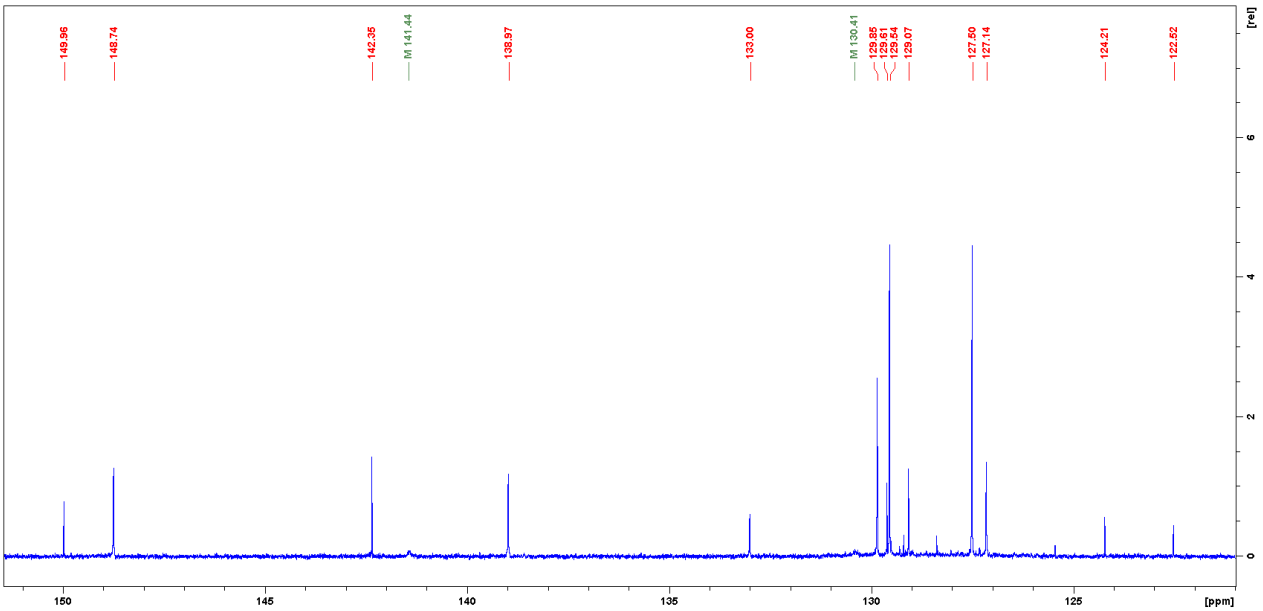

Figure S27. Magnified aromatic region of the $^{13}C\{^{1}H\}$ NMR spectrum of 11-*tert*-butyl-2,8-dihydroxy-3,7-diphenyl-2,8-diboratriangulene (**6**) (100 MHz, $CDCl_3$, 298 K).

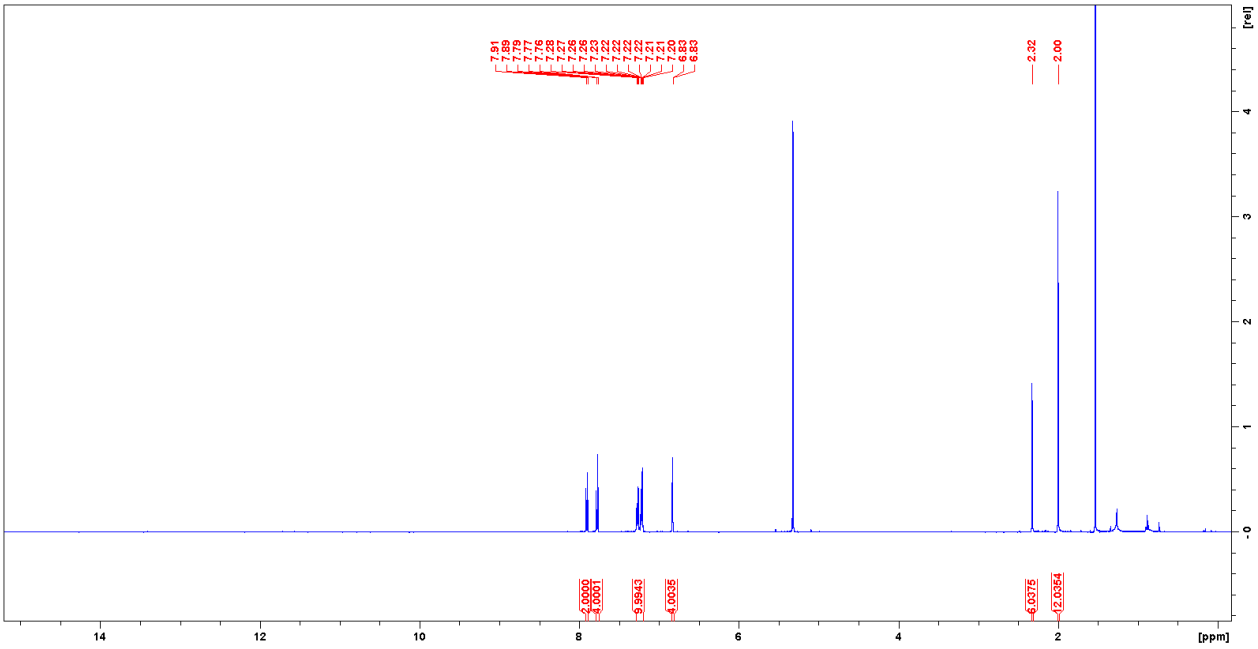

Figure S28. ^{1}H NMR spectrum of 1,6-dimesityl-2,7-diphenyl-1,6-diborapyrene (**7**) (400 MHz, CD_2Cl_2, 298 K).

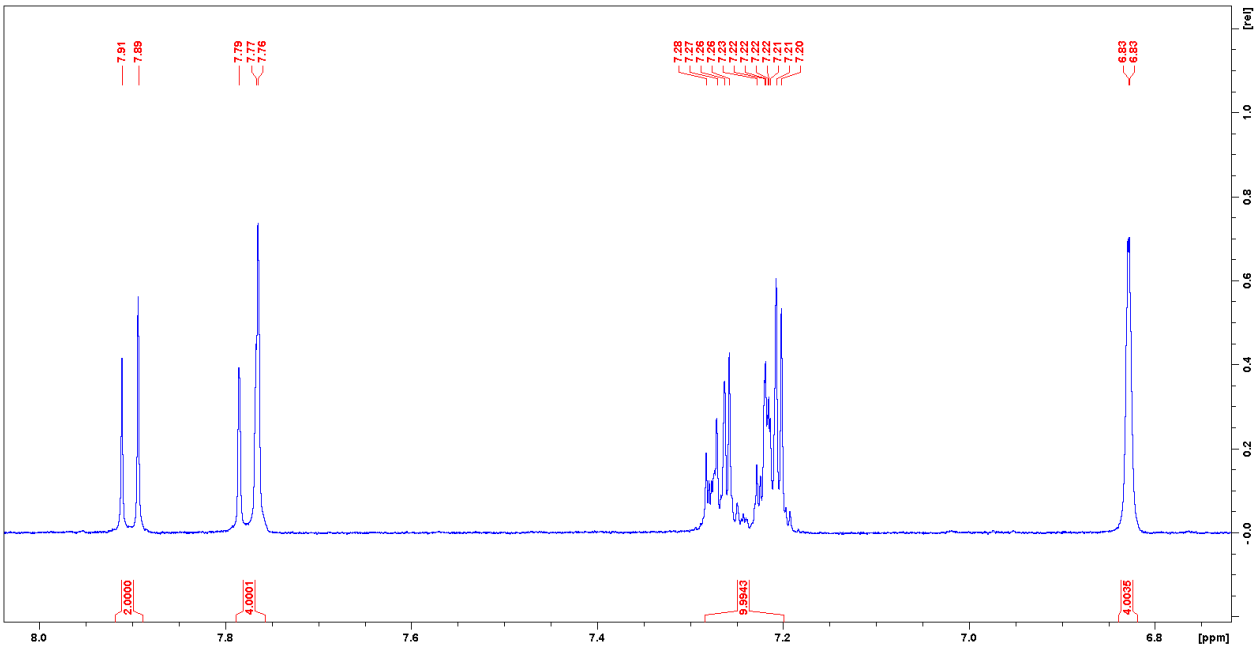

Figure S29. Magnified aromatic region of the ^{1}H NMR spectrum of 1,6-dimesityl-2,7-diphenyl-1,6-diborapyrene (**7**) (400 MHz, CD_2Cl_2, 298 K).

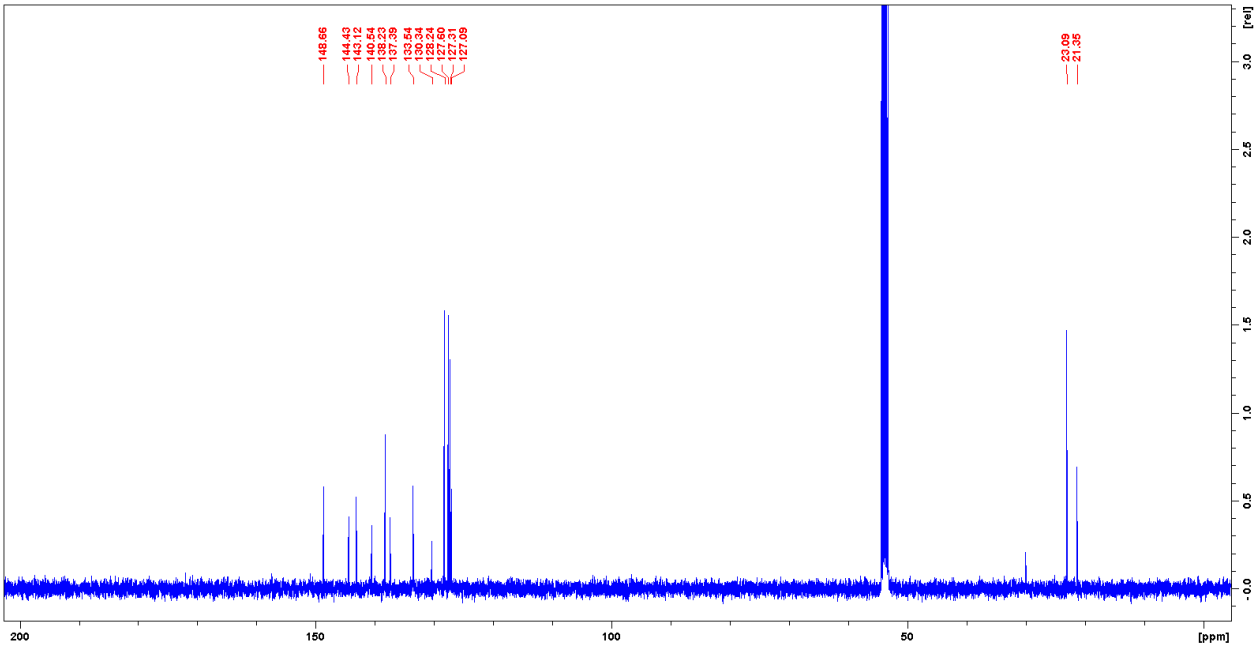

Figure S30. $^{13}C\{^{1}H\}$ NMR spectrum of 1,6-dimesityl-2,7-diphenyl-1,6-diborapyrene (**7**) (100 MHz, CD_2Cl_2, 298 K).

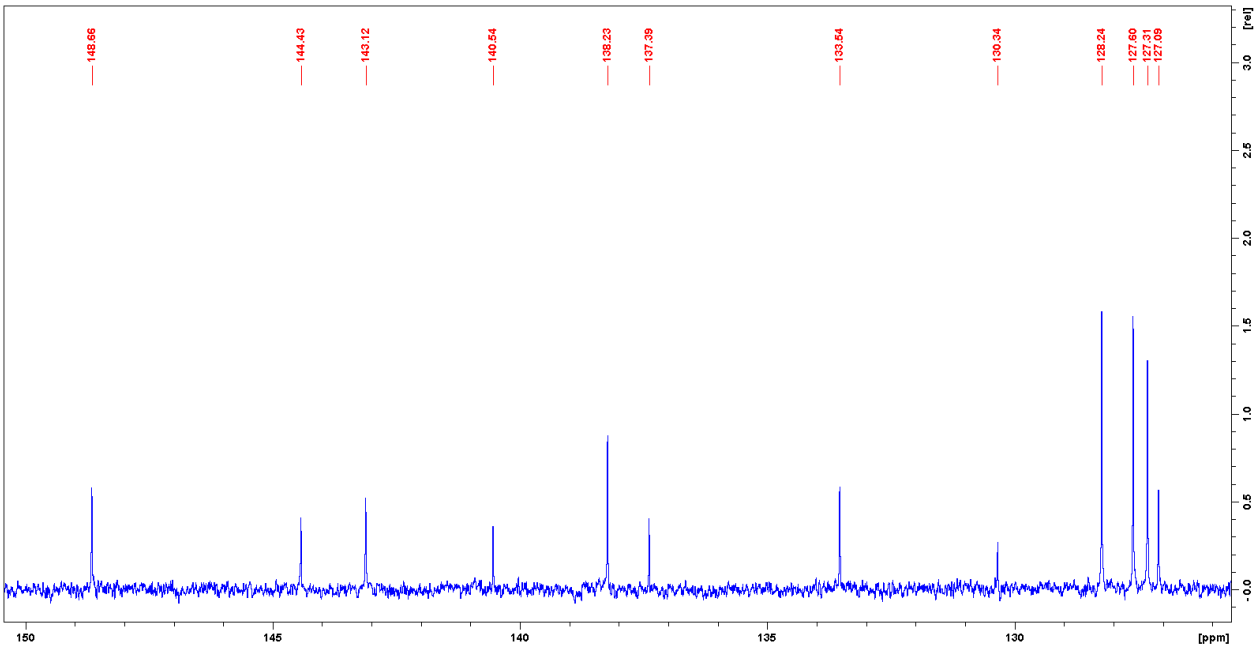

Figure S31. Magnified aromatic region of the $^{13}C\{^{1}H\}$ NMR spectrum of 1,6-dimesityl-2,7-diphenyl-1,6-diborapyrene (**7**) (100 MHz, CD_2Cl_2, 298 K). (7)

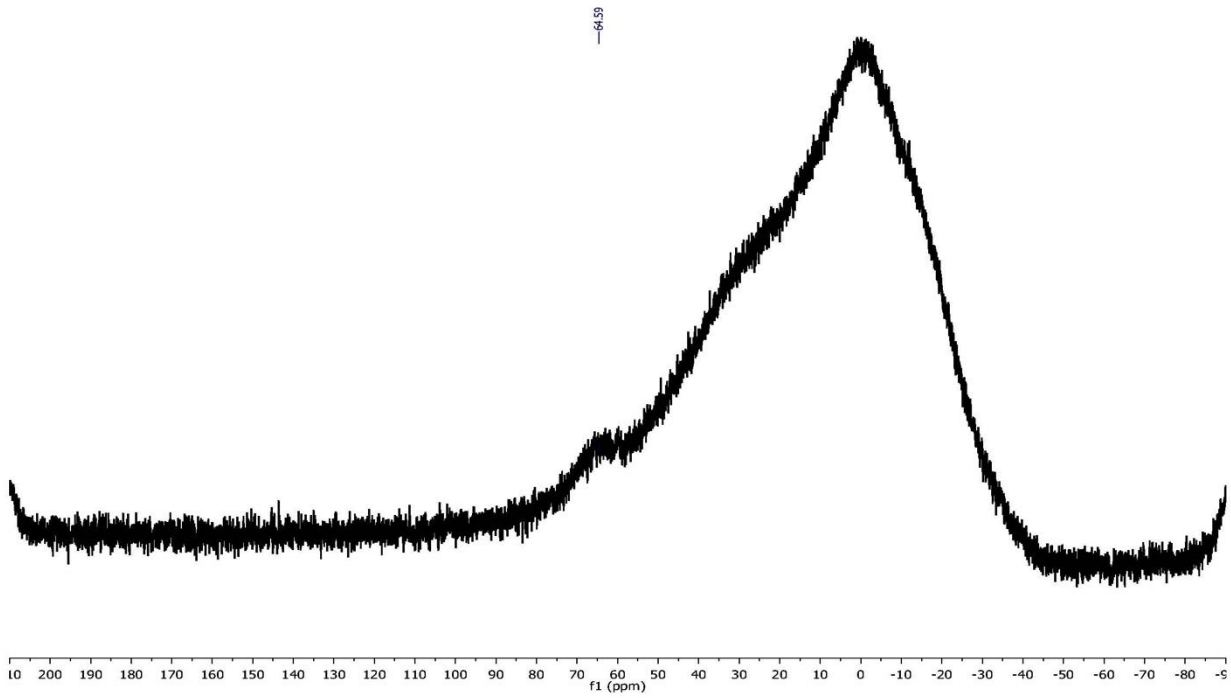

Figure S32. ^{11}B NMR spectrum of 1,6-dimesityl-2,7-diphenyl-1,6-diborapyrene (**7**) (128 MHz, CD_2Cl_2, 298 K).

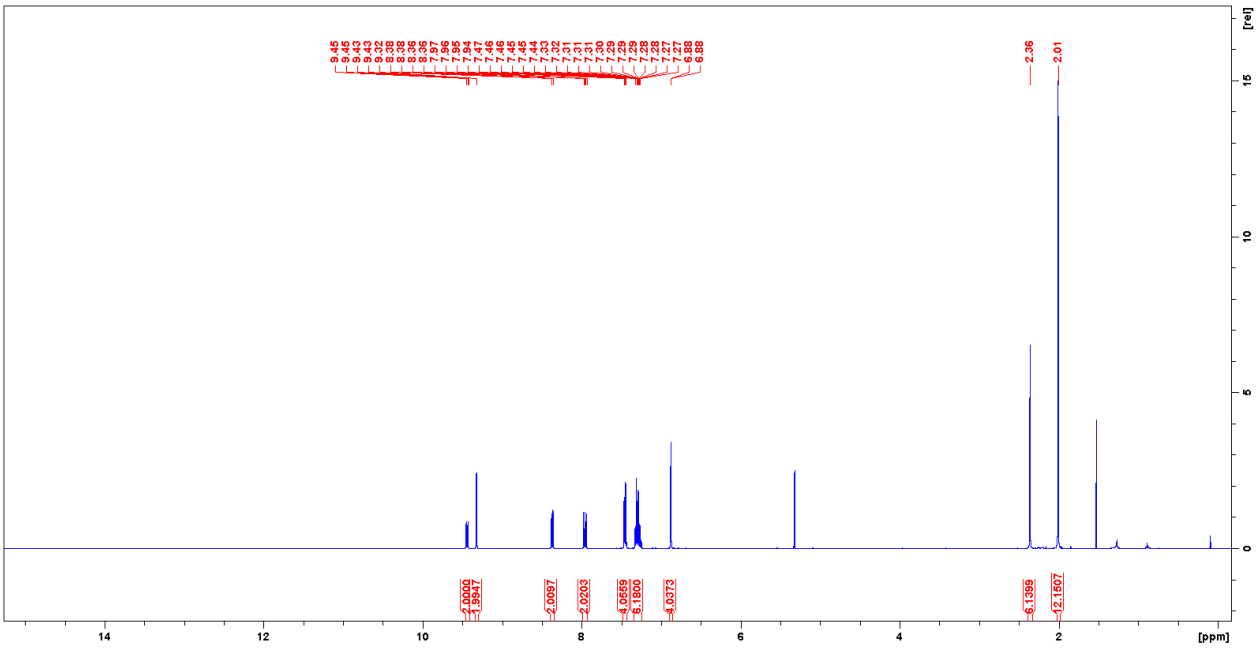

Figure S33. ^{1}H NMR spectrum of 3,9-dimesityl-2,8-diphenyl-3,9-diboraperylene (**8**) (400 MHz, CD_2Cl_2, 298 K).

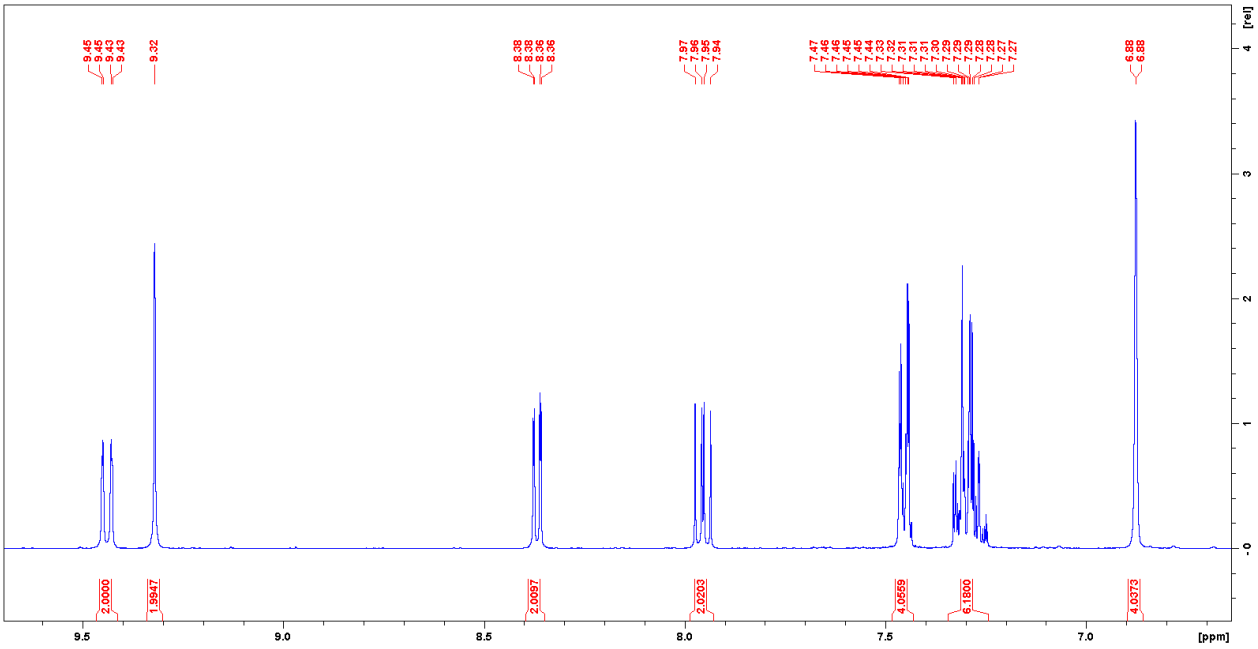

Figure S34. Magnified aromatic region of the ^{1}H NMR spectrum of 3,9-dimesityl-2,8-diphenyl-3,9-diboraperylene (**8**) (400 MHz, CD_2Cl_2, 298 K).

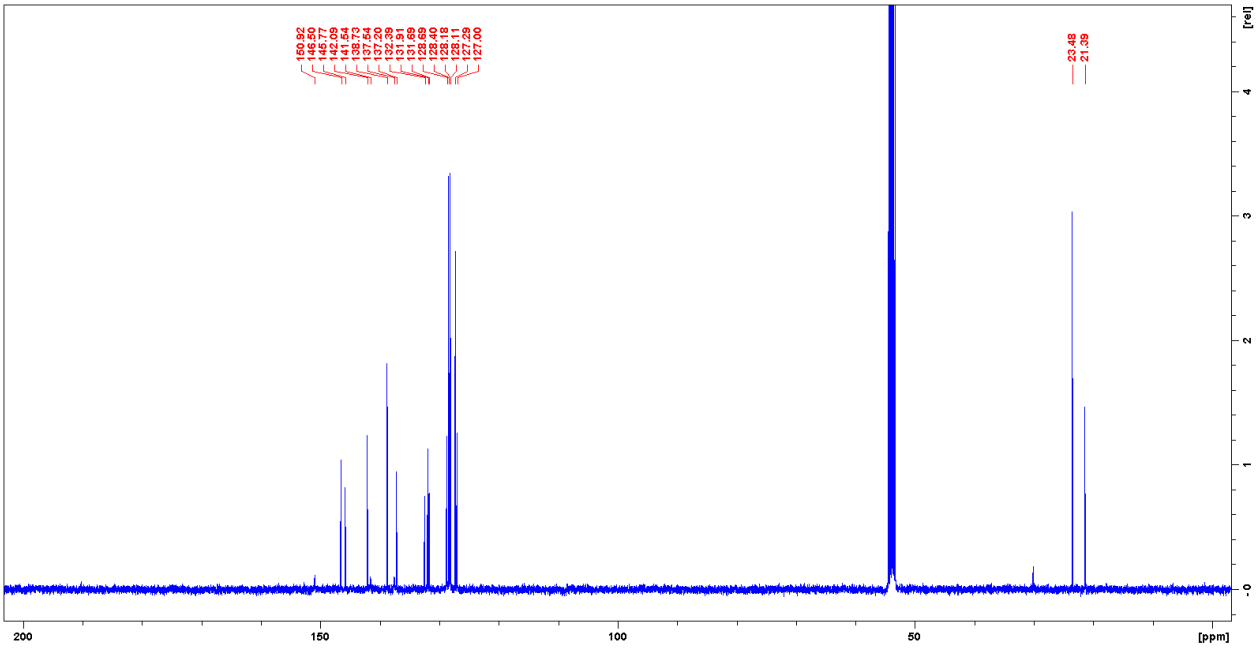

Figure S35. ^{13}C{^{1}H} NMR spectrum of 3,9-dimesityl-2,8-diphenyl-3,9-diboraperylene (**8**) (100 MHz, CD_2Cl_2, 298 K).

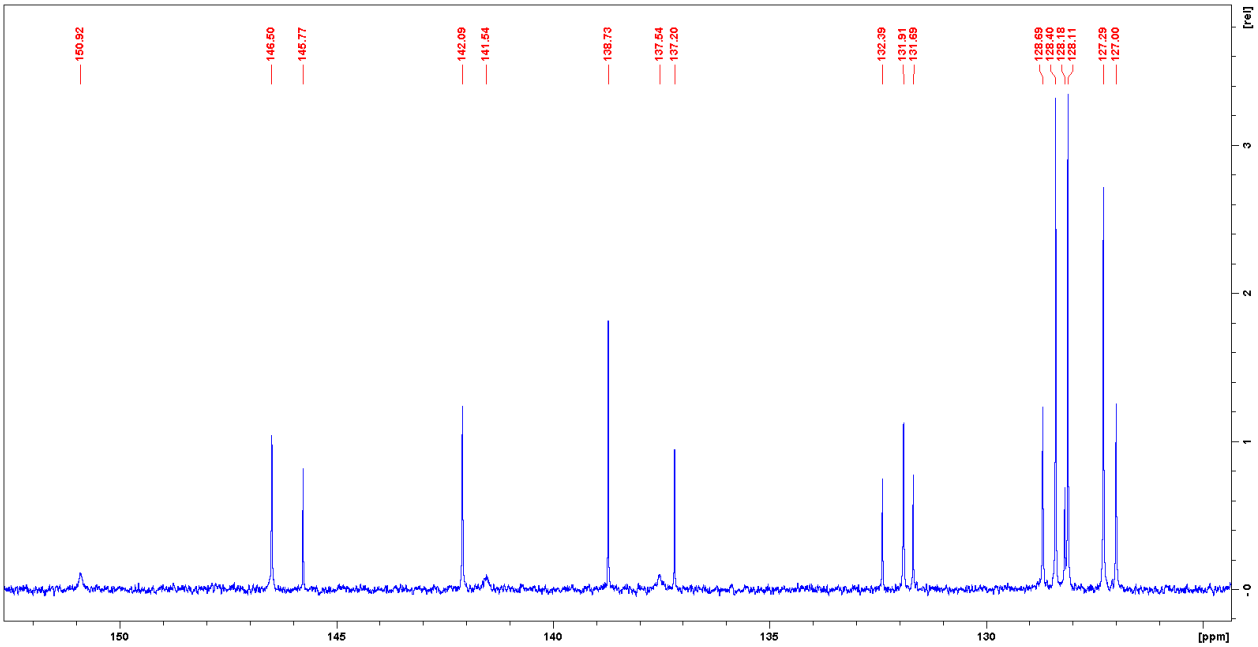

Figure S36. Magnified aromatic region of the $^{13}C\{^{1}H\}$ NMR spectrum of 3,9-dimesityl-2,8-diphenyl-3,9-diboraperylene (**8**) (100 MHz, CD_2Cl_2, 298 K).

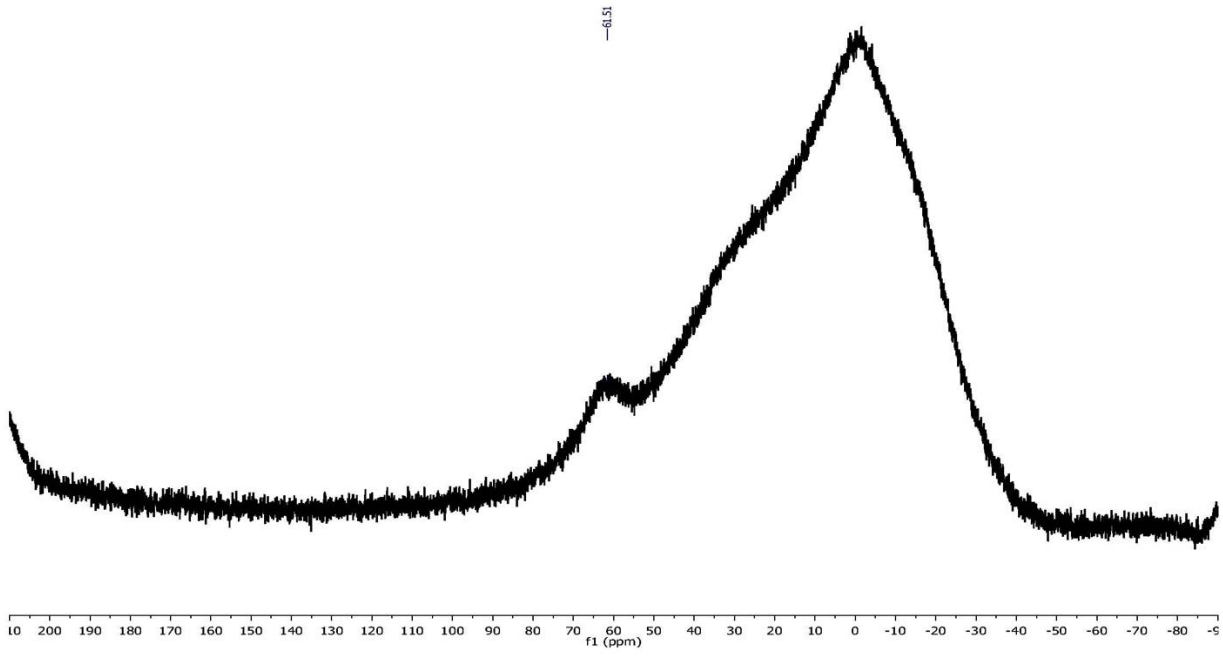

Figure S37. ^{11}B NMR spectrum of 3,9-dimesityl-2,8-diphenyl-3,9-diboraperylene (**8**) (128 MHz, CD_2Cl_2, 298 K).

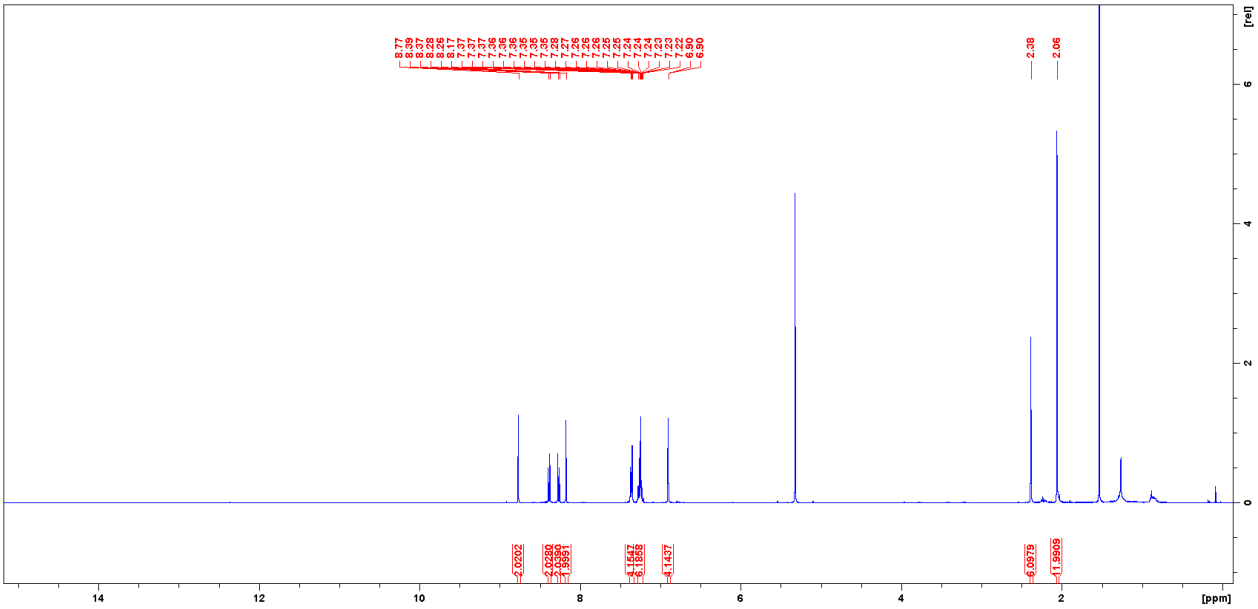

Figure S38. ^{1}H NMR spectrum of 1,7-dimesityl-2,8-diphenyl-1,7-diboraanthanthrene (**9**) (400 MHz, CD_2Cl_2, 298 K).

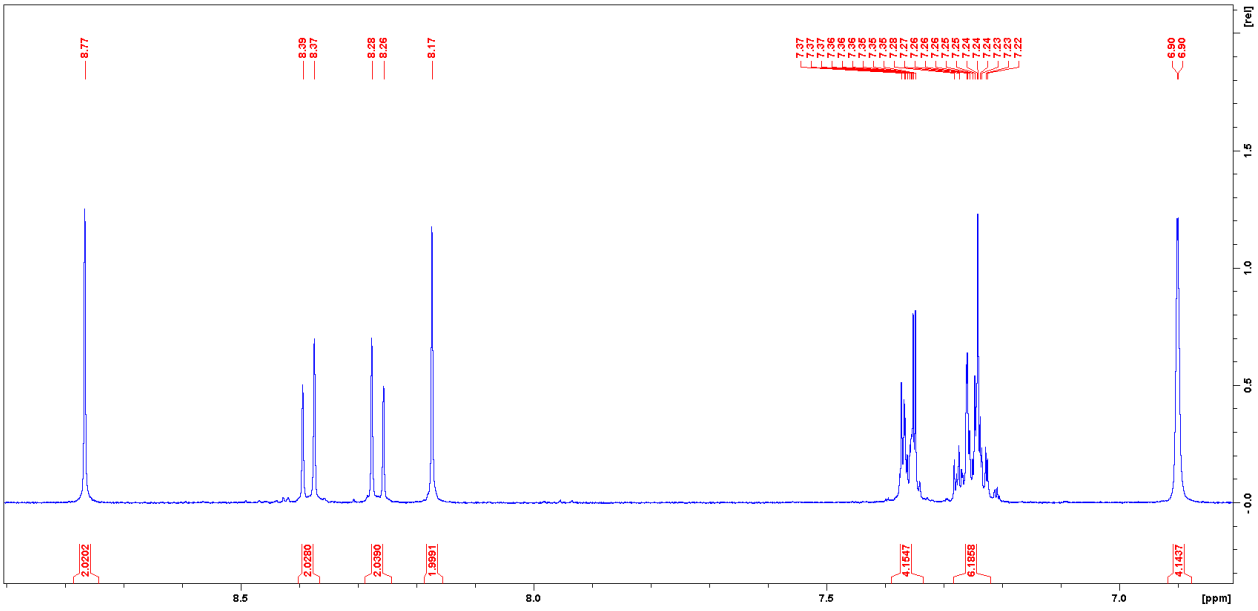

Figure S39. Magnified aromatic region of the ^{1}H NMR spectrum of 1,7-dimesityl-2,8-diphenyl-1,7-diboraanthanthrene (**9**) (400 MHz, CD_2Cl_2, 298 K).

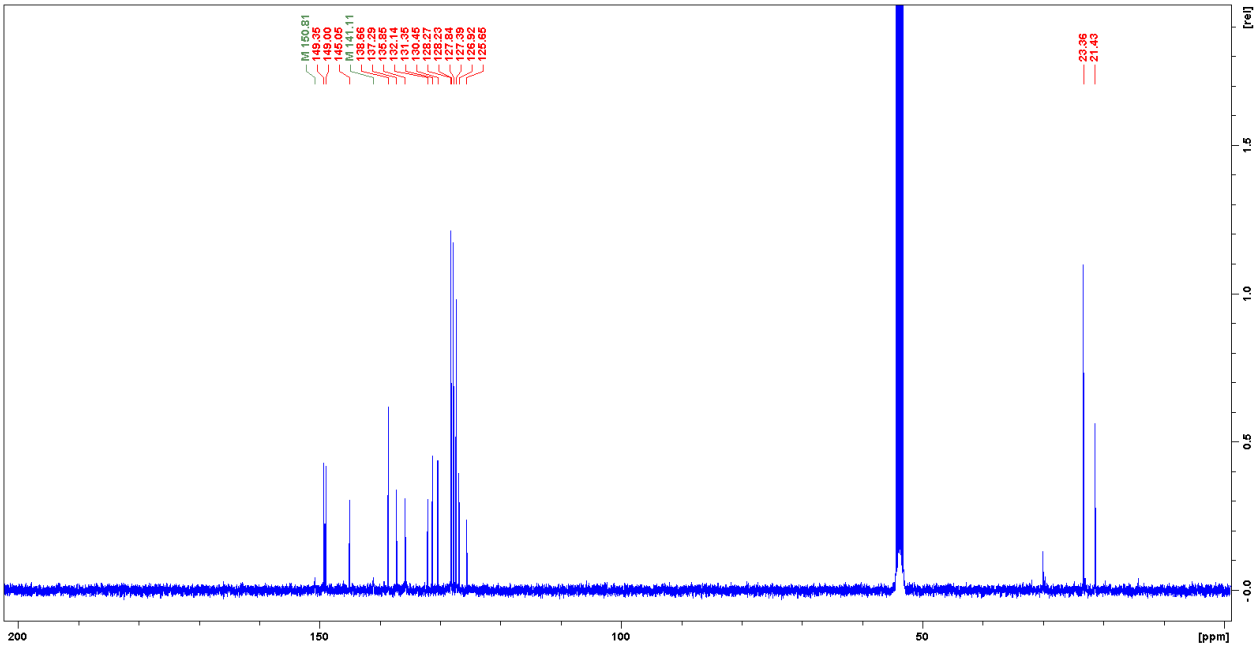

Figure S40. $^{13}C\{^{1}H\}$ NMR spectrum of 1,7-dimesityl-2,8-diphenyl-1,7-diboraanthanthrene (**9**) (100 MHz, CD_2Cl_2, 298 K).

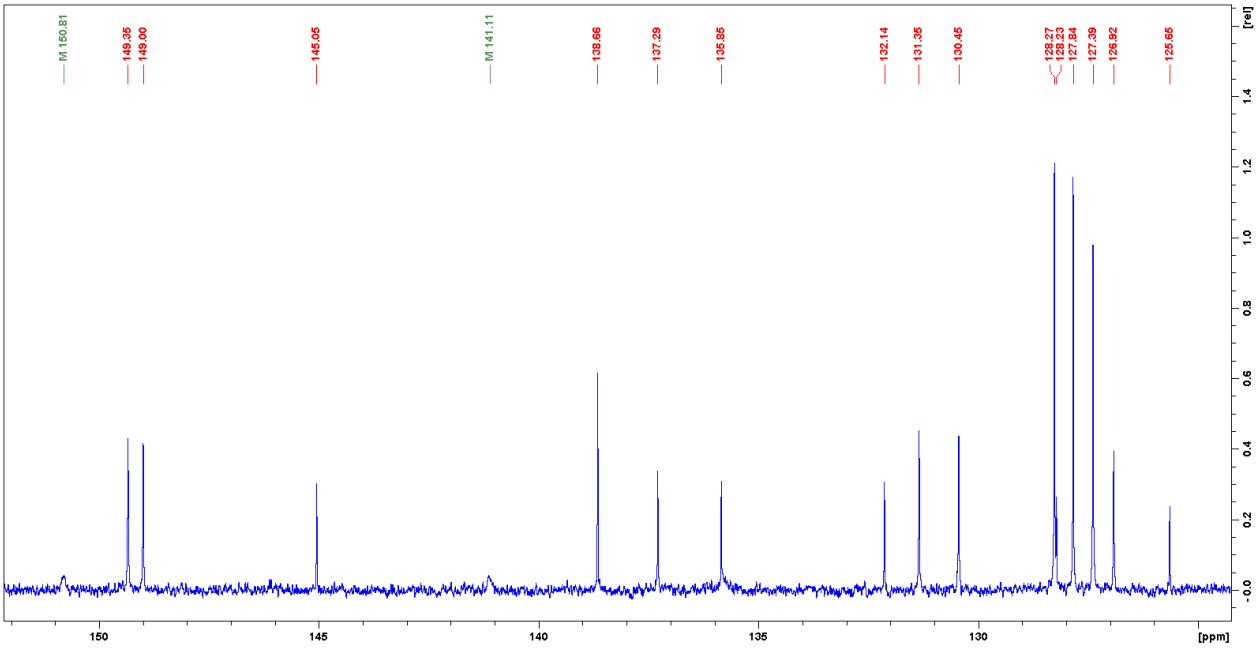

Figure S41. Magnified aromatic region of the $^{13}C\{^{1}H\}$ NMR spectrum of 1,7-dimesityl-2,8-diphenyl-1,7-diboraanthanthrene (**9**) (100 MHz, CD_2Cl_2, 298 K).

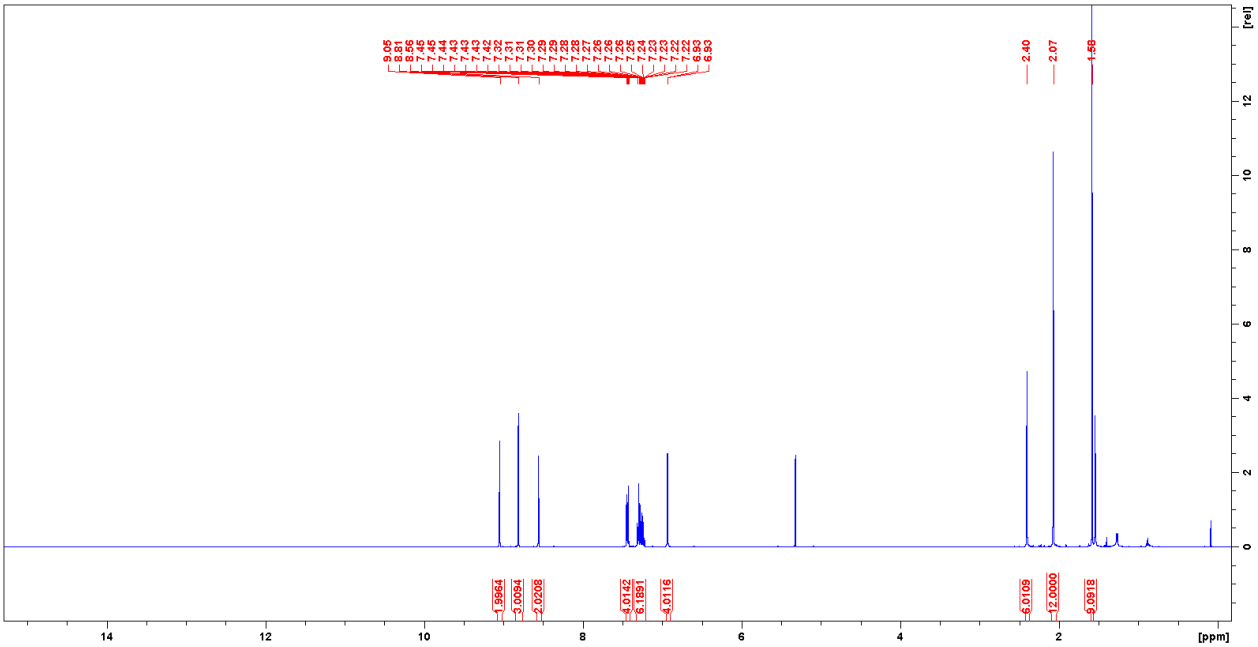

Figure S42. ^{1}H NMR spectrum 11-*tert*-butyl-2,8-dimesityl-3,7-diphenyl-2,8-diboratriangulene (**10**) (400 MHz, CD_2Cl_2, 298 K).

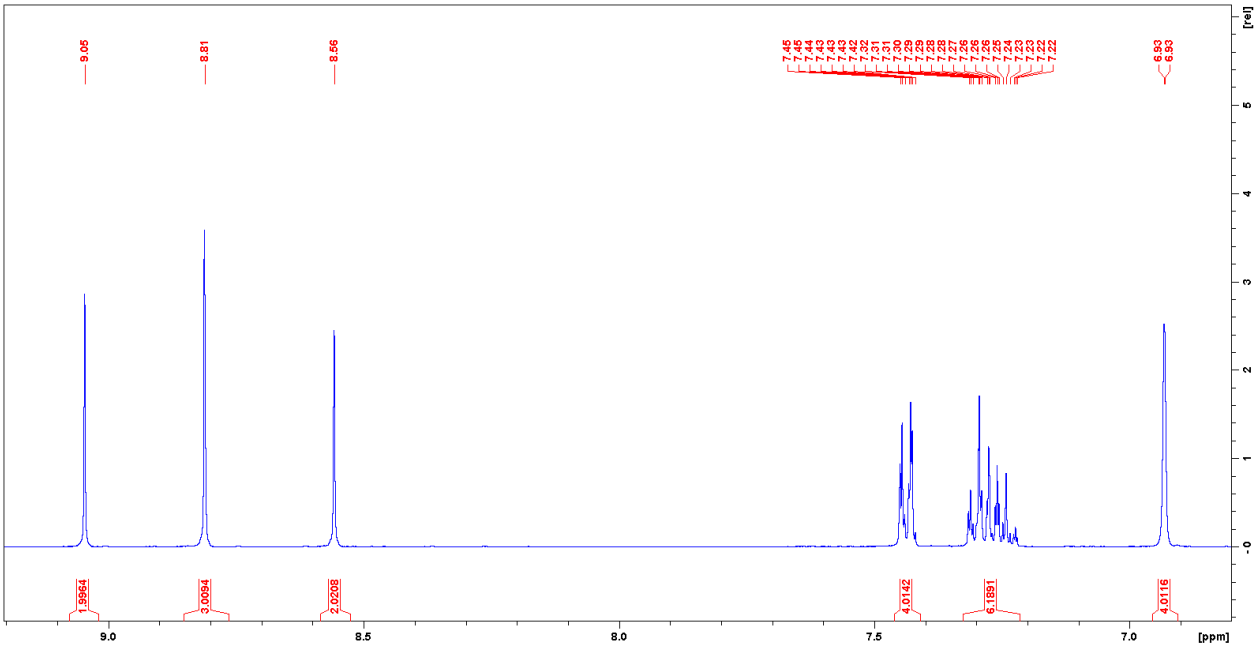

Figure S43. Magnified aromatic region of the ^{1}H NMR spectrum of 11-*tert*-butyl-2,8-dimesityl-3,7-diphenyl-2,8-diboratriangulene (**10**) (400 MHz, CD_2Cl_2, 298 K).

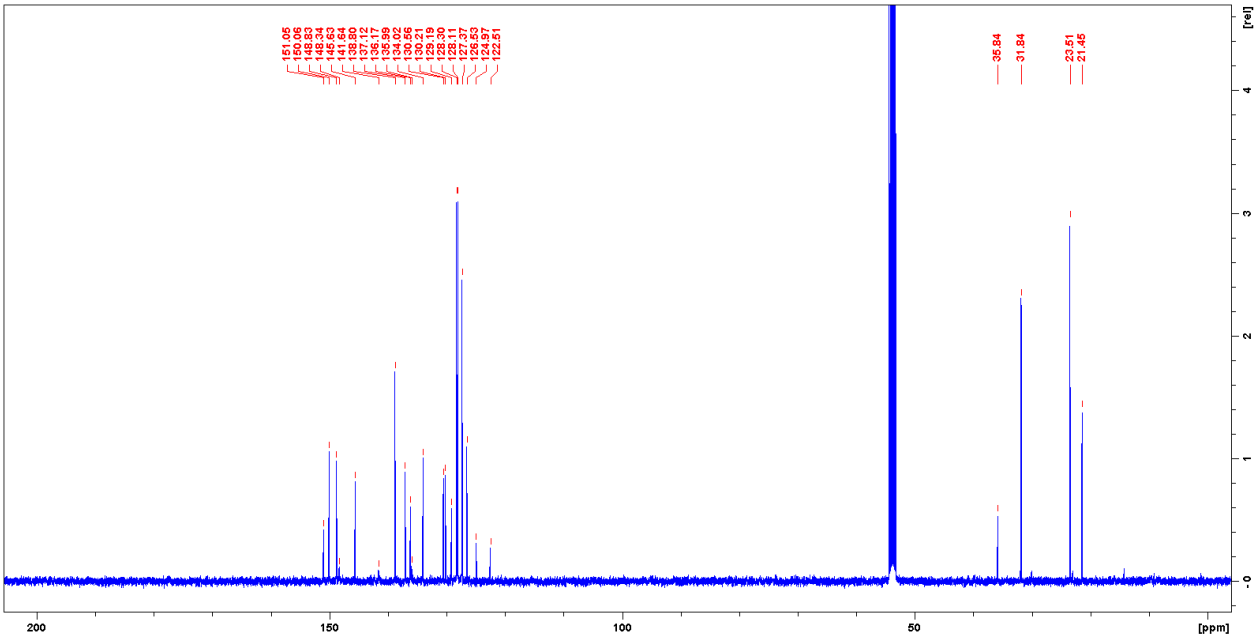

Figure S44. $^{13}C\{^{1}H\}$ NMR spectrum of 11-*tert*-butyl-2,8-dimesityl-3,7-diphenyl-2,8-diboratriangulene (**10**) (100 MHz, CD_2Cl_2, 298 K).

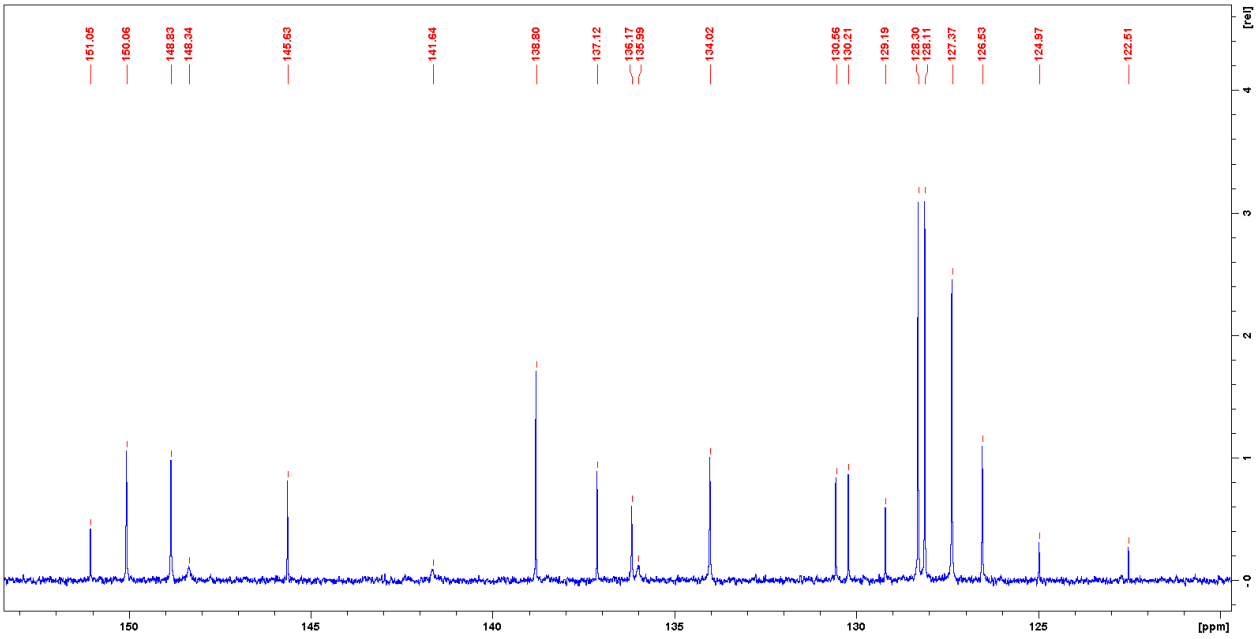

Figure S45. Magnified aromatic region of the $^{13}C\{^{1}H\}$ NMR spectrum of 11-*tert*-butyl-2,8-dimesityl-3,7-diphenyl-2,8-diboratriangulene (**10**) (100 MHz, CD_2Cl_2, 298 K).

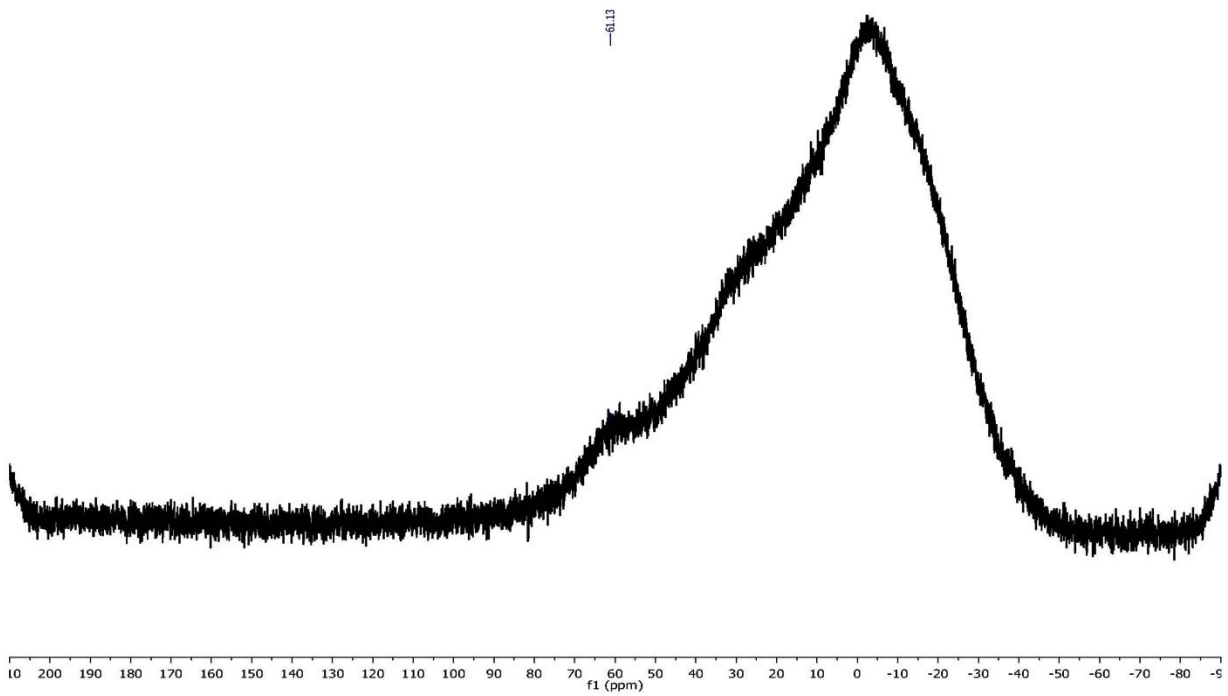

Figure S46. ^{11}B NMR spectrum of 11-*tert*-butyl-2,8-dimesityl-3,7-diphenyl-2,8-diboratriangulene (**10**) (128 MHz, CD_2Cl_2, 298 K).

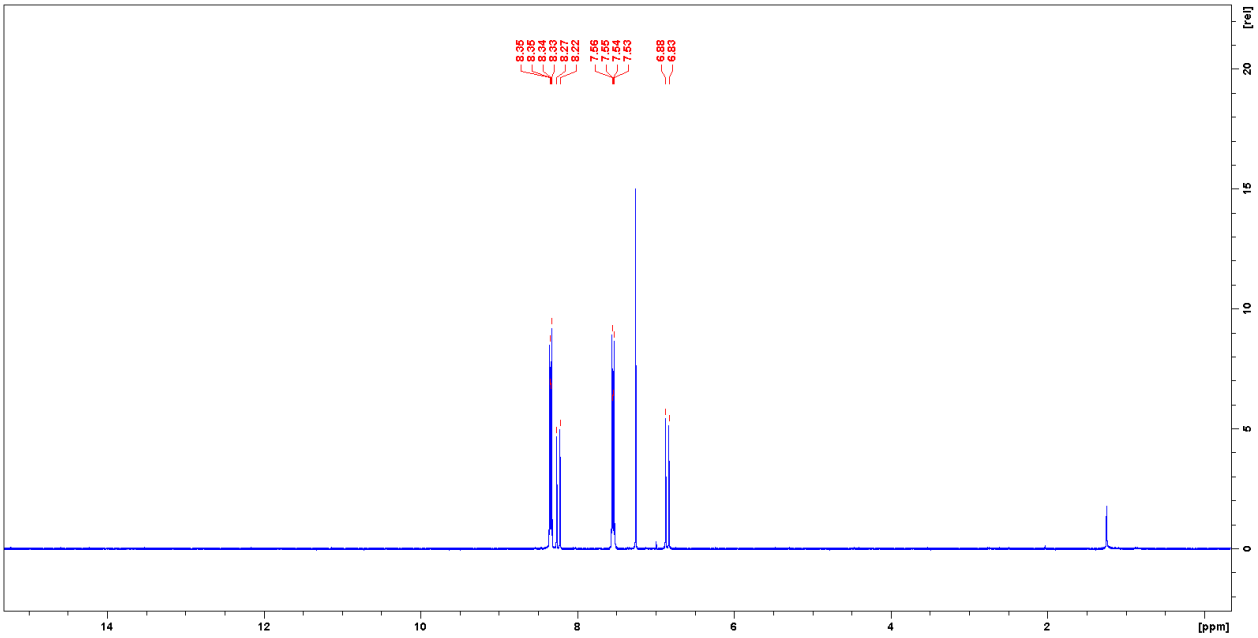

Figure S47. ^{1}H NMR spectrum of 9,10-bis(2,3,4,5,6-pentafluorostyryl)anthracene (400 MHz, $CDCl_3$, 298 K).

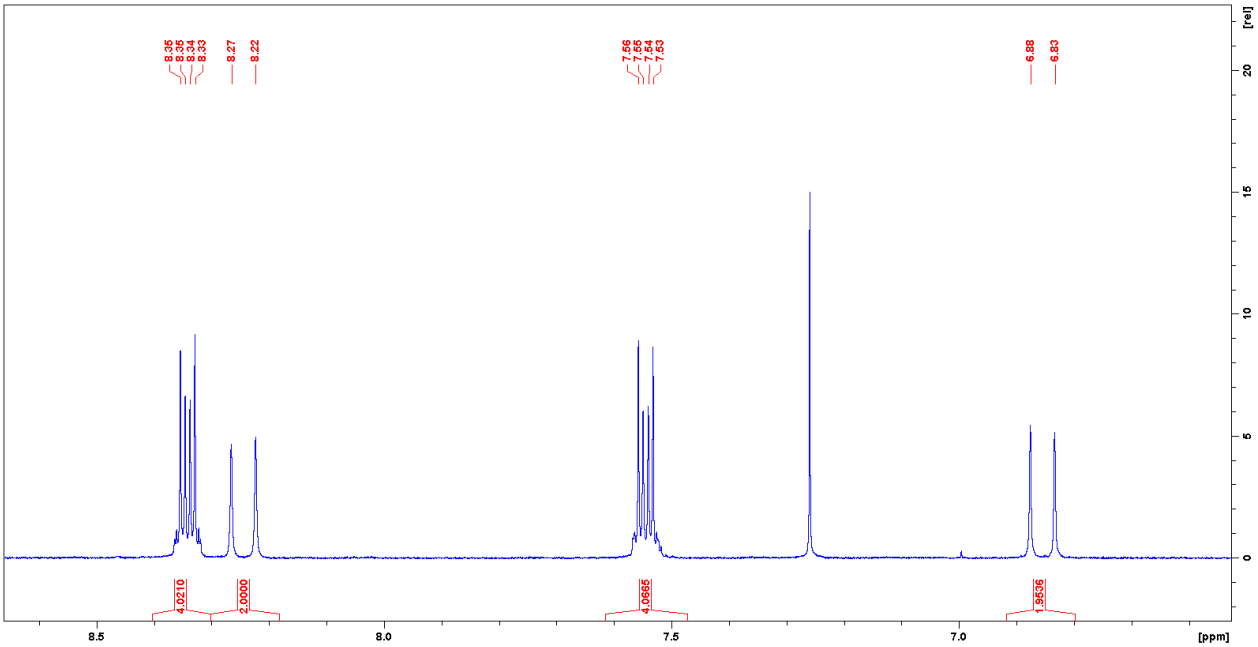

Figure S48. Magnified aromatic region of the ^{1}H NMR spectrum of 9,10-bis(2,3,4,5,6-pentafluorostyryl)anthracene (400 MHz, $CDCl_3$, 298 K).

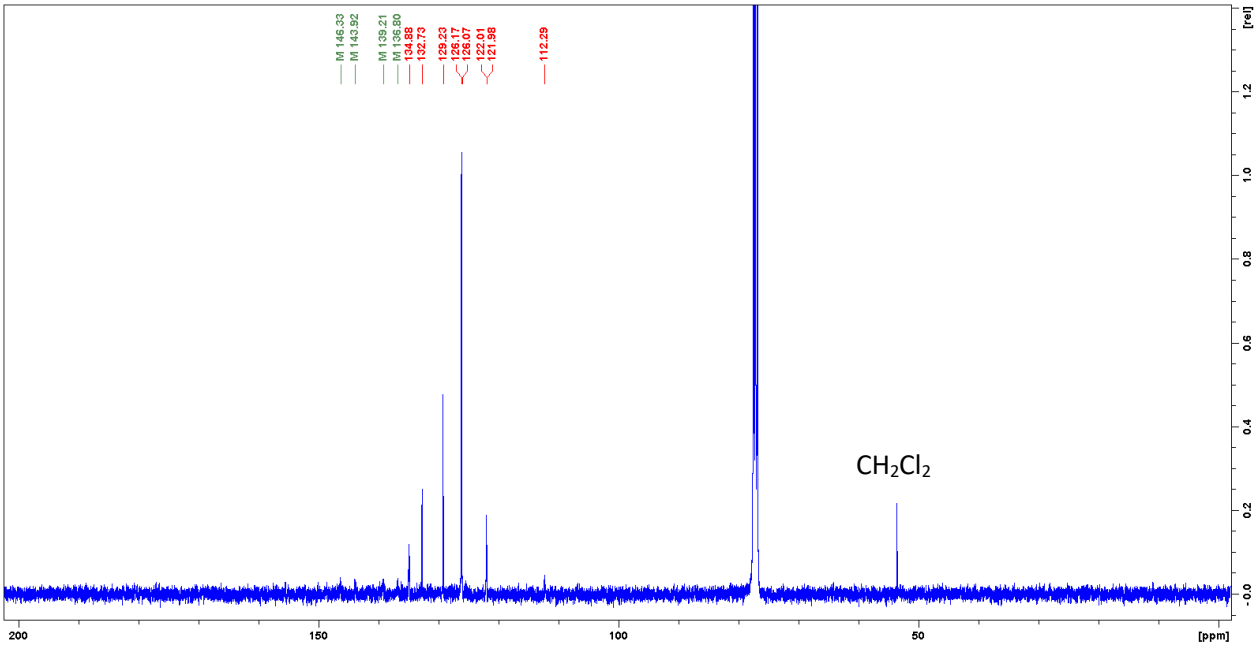

Figure S49. $^{13}C\{^{1}H\}$ NMR spectrum of 9,10-bis(2,3,4,5,6-pentafluorostyryl)anthracene (100 MHz, $CDCl_3$, 298 K).

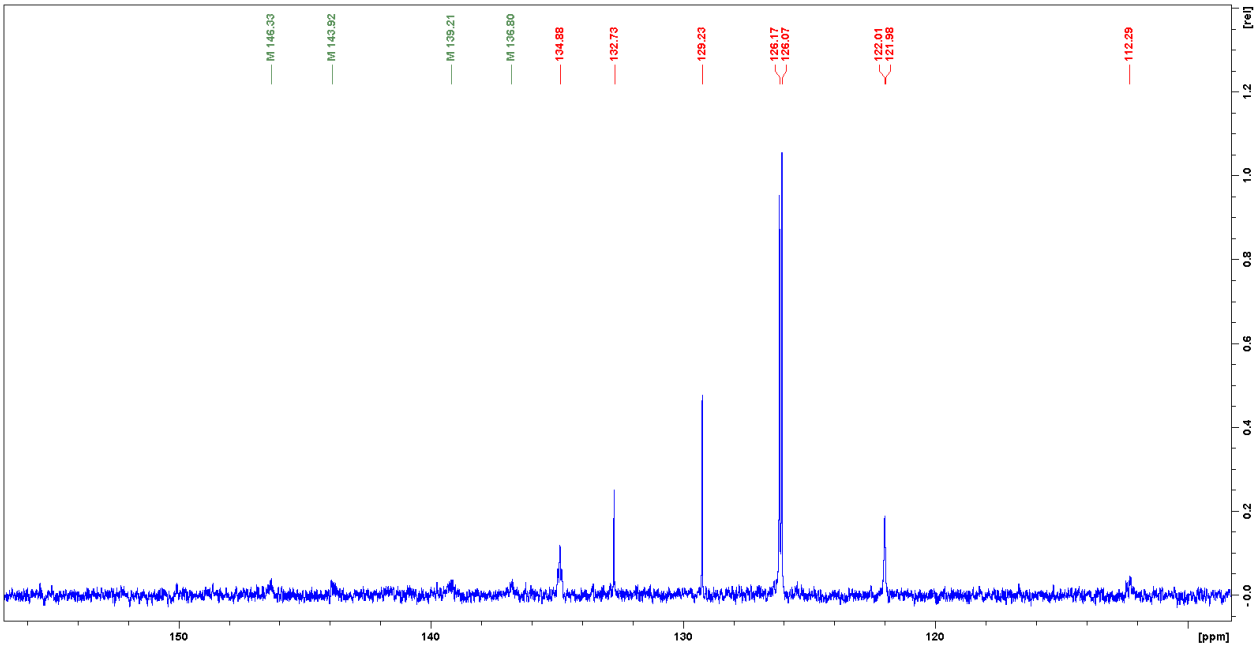

Figure S50. Magnified aromatic region of the $^{13}C\{^{1}H\}$ NMR spectrum of 9,10-bis(2,3,4,5,6-pentafluorostyryl)anthracene (100 MHz, $CDCl_3$, 298 K).

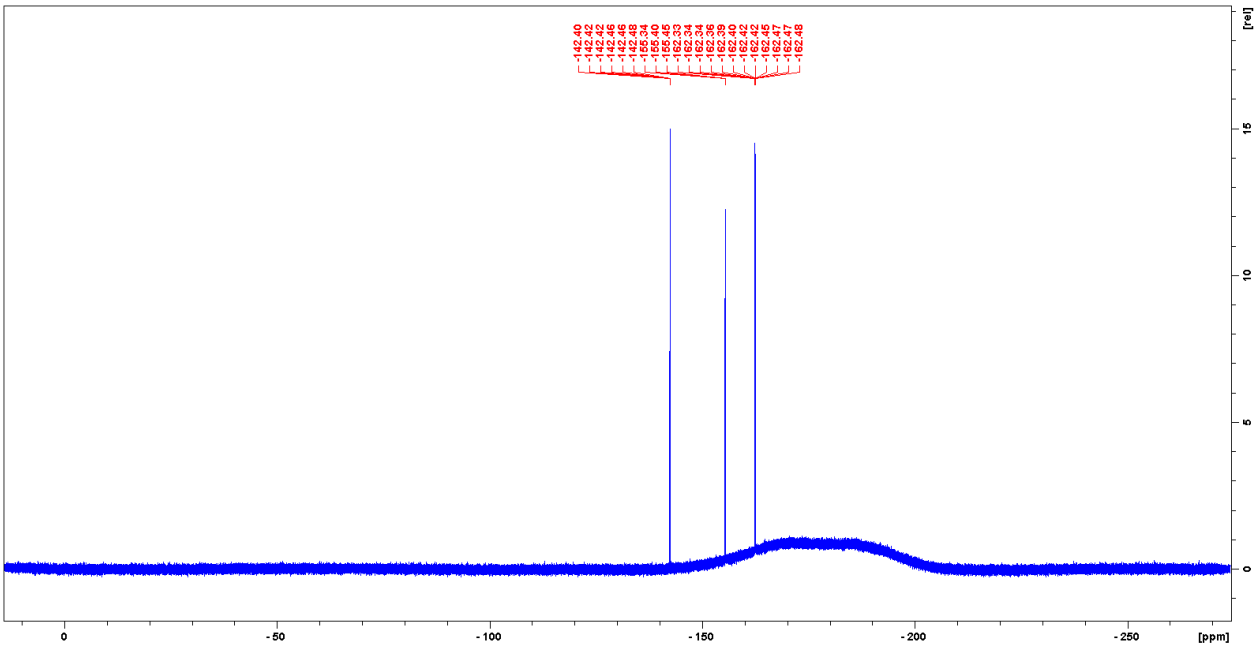

Figure S51. ^{19}F NMR spectrum of 9,10-bis(2,3,4,5,6-pentafluorostyryl)anthracene (376 MHz, $CDCl_3$, 298 K).

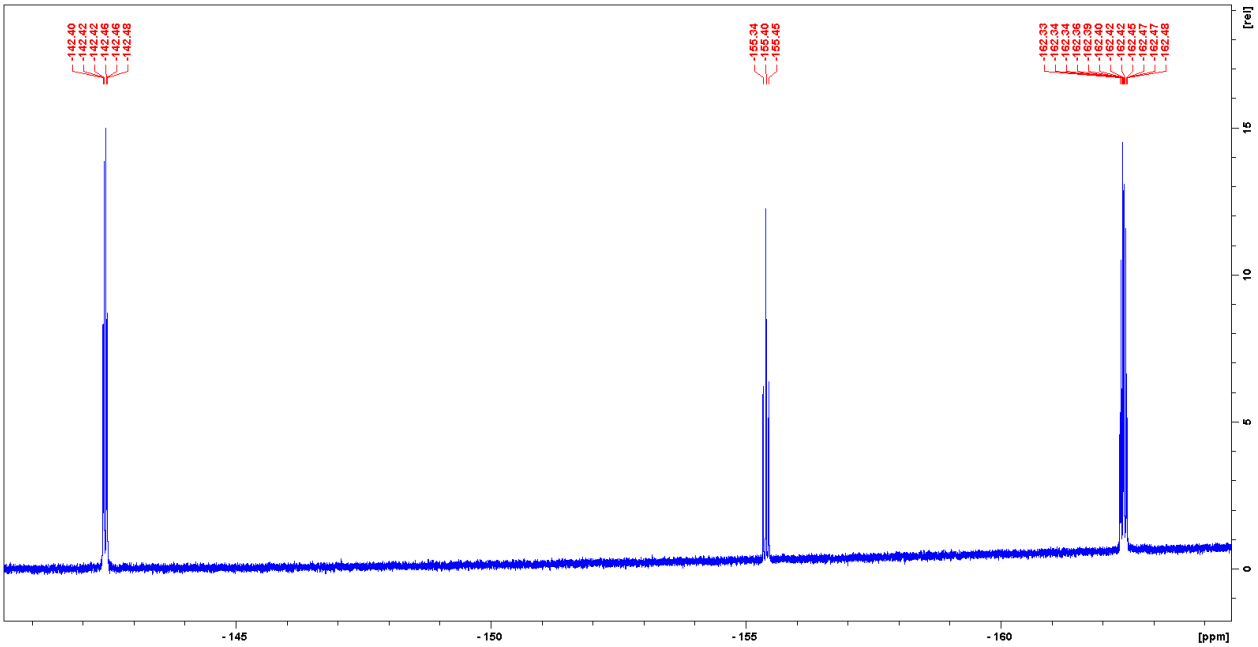

Figure S52. Expansion of the ^{19}F NMR spectrum of 9,10-bis(2,3,4,5,6-pentafluorostyryl)anthracene (376 MHz, $CDCl_3$, 298 K).

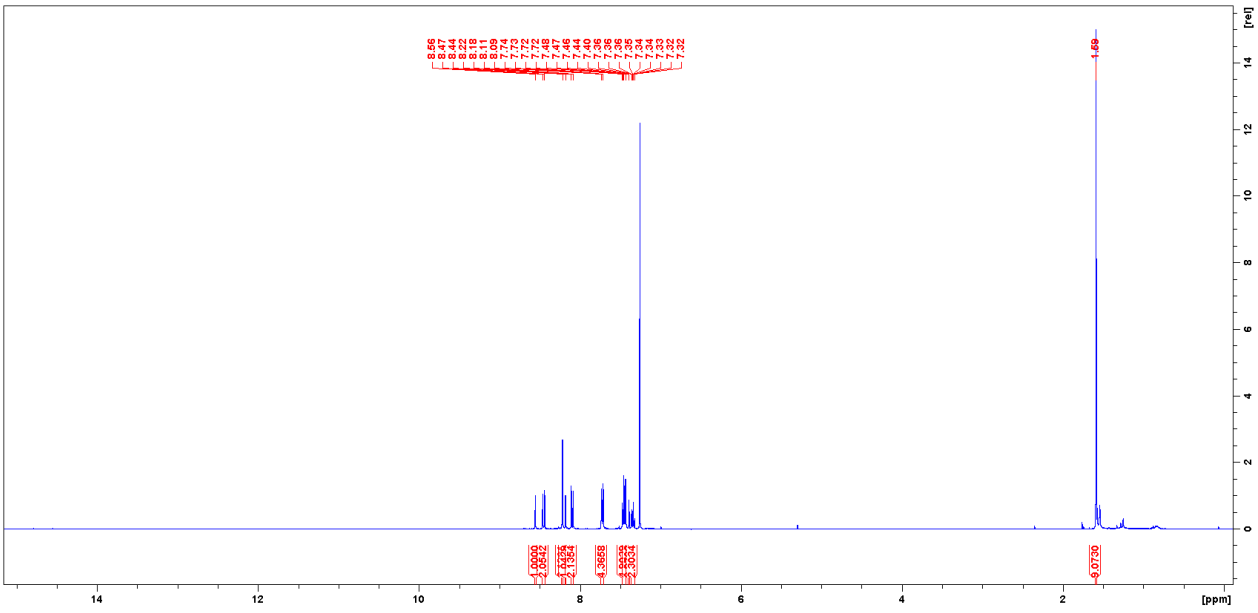

Figure S53. ^{1}H NMR spectrum of 7-(*t*-butyl)-1,3-distyrylpyrene (400 MHz, $CDCl_3$, 298 K).

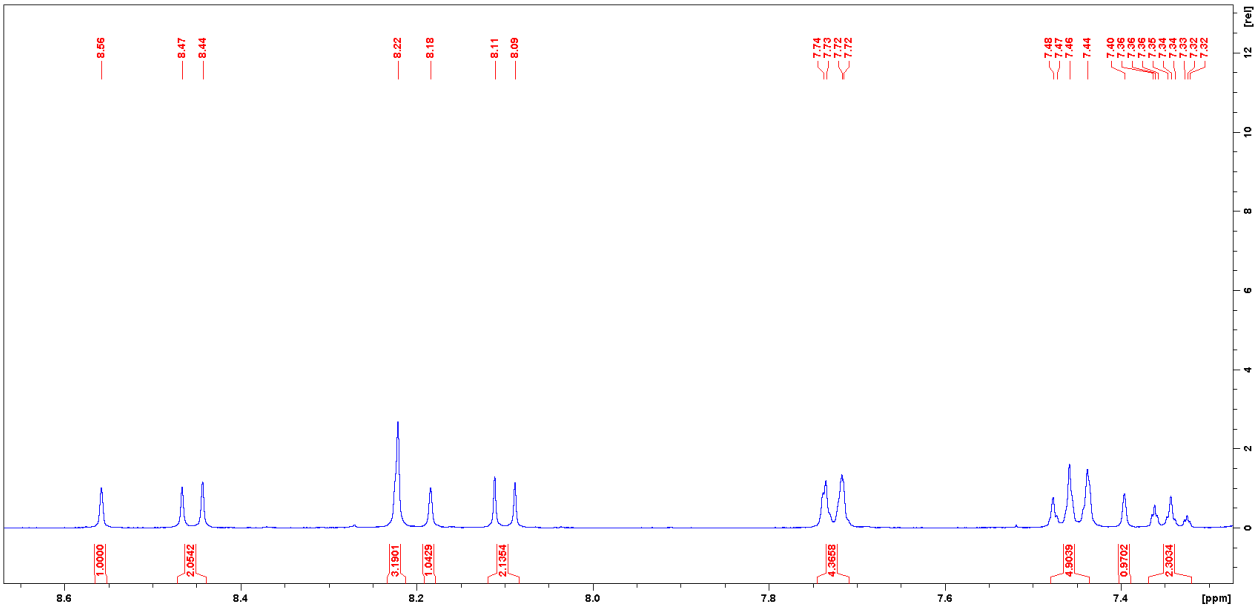

Figure S54. Magnified aromatic region of the ^{1}H NMR spectrum of 7-(*t*-butyl)-1,3-distyrylpyrene (400 MHz, $CDCl_3$, 298 K).

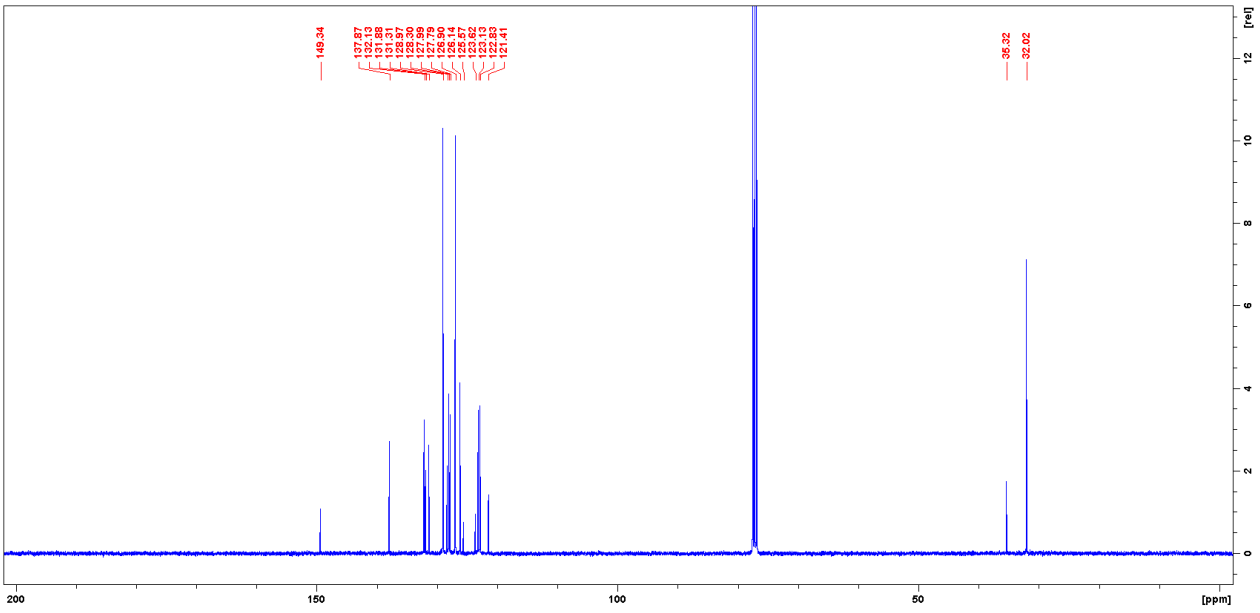

Figure S55. ^{13}C{^{1}H} NMR spectrum of 7-(*t*-butyl)-1,3-distyrylpyrene (100 MHz, $CDCl_3$, 298 K).

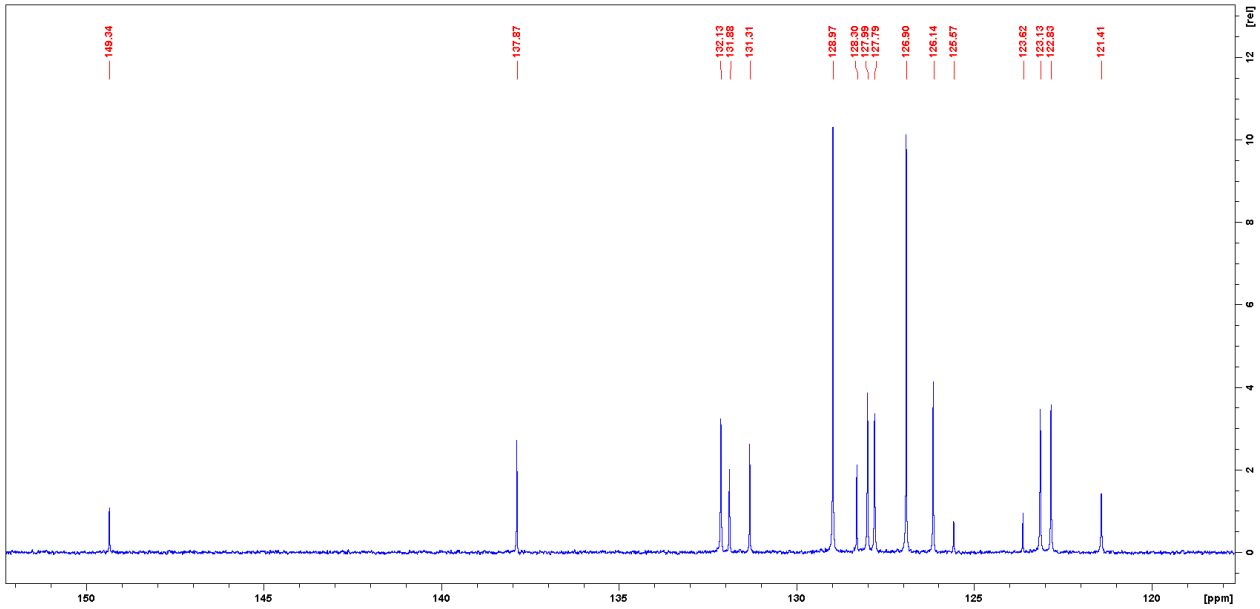

Figure S56. Magnified aromatic region of the $^{13}C\{^{1}H\}$ NMR spectrum of 7-(*t*-butyl)-1,3-distyrylpyrene (100 MHz, $CDCl_3$, 298 K).

4. Simulated and Measured HR-MS Spectra

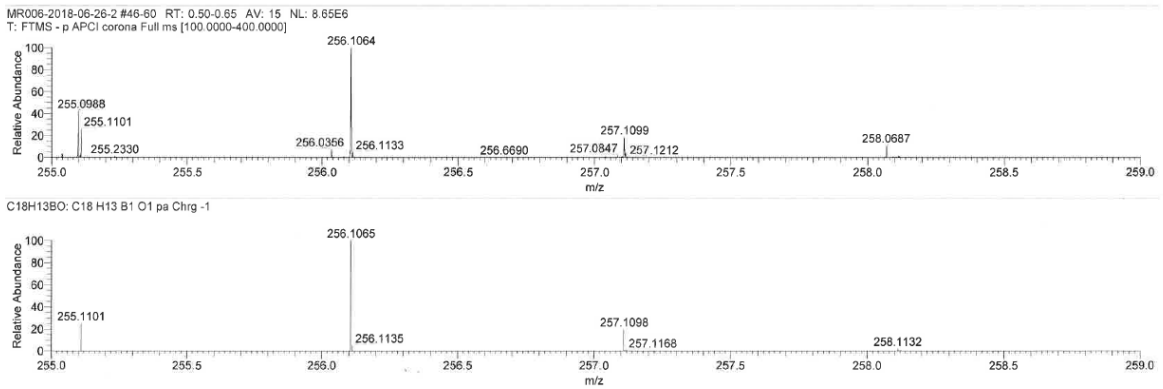

Figure S57. Simulated (bottom) and found (top) patterns of the high-resolution mass spectrum of **1** (ASAP, negative mode) *m/z*: $[M]^-$ Calc'd for $C_{18}H_{13}BO$.

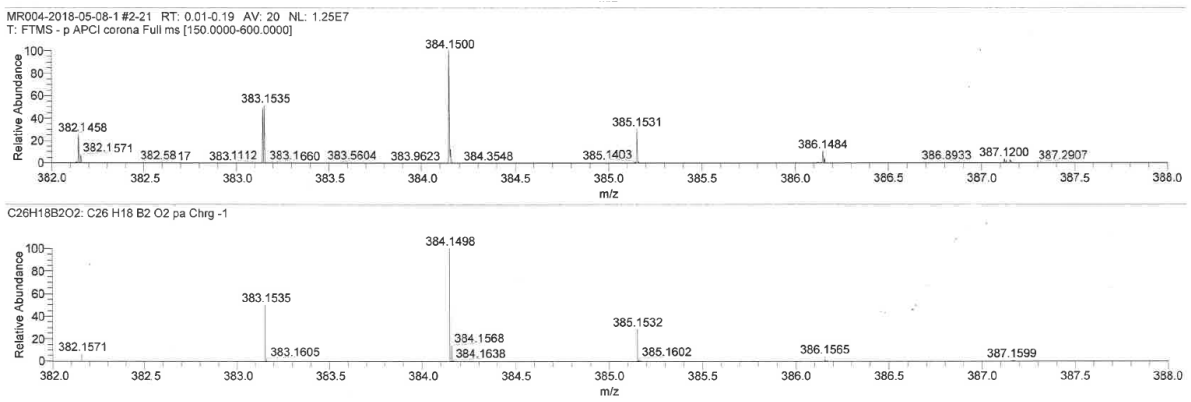

Figure S58. Simulated (bottom) and found (top) patterns of the high-resolution mass spectrum of **2** (ASAP, negative mode) *m/z*: $[M]^-$ Calc'd for $C_{26}H_{18}B_2O_2$.

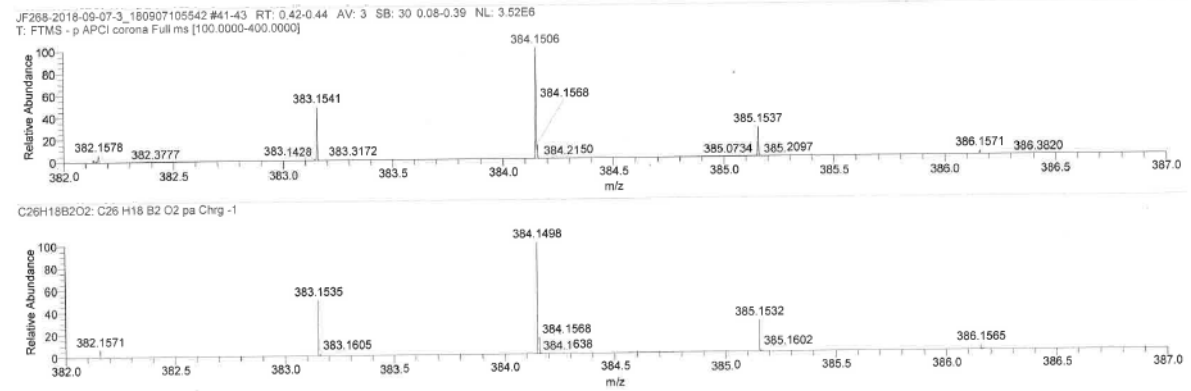

Figure S59. Simulated (bottom) and found (top) patterns of the high-resolution mass spectrum of **3** (ASAP, negative mode) *m/z*: $[M]^-$ Calc'd for $C_{26}H_{18}B_2O_2$.

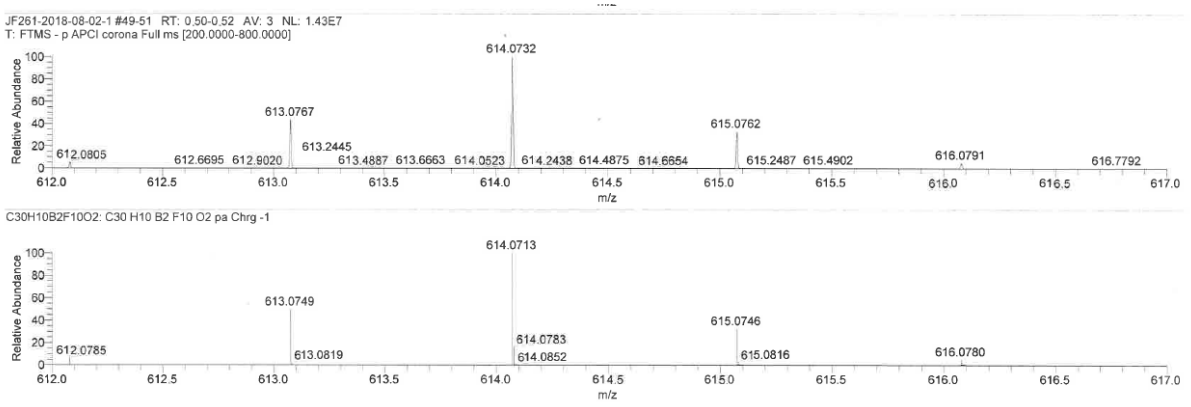

Figure S60. Simulated (bottom) and found (top) patterns of the high-resolution mass spectrum of **4b** (ASAP, negative mode) *m/z*: $[M]^-$ Calc'd for $C_{30}H_{10}B_2F_{10}O_2$.

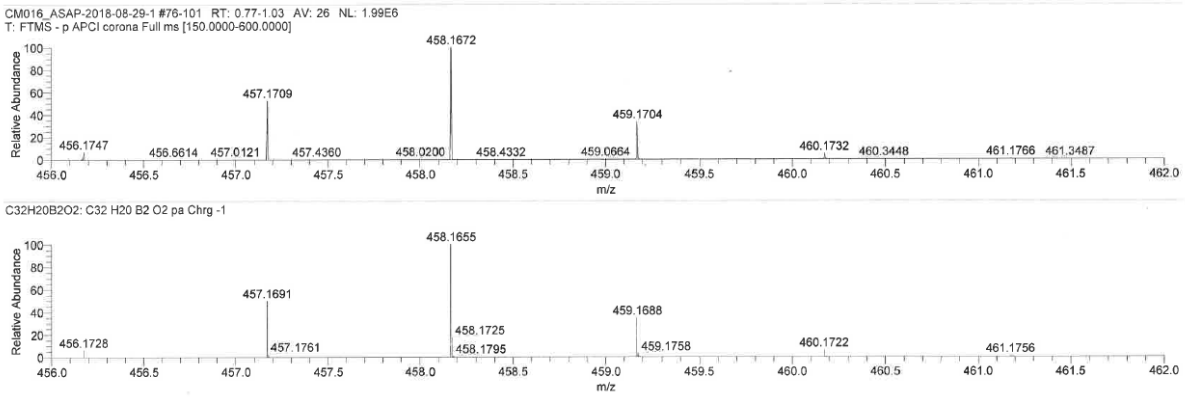

Figure S61. Simulated (bottom) and found (top) patterns of the high-resolution mass spectrum of **5** (ASAP, negative mode) *m/z*: $[M]^-$ Calc'd for $C_{32}H_{20}B_2O_2$.

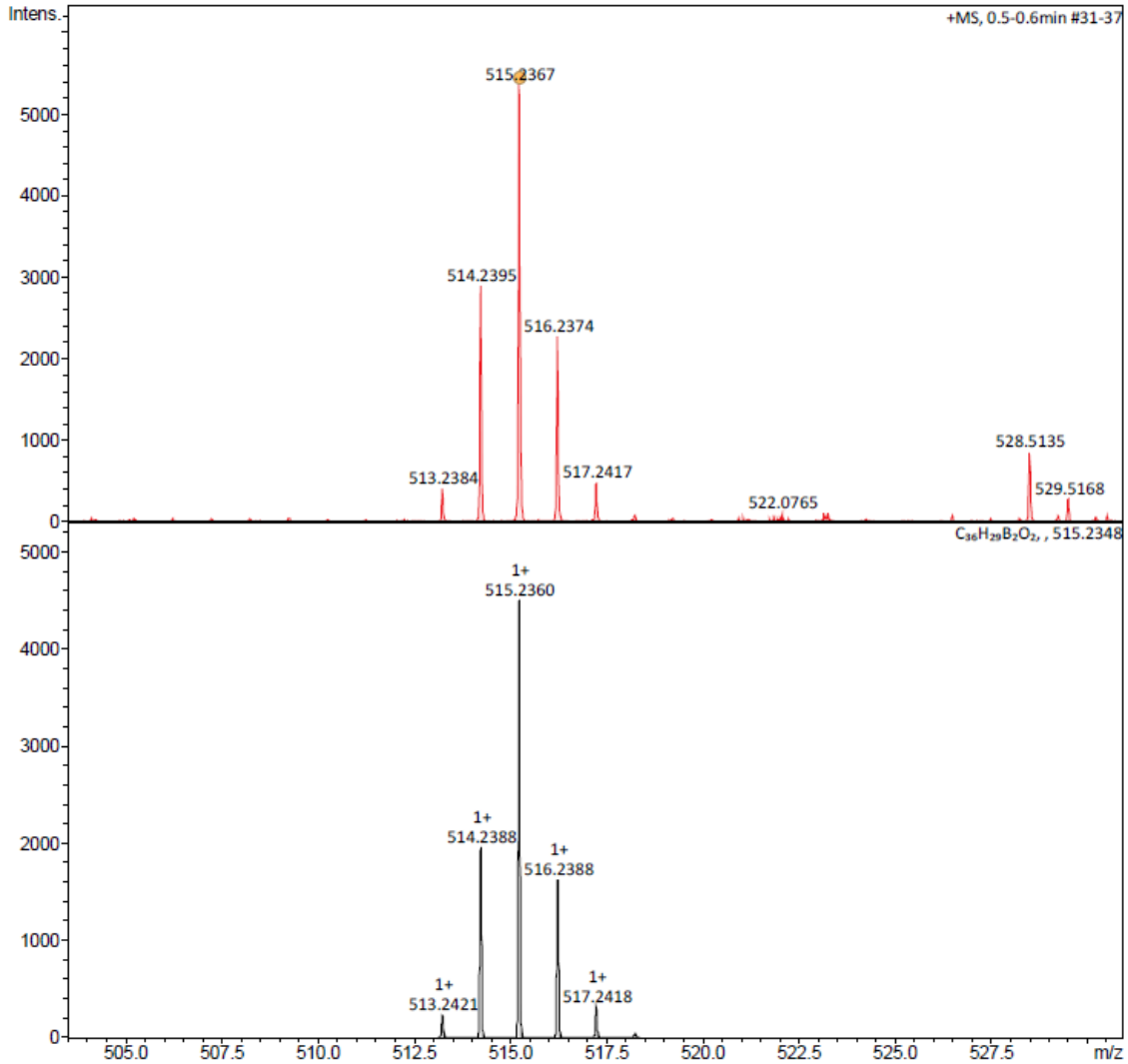

Figure S62. Simulated (bottom) and found (top) patterns of the high-resolution mass spectrum of **6** (ESI-TOF, positive mode) *m/z*: $[M+1]^+$ Calc'd for $C_{36}H_{29}B_2O_2$.

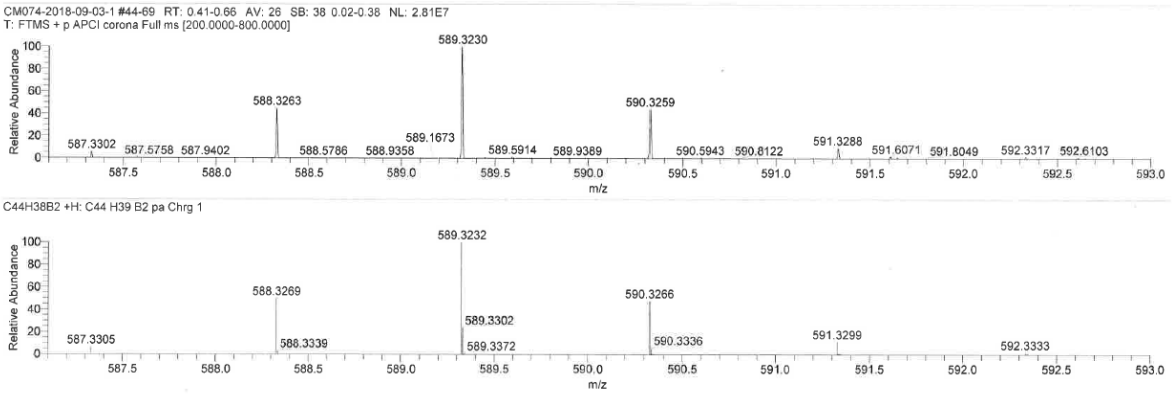

Figure S63. Simulated (bottom) and found (top) patterns of the high-resolution mass spectrum of **7** (ASAP, positive mode) *m/z*: $[M+1]^+$ Calc'd for $C_{44}H_{39}B_2$.

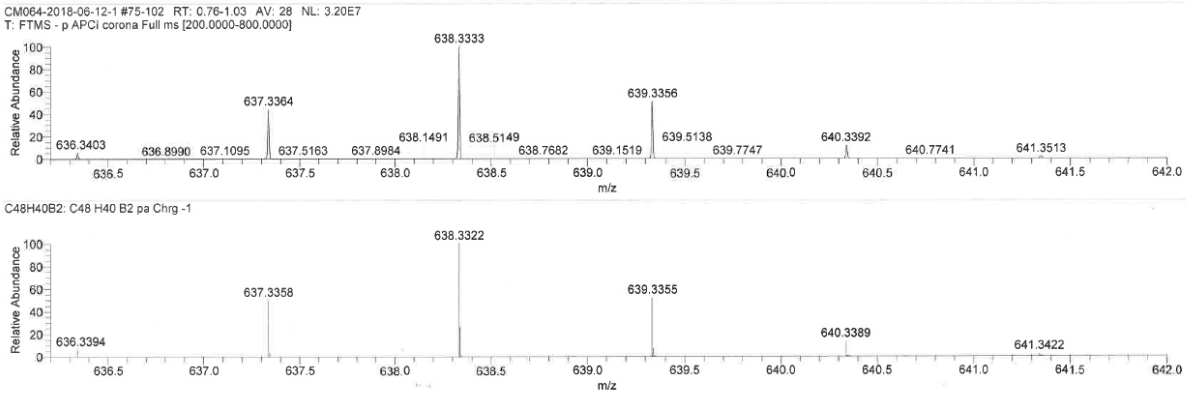

Figure S64. Simulated (bottom) and found (top) patterns of the high-resolution mass spectrum of **8** (ASAP, negative mode) *m/z*: $[M]^-$ Calc'd for $C_{48}H_{40}B_2$.

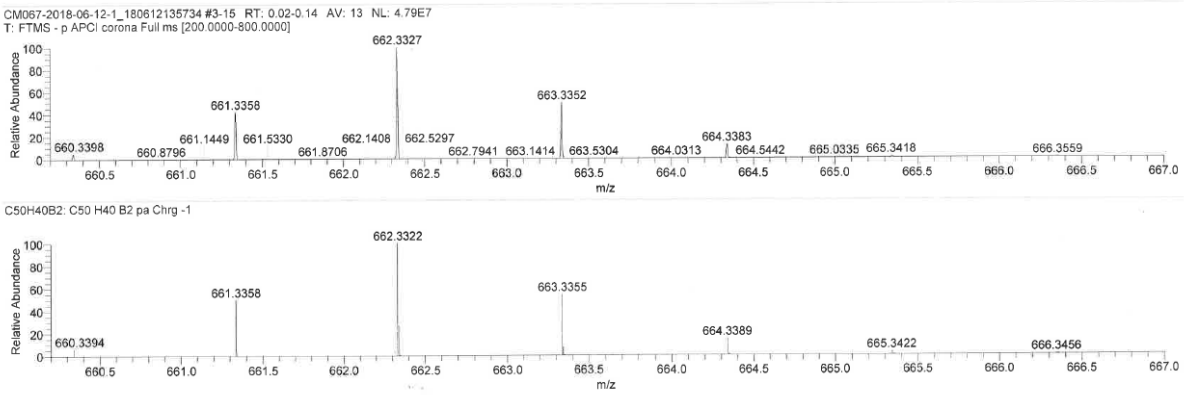

Figure S65. Simulated (bottom) and found (top) patterns of the high-resolution mass spectrum of **9** (ASAP, negative mode) *m/z*: $[M]^-$ Calc'd for $C_{50}H_{40}B_2$.

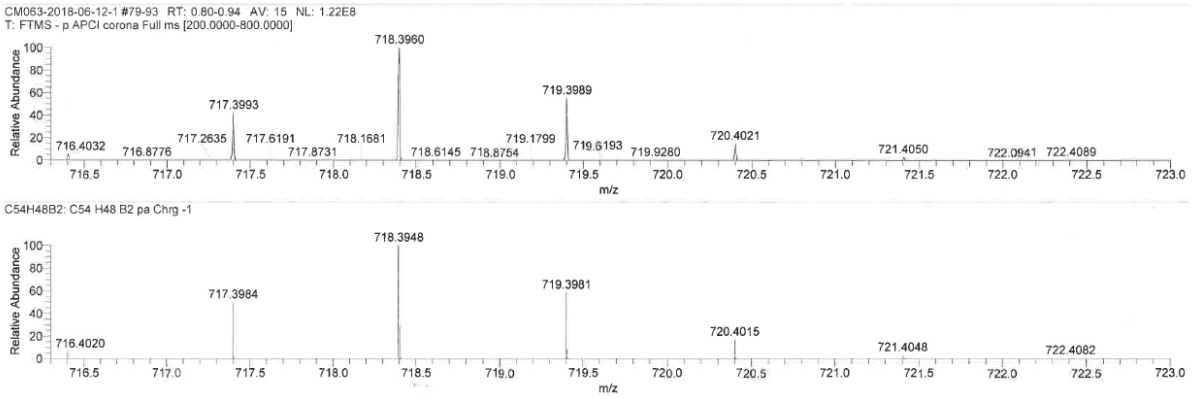

Figure S66. Simulated (bottom) and found (top) patterns of the high-resolution mass spectrum of **10** (ASAP, negative mode) *m/z*: $[M]^-$ Calc'd for $C_{54}H_{48}B_2$.

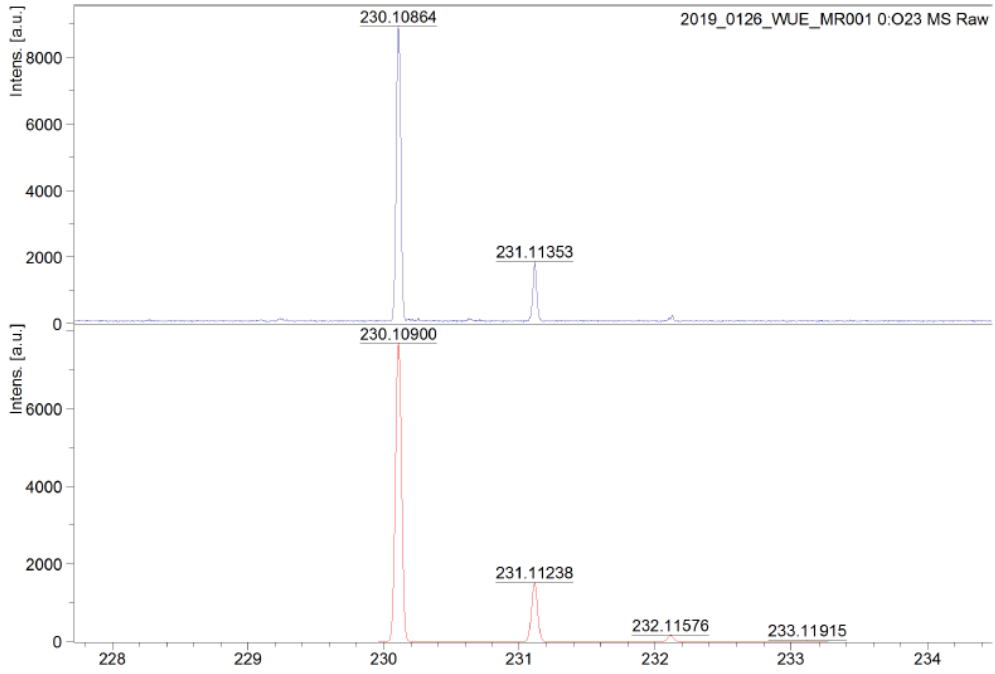

Figure S67. Simulated (bottom) and found (top) patterns of the high-resolution mass spectrum of 1-styrylnaphthalene (MALDI-TOF, positive mode) *m/z*: $[M]^+$ Calc'd for $C_{18}H_{14}$.

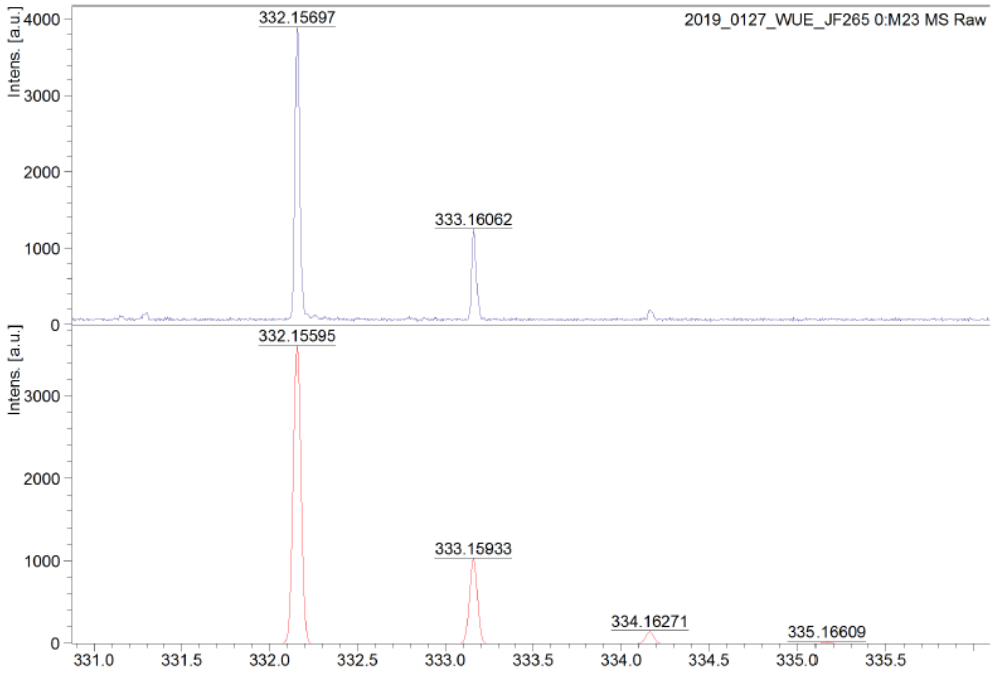

Figure S68. Simulated (bottom) and found (top) patterns of the high-resolution mass spectrum of 1,5-di(styryl)naphthalene (MALDI-TOF, positive mode) *m/z*: $[M]^+$ Calc'd for $C_{26}H_{20}$.

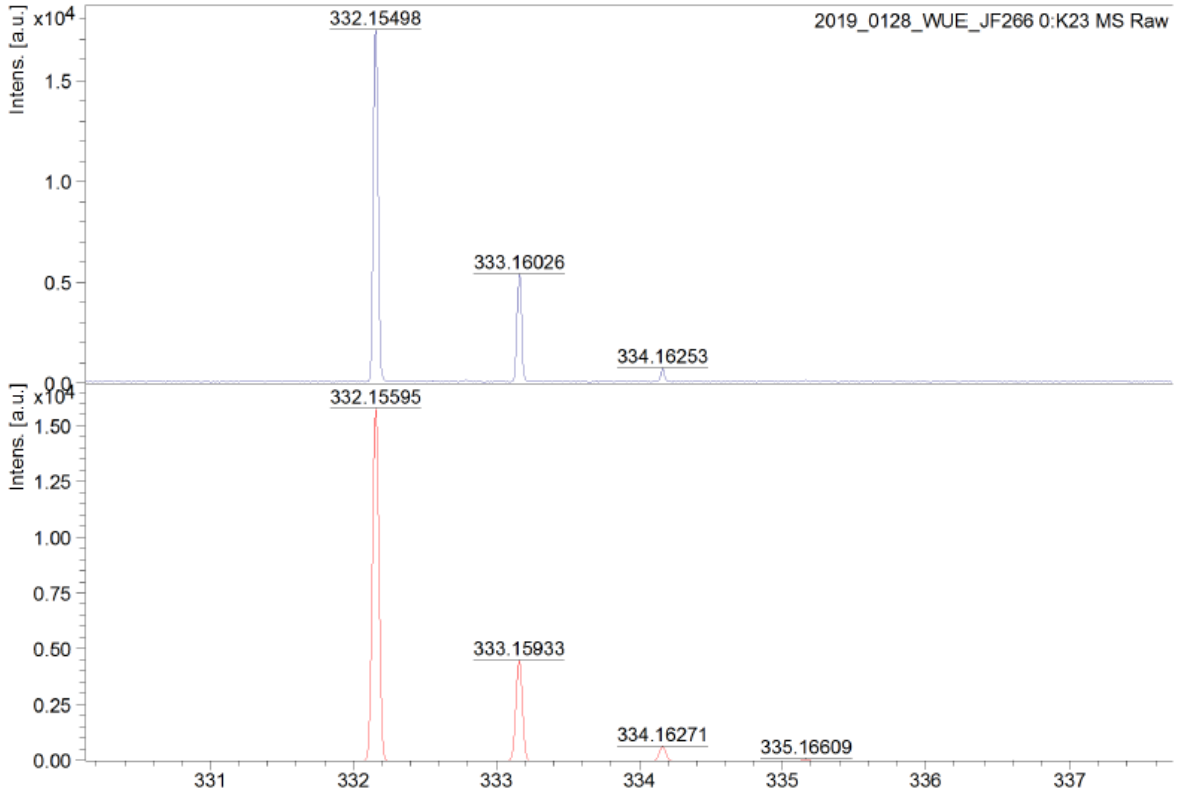

Figure S69. Simulated (bottom) and found (top) patterns of the high-resolution mass spectrum of 1,4-di(styryl)naphthalene (MALDI-TOF, positive mode) *m/z*: $[M]^+$ Calc'd for $C_{26}H_{20}$.

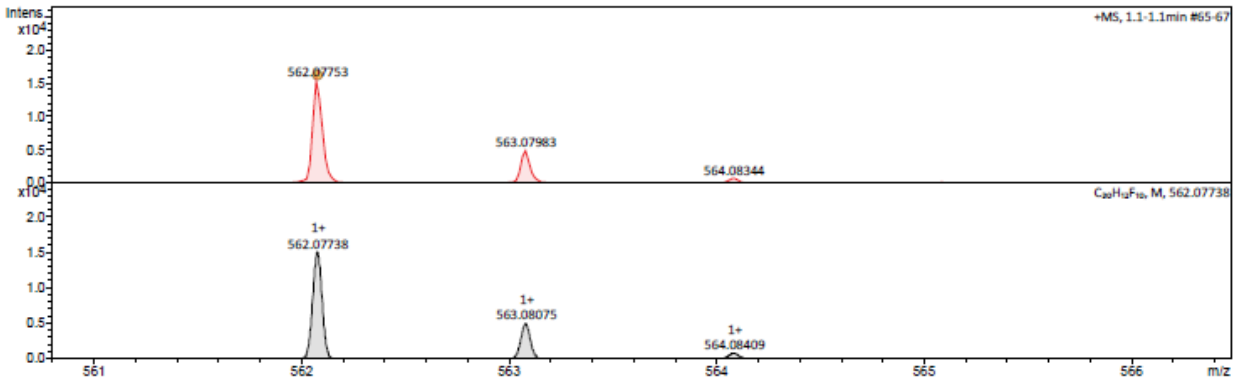

Figure S70. Simulated (bottom) and found (top) patterns of the high-resolution mass spectrum of 9,10-bis(2,3,4,5,6-pentafluorostyryl)anthracene (ESI-TOF, positive mode) *m/z*: $[M]^+$ Calc'd for $C_{30}H_{12}F_{10}$.

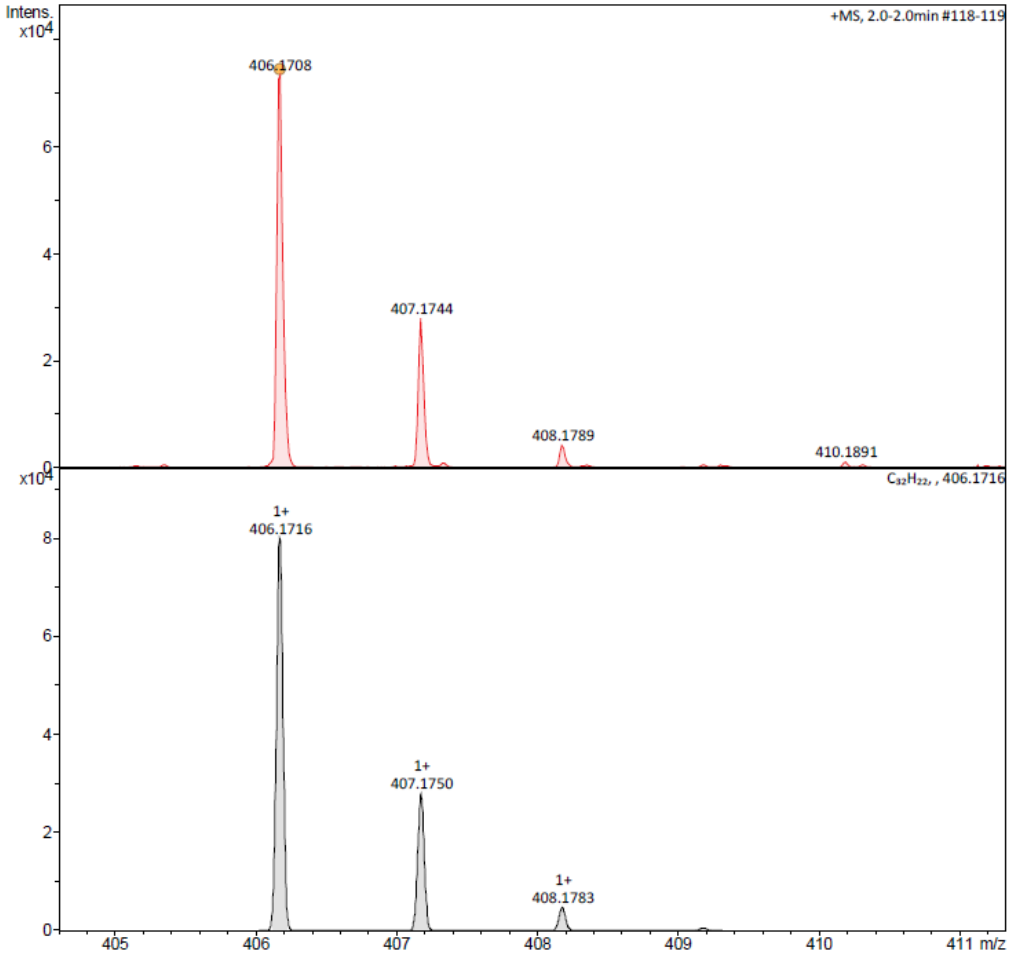

Figure S71. Simulated (bottom) and found (top) patterns of the high-resolution mass spectrum of 1,6-distyrylpyrene (ESI-TOF, positive mode) *m/z*: $[M]^+$ Calc'd for $C_{32}H_{22}$.

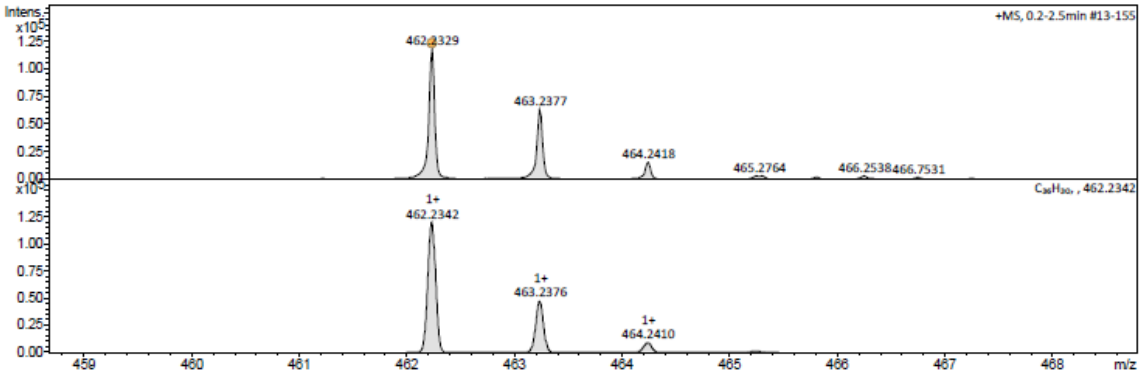

Figure S72. Simulated (bottom) and found (top) patterns of the high-resolution mass spectrum of 7-(*tert*-butyl)-1,3-distyryl-pyrene (ESI-TOF, positive mode) *m/z*: $[M]^+$ Calc'd for $C_{36}H_{30}$.

5. UV-Vis and Fluorescence Spectroscopy

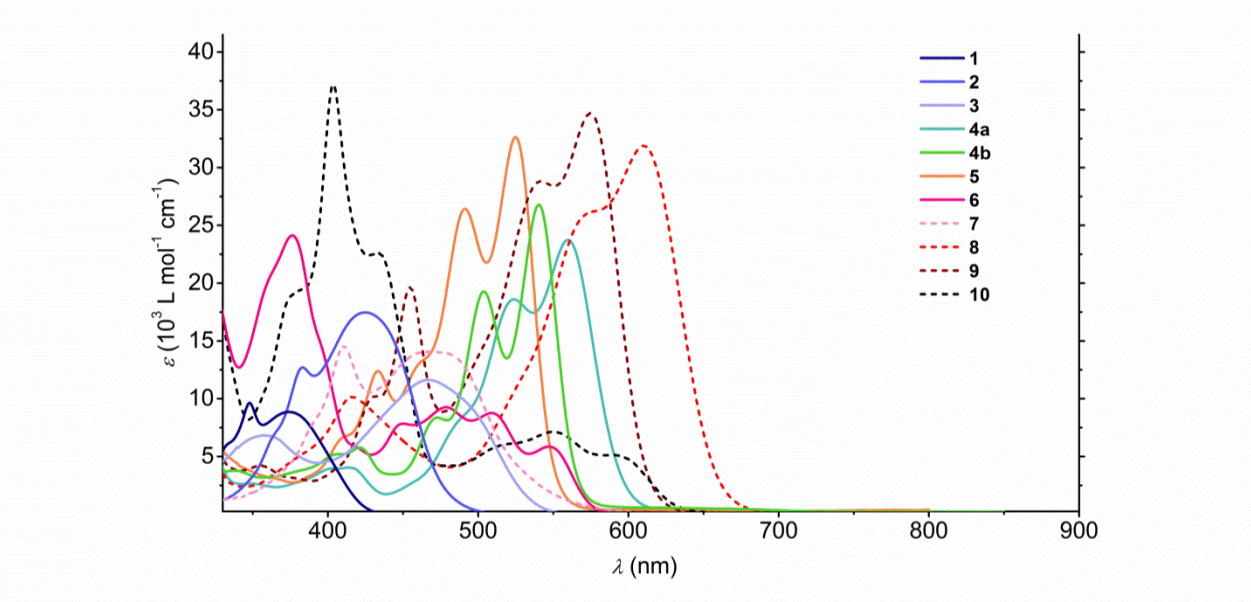

Figure S73. UV-Vis absorption (solid lines: **1**-**4** 10^{-5} M in $CHCl_3$, 298 K; **5**-**10** 10^{-6} M - 10^{-5} M in CH_2Cl_2, 298 K) spectra of boron-containing PAHs **1**-**10**. Borinic acids **1**-**6** are depicted with solid lines and mesityl boranes **7**-**10** are depicted with dashed lines.

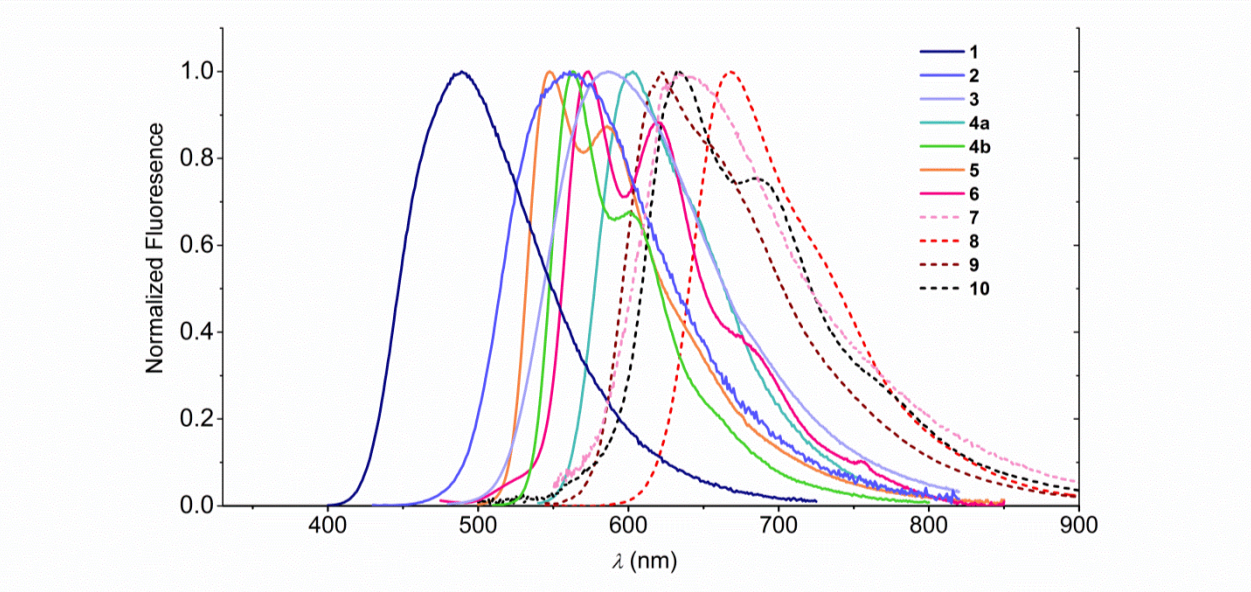

Figure S74. Fluorescence (dashed lines: **1-4** 10^{-5} M in $CHCl_3$, 298 K; **5-10** 10^{-7} M - 10^{-4} M in CH_2Cl_2, 298 K) spectra of boron-containing PAHs **1-10**. Borinic acids **1-6** are depicted with solid lines and mesityl boranes **7-10** are depicted with dashed lines.

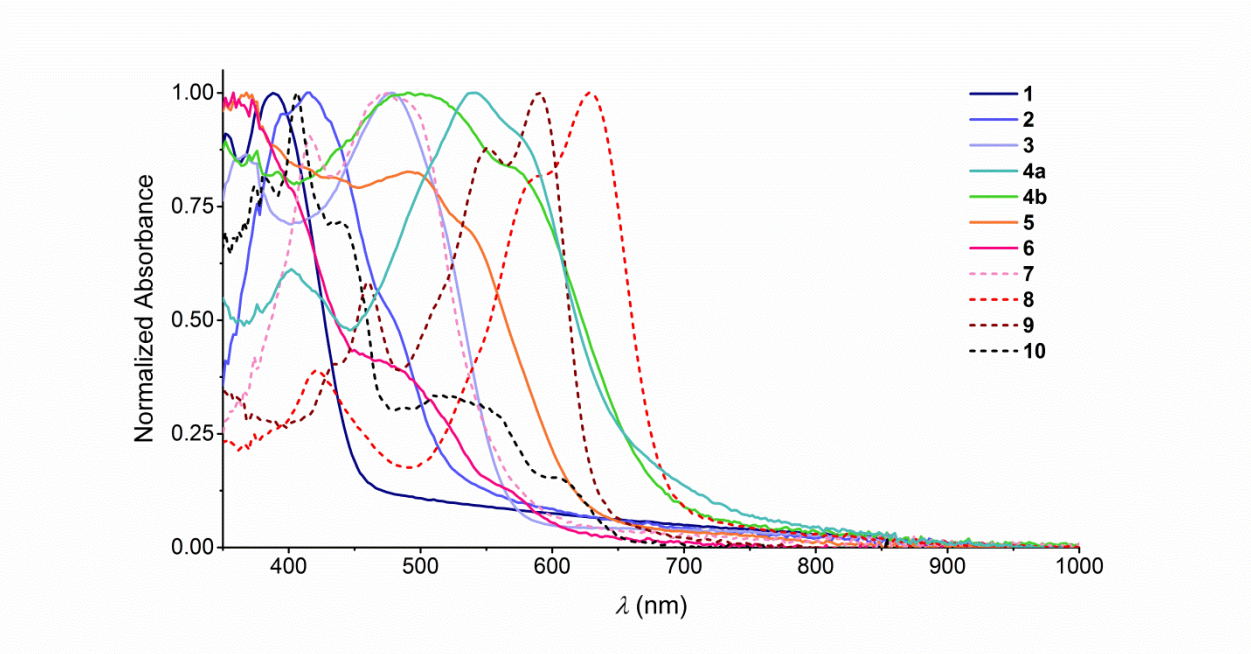

Figure S75. UV-Vis absorption (thin film, 298 K) spectra of boron-containing PAHs **1-10**. Borinic acids **1-6** are depicted with solid lines and mesityl boranes **7-10** are depicted with dashed lines.

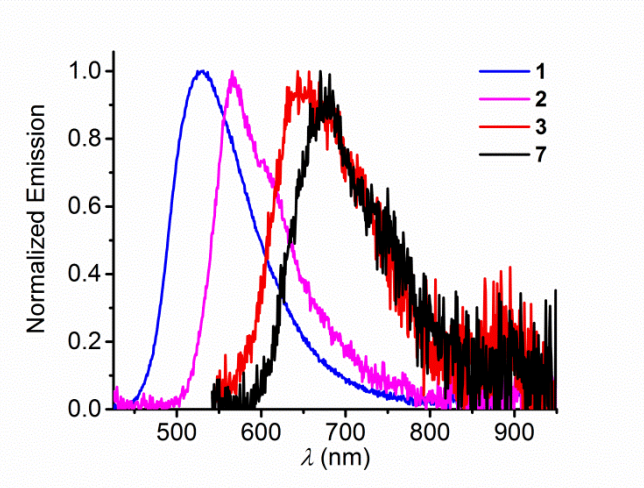

Figure S76. Normalized solid-state emission spectra (298 K) of **1**, **2**, **3** and **7** measured at excitation wavelengths of 370 nm, 410 nm, 475 nm and 510 nm, respectively.

6. Cyclic Voltammetry

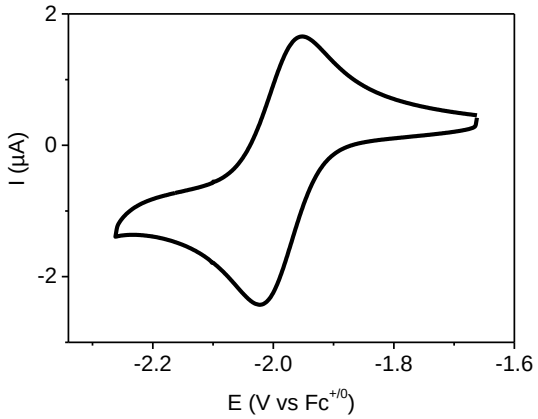

Figure S77. Cyclic voltammogram of 1-hydroxy-2-phenyl-1-boraphenalene (**1**) (1 x 10^{-3} M, 0.1 M *n*-Bu_4NPF_6 in DMSO, vs. $Fc^{+/0}$, 298 K).

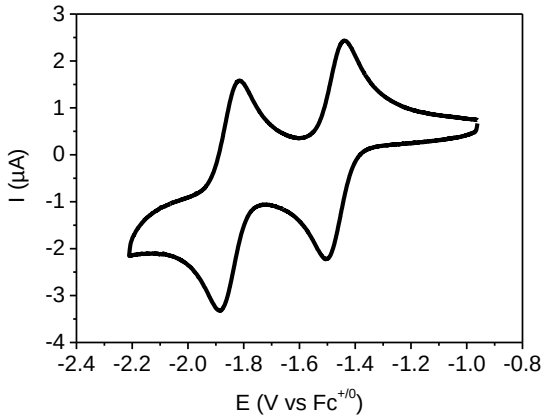

Figure S78. Cyclic voltammogram of 1,6-dihydroxy-2,7-diphenyl-1,6-diborapyrene (**2**) (9 x 10^{-4} M, 0.1 M *n*-Bu_4NPF_6 in DMSO, vs. $Fc^{+/0}$, 298 K).

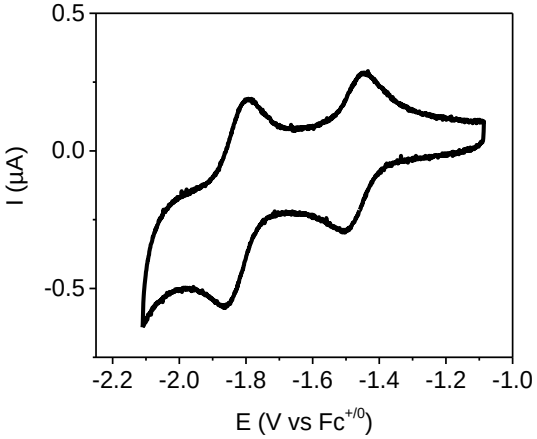

Figure S79. Cyclic voltammogram of 1,8-dihydroxy-2,7-diphenyl-1,8-diborapyrene (**3**) (3 x 10^{-5} M, 0.1 M *n*-Bu_4NPF_6 in DMSO, vs. $Fc^{+/0}$, 298 K).

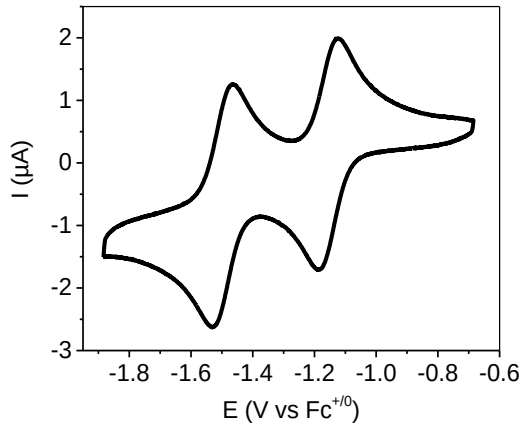

Figure S80. Cyclic voltammogram of 3,9-dihydroxy-2,8-bis(pentafluorophenyl)-3,9-diboraperylene (**4b**) (7 x 10^{-4} M, 0.1 M *n*-Bu_4NPF_6 in DMSO, vs. $Fc^{+/0}$, 298 K).

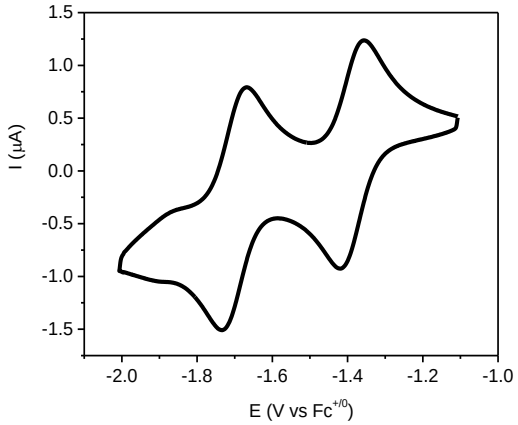

Figure S81. Cyclic voltammogram of 1,7-dihydroxy-2,8-diphenyl-1,7-diboraanthanthrene (**5**) (3 x 10^{-4} M, 0.1 M *n*-Bu_4NPF_6 in DMSO, vs. $Fc^{+/0}$, 298 K).

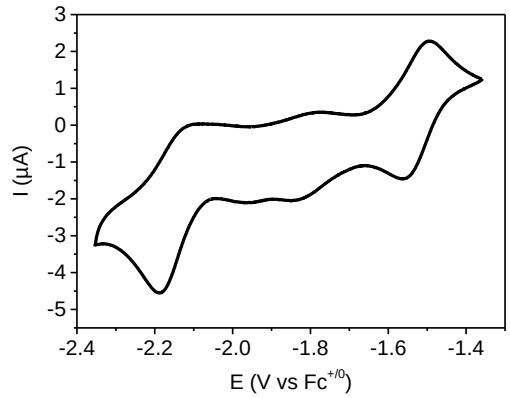

Figure S82. Full cyclic voltammogram of 11-*tert*-butyl-2,8-dihydroxy-3,7-diphenyl-2,8-diboratriangulene (**6**) (3 x 10^{-4} M, 0.1 M *n*-Bu_4NPF_6 in DMSO, vs. $Fc^{+/0}$, 298 K).

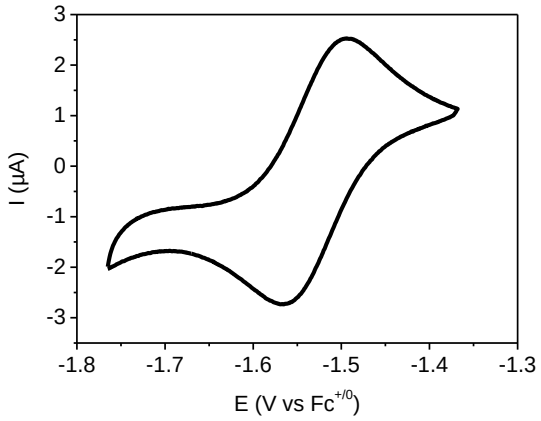

Figure S83. Cyclic voltammogram of the first reduction of 11-*tert*-butyl-2,8-dihydroxy-3,7-diphenyl-2,8-diboratriangulene (**6**) (3 x 10^{-4} M, 0.1 M *n*-Bu_4NPF_6 in DMSO, vs. $Fc^{+/0}$, 298 K).

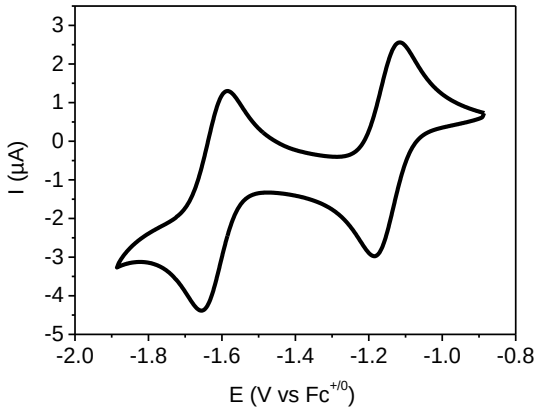

Figure S84. Cyclic voltammogram of 1,6-dimesityl-2,7-diphenyl-1,6-diborapyrene (**7**) (3 x 10^{-4} M, 0.1 M *n*-Bu_4NPF_6 in CH_2Cl_2, vs. $Fc^{+/0}$, 298 K).

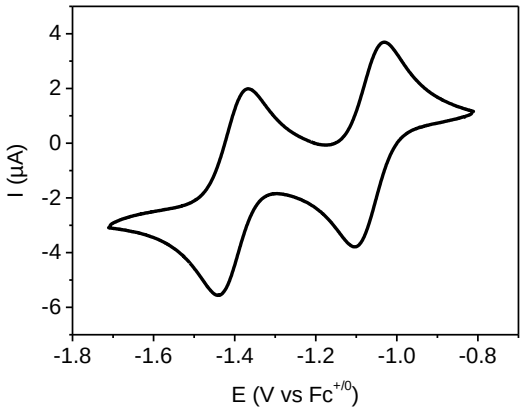

Figure S85. Cyclic voltammogram of 3,9-dimesityl-2,8-diphenyl-3,9-diboraperylene (**8**) (3 x 10^{-4} M, 0.1 M *n*-Bu_4NPF_6 in CH_2Cl_2, vs. $Fc^{+/0}$, 298 K).

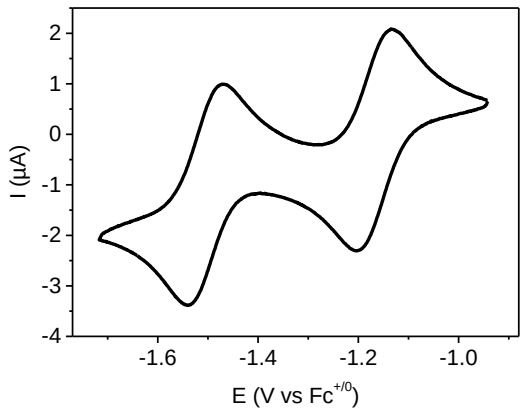

Figure S86. Cyclic voltammogram of 1,7-dimesityl-2,8-diphenyl-1,7-diboraanthanthrene (**9**) (3 x 10^{-4} M, 0.1 M *n*-Bu_4NPF_6 in CH_2Cl_2, vs. $Fc^{+/0}$, 298 K).

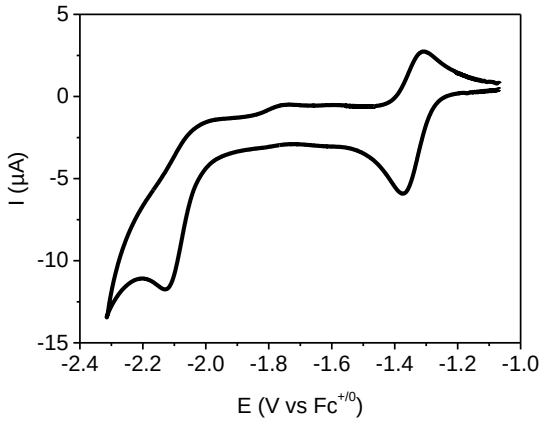

Figure S87. Full cyclic voltammogram of 11-*tert*-butyl-2,8-dimesityl-3,7-diphenyl-2,8-diboratriangulene (**10**) (3 x 10^{-4} M, 0.1 M *n*-Bu_4NPF_6 in CH_2Cl_2, vs. $Fc^{+/0}$, 298 K).

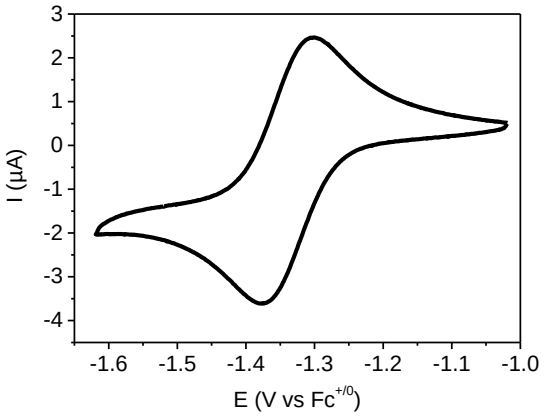

Figure S88. Cyclic voltammogram of the first reduction of 11-*tert*-butyl-2,8-dimesityl-3,7-diphenyl-2,8-diboratriangulene (**10**) (3 x 10^{-4} M, 0.1 M *n*-Bu_4NPF_6 in CH_2Cl_2, vs. $Fc^{+/0}$, 298 K).

7. X-ray Crystallography

Crystal data for 1-hydroxy-2-phenyl-1-boraphenalene ***2*** ($C_{26}H_{18}B_2O_2$, • 2(C_2H_6OS)): *M*r = 540.28, 0.187x0.067x0.018 mm^3, triclinic space group P-1, *a* = 5.7757(6) Å, α = 70.856(5)°, *b* = 10.0831(12) Å, β = 84.636(5)° *c* = 12.4448(14) Å, γ = 73.657(5)°, *V* = 657.00(13) $Å^3$, *Z* = 1, ρ(*calcd)* = 1.366 g·cm^{-3}, μ = 2.124 mm^{-1}, $F_{(000)}$ = 284, *GooF*(F^2) = 1.057, R_1 = 0.0333, wR^2 = 0.0897 for I>2σ(I), R_1 = 0.0342, wR^2 = 0.0906 for all data, 2582 unique reflections [θ ≤ 72.424 °] with a completeness of 99.3% and 175 parameters, 0 restraints.

Crystal data for 3,9-dihydroxy-2,8-bis(pentafluorophenyl)-3,9-diboraperylene ***4*** ($C_{30}H_{10}B_2F_{10}O_2$ • 2 (C_2H_6OS)): *M*r = 789.59, 0.511x0.027x0.027 mm^3, triclinic space group P-1 *a* = 14.7128(5) Å, α = 74.5203(18)°, *b* = 14.9182(5) Å, β = 87.2248(19) ° *c* = 16.4821(6) Å, γ = 86.8565(18)°, *V* = 3479.0(2) $Å^3$, *Z* = 2, ρ(*calcd)* = 1.507 g·cm^{-3}, μ = 2.373 mm^{-1}, $F_{(000)}$ = 1602, *GooF*(F^2) = 1.050, R_1 = 0.0758, wR^2 = 0.2050 for I>2σ(I), R_1 = 0.0871, wR^2 = 0.2149 for all data, 13706 unique reflections [θ ≤ 72.665°] with a completeness of 99.0% and 1077 parameters, 61 restraints.

Crystal data for 1,7-dihydoxy-2,8-diphenyl-1,7-diboraanthanthrene ***9*** ($C_{32}H_{20}B_2O_2$ • 4 ($C_4H_6O_2$)): *M*r = 810.51, 0.272x0.053x0.022 mm^3, triclinic space group P-1, *a* = 5.6393(4) Å, α =

80.086(3)°, *b* = 12.8559(8) Å, β = 89.946(3)°, *c* = 14.1348(9) Å, γ = 85.751(3)°, *V* = 1006.60(12) Å^3, *Z* = 1, ρ(*calcd)* = 1.337 g·cm^{-3}, μ = 0.742 mm^{-1}, $F_{(000)}$ = 430, *GooF*(F^2) = 1.055, R_1 = 0.0570, wR^2 = 0.1559 for I>2σ(I), R_1 = 0.0653, wR^2 = 0.1655 for all data, 3919 unique reflections [θ ≤ 72.723°] with a completeness of 98.4% and 341 parameters, 8 restraints.

Crystal data for 3,9-dimesityl-2,8-diphenyl-3,9-diboraperylene ***8*** ($C_{48}H_{40}B_2$): *M*r = 638.42, 0.168x0.094x0.082 mm^3, monoclinic space group $P2_1/n$, *a* = 9.4061(5) Å, α = 90°, *b* = 11.8145(7) Å, β = 95.270(2) ° *c* = 15.8718(9) Å, γ = 90°, *V* = 1756.35(17) Å^3, *Z* = 2, ρ(*calcd)* = 1.207 g·cm^{-3}, μ = 0.504 mm^{-1}, $F_{(000)}$ = 676, *GooF*(F^2) = 1.034, R_1 = 0.0419, wR^2 = 0.1082 for I>2σ(I), R_1 = 0.0465, wR^2 = 0.1130 for all data, 3467 unique reflections [θ ≤ 72.214°] with a completeness of 99.9% and 229 parameters, 0 restraints.

Crystal data for 9,10-bis(2,3,4,5,6-pentafluorostyryl)anthracene ($C_{30}H_{12}F_{10}$): *M*r = 562.40, 0.534x0.055x0.034 mm^3, monoclinic space group $P2_1/c$, *a* = 13.5878(4) Å, α = 90°, *b* = 7.1239(2) Å, β = 98.4482(13) ° *c* = 22.9259(7) Å, γ = 90°, *V* = 2195.10(11) Å^3, *Z* = 4, ρ(*calcd)* = 1.702 g·cm^{-3}, μ = 1.400 mm^{-1}, $F_{(000)}$ = 1128, *GooF*(F^2) = 1.083, R_1 = 0.0600, wR^2 = 0.1643 for I>2σ(I), R_1 = 0.0647, wR^2 = 0.1684 for all data, 4325 unique reflections [θ ≤ 72.126°] with a completeness of 99.9% and 361 parameters, 0 restraints.

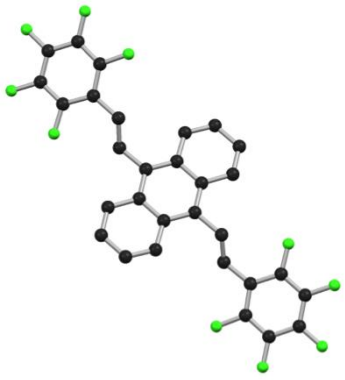

Figure S89. Solid state structure of 9,10-bis(2,3,4,5,6-pentafluorostyryl)anthracene. C: black, F: green. H atoms omitted for clarity.

8. Computations

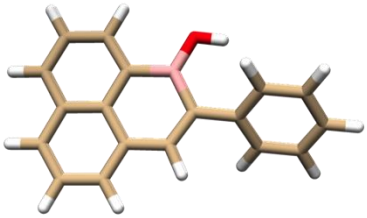

Figure S90. Geometry-optimized structure of **1** by DFT calculations at the B3LYP/6-31++G** level of theory.

Figure S91. Frontier molecular orbitals of **1** by DFT calculations at the B3LYP/6-31++G** level of theory. Isovalues for orbitals: 0.02 a.u.

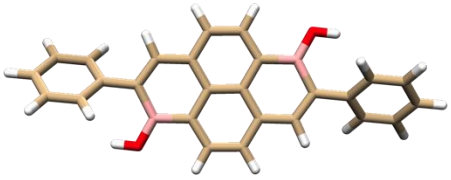

Figure S92. Geometry-optimized structure of **2** by DFT calculations at the B3LYP/6-31++G** level of theory.

LUMO
−2.97 eV

HOMO
−6.00 eV

Figure S93. Frontier molecular orbitals of **2** by DFT calculations at the B3LYP/6-31++G** level of theory. Isovalues for orbitals: 0.02 a.u.

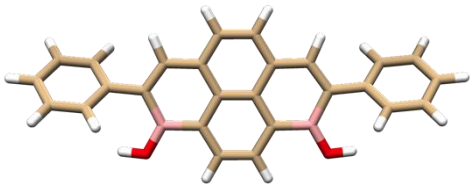

Figure S94. Geometry-optimized structure of **3** by DFT calculations at the B3LYP/6-31++G** level of theory.

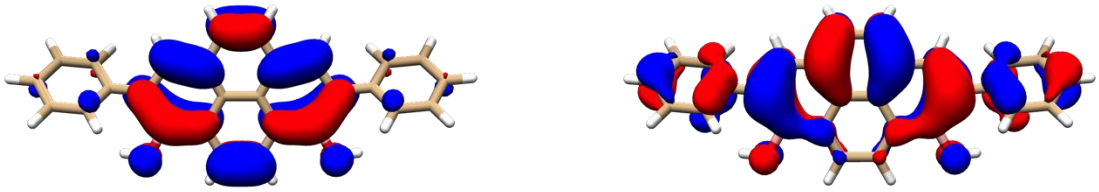

LUMO
−2.97 eV

HOMO
−5.81 eV

Figure S95. Frontier molecular orbitals of **3** by DFT calculations at the B3LYP/6-31++G** level of theory. Isovalues for orbitals: 0.02 a.u.

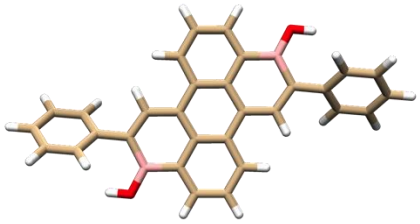

Figure S96. Geometry-optimized structure of **4a** by DFT calculations at the B3LYP/6-31++G** level of theory.

Figure S97. Frontier molecular orbitals of **4a** by DFT calculations at the B3LYP/6-31++G** level of theory. Isovalues for orbitals: 0.02 a.u.

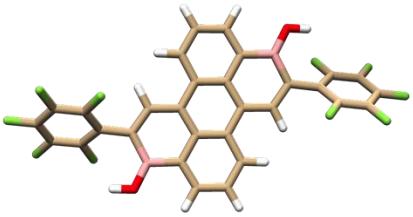

Figure S98. Geometry-optimized structure of **4b** by DFT calculations at the B3LYP/6-31++G** level of theory.

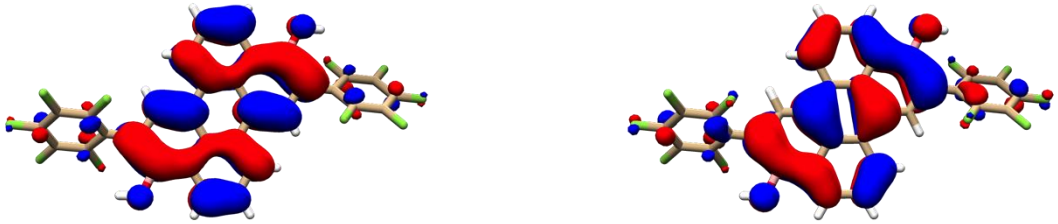

Figure S99. Frontier molecular orbitals of **4b** by DFT calculations at the B3LYP/6-31++G** level of theory. Isovalues for orbitals: 0.02 a.u.

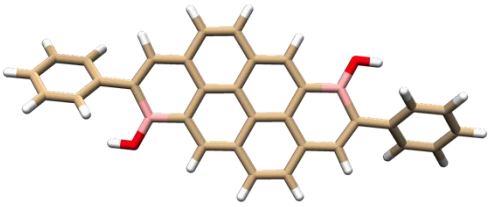

Figure S100. Geometry-optimized structure of **5** by DFT calculations at the B3LYP/6-31++G** level of theory.

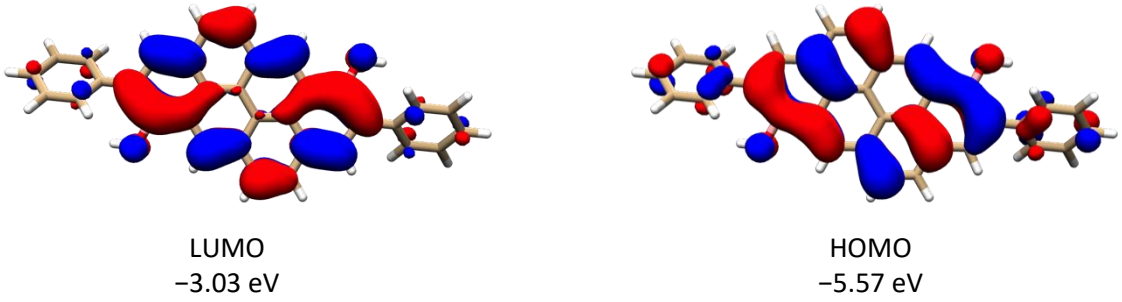

Figure S101. Frontier molecular orbitals of **5** by DFT calculations at the B3LYP/6-31++G** level of theory. Isovalues for orbitals: 0.02 a.u.

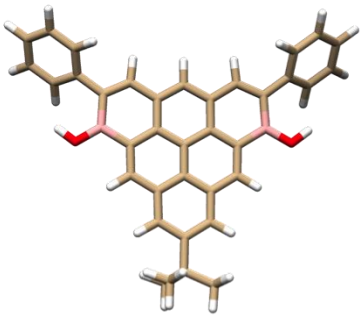

Figure S102. Geometry-optimized structure of **6** by DFT calculations at the B3LYP/6-31++G** level of theory.

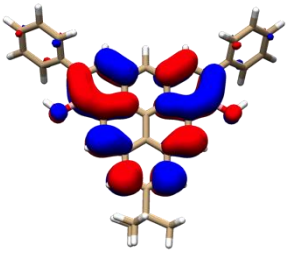

LUMO
−2.81 eV

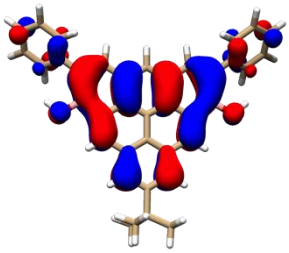

HOMO
−5.47 eV

Figure S103. Frontier molecular orbitals of **6** by DFT calculations at the B3LYP/6-31++G** level of theory. Isovalues for orbitals: 0.02 a.u.

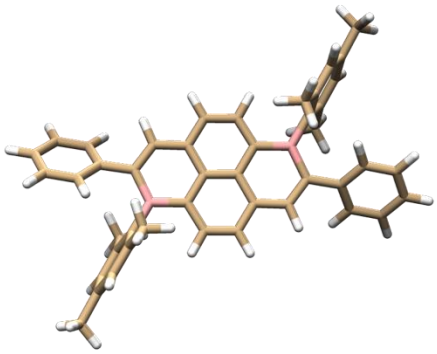

Figure S104. Geometry-optimized structure of **7** by DFT calculations at the B3LYP/6-31++G** level of theory.

Figure S105. Frontier molecular orbitals of **7** by DFT calculations at the B3LYP/6-31++G** level of theory. Isovalues for orbitals: 0.02 a.u.

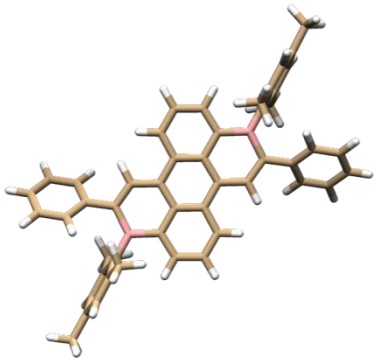

Figure S106. Geometry-optimized structure of **8** by DFT calculations at the B3LYP/6-31++G** level of theory.

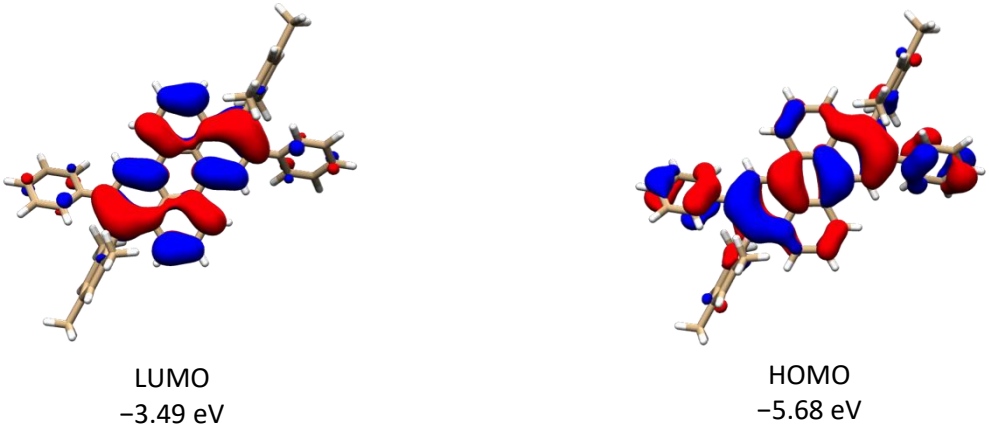

Figure S107. Frontier molecular orbitals of **8** by DFT calculations at the B3LYP/6-31++G** level of theory. Isovalues for orbitals: 0.02 a.u.

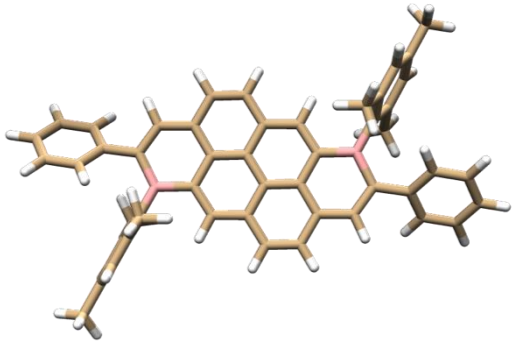

Figure S108. Geometry-optimized structure of **9** by DFT calculations at the B3LYP/6-31++G** level of theory.

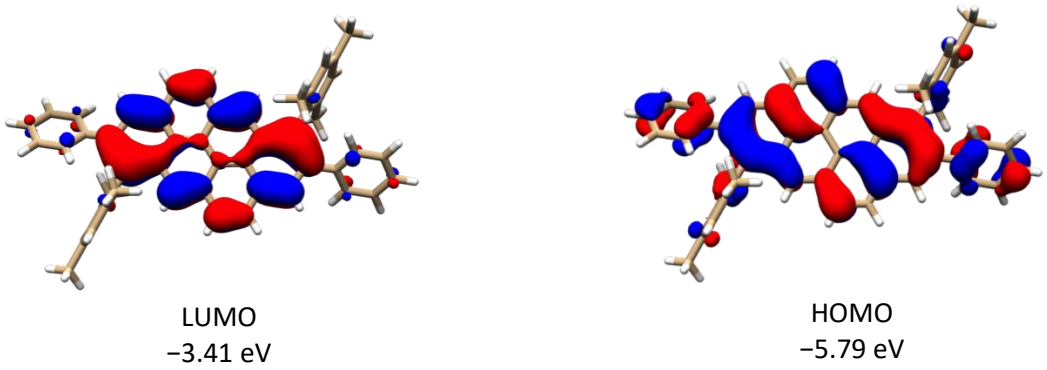

Figure S109. Frontier molecular orbitals of **9** by DFT calculations at the B3LYP/6-31++G** level of theory. Isovalues for orbitals: 0.02 a.u.

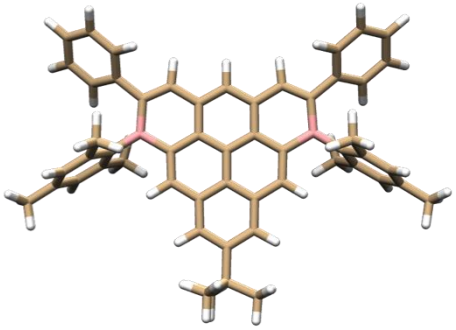

Figure S110. Geometry-optimized structure of **10** by DFT calculations at the B3LYP/6-31++G** level of theory.

LUMO
−3.03 eV

HOMO
−5.57 eV

Figure S111. Frontier molecular orbitals of **10** by DFT calculations at the B3LYP/6-31++G** level of theory. Isovalues for orbitals: 0.02 a.u.

Table S1. Cartesian coordinates and absolute energy of the geometry-optimized structure (B3LYP/6-31++G**) of compound **1**.

	x	y	z
C	–1.83400600	–2.51587000	0.20261100
C	–3.24308100	–2.60298500	0.21614700
C	–4.00710400	–1.45781000	0.12995600
C	–3.38705400	–0.18111600	0.02634800
C	–1.96039200	–0.08897400	0.01037800
C	–1.18106300	–1.29101500	0.10099400
C	–4.14972900	1.01330200	–0.06414600
C	–3.52907000	2.24315400	–0.16862100
C	–2.12011800	2.32279300	–0.18636000
C	–1.32239800	1.18450100	–0.09690800
B	0.23356900	1.24617900	–0.11486200
C	1.01469200	–0.09900500	0.02284800
C	0.27456300	–1.24212000	0.09985700
O	0.84161400	2.46615700	–0.28258900
C	2.49882100	–0.16191500	0.02241300
C	3.19730100	–1.04970000	–0.81835500
C	4.59208000	–1.10137500	–0.81297000
C	5.32681300	–0.26121000	0.02929600
C	4.65165100	0.62857200	0.86846000
C	3.25532700	0.68058800	0.86202600
H	–1.24328300	–3.42593900	0.27362300
H	–3.72009600	–3.57524000	0.29535600
H	–5.09246000	–1.51694500	0.13940700
H	–5.23481500	0.94447400	–0.05091700
H	–4.12391200	3.14940400	–0.23823800
H	–1.64078400	3.29419500	–0.27165600
H	0.77610400	–2.20682100	0.19151200

H	1.80608100	2.41254400	–0.31737500
H	2.63618700	–1.69011500	–1.49309800
H	5.10659500	–1.79315200	–1.47425000
H	6.41211600	–0.29949300	0.03055800
H	5.21029900	1.27872900	1.53606600
H	2.74382700	1.34930400	1.55019000

E = –793.96553969 a.u.

Table S2. Cartesian coordinates and absolute energy of the geometry-optimized structure (B3LYP/6-31++G**) of compound **2**.

	x	y	z
B	–2.94860800	–1.31159300	–0.02652200
C	–5.94499100	–0.60811400	0.92156100
H	–5.44334100	–1.24760100	1.64389000
C	–7.33924700	–0.51883300	0.93847700
H	–7.90715200	–1.11328700	1.64874300
C	–8.00025800	0.33782700	0.05477900
H	–9.08410900	0.40477600	0.06427800
C	–7.25384200	1.10754900	–0.84277900
H	–7.75792500	1.77259500	–1.53853500
C	–5.86113800	1.01882200	–0.85901000
H	–5.29150400	1.60307700	–1.57613400
C	–5.17677600	0.16369000	0.02618200
C	–3.69566700	0.06188300	0.01714700
C	–2.92245400	1.18380700	–0.00192000
H	–3.39324500	2.16767400	0.01932700
C	–1.46393100	1.19000400	–0.01817900
C	–0.78096200	2.40516800	–0.02133100
H	–1.34991600	3.33194600	–0.01961200
C	0.62409800	2.45296700	–0.02700200
H	1.12568100	3.41661900	–0.03324700
C	1.39045700	1.29028000	–0.02317600
C	0.71253500	0.03211400	–0.01919600
O	–3.58828000	–2.52234100	–0.10187900
H	–4.55172900	–2.44737000	–0.13189900
B	2.94860800	1.31158800	–0.02651200
C	5.94499400	0.60808300	0.92152300
H	5.44334500	1.24754100	1.64387900
C	7.33925100	0.51881200	0.93842200
H	7.90716000	1.11324200	1.64870400
C	8.00025800	–0.33781000	0.05468400
H	9.08411000	–0.40475200	0.06416900

C	7.25383900	–1.10750100	–0.84289800
H	7.75791900	–1.77251500	–1.53868700
C	5.86113400	–1.01878300	–0.85911200
H	5.29149700	–1.60301100	–1.57625500
C	5.17677500	–0.16369300	0.02612400
C	3.69566600	–0.06189100	0.01710300
C	2.92245400	–1.18381400	–0.00199200
H	3.39324600	–2.16768200	0.01922100
C	1.46393000	–1.19001100	–0.01823200
C	0.78096100	–2.40517400	–0.02141500
H	1.34991500	–3.33195200	–0.01973300
C	–0.62409900	–2.45297300	–0.02707500
H	–1.12568200	–3.41662400	–0.03334600
C	–1.39045700	–1.29028500	–0.02320300
C	–0.71253400	–0.03212100	–0.01918900
O	3.58828200	2.52233700	–0.10181200
H	4.55173200	2.44736500	–0.13183400

E = –1202.01008512 a.u.

Table S3. Cartesian coordinates and absolute energy of the geometry-optimized structure (B3LYP/6-31++G**) of the anion of compound **2**.

	x	y	z
B	–2.93652800	–1.32670100	–0.01275600
C	–5.95455600	–0.65883400	0.86468800
H	–5.46552000	–1.34399300	1.55266600
C	–7.34778200	–0.55519900	0.87640700
H	–7.92645100	–1.18719200	1.54641400
C	–7.99734200	0.36433600	0.04741700
H	–9.08106700	0.44585200	0.05477400
C	–7.22822500	1.17914900	–0.79173500
H	–7.71652200	1.89654600	–1.44767500
C	–5.83743300	1.06948100	–0.80675900
H	–5.25616900	1.68979700	–1.48321900
C	–5.15663700	0.15026600	0.02325600
C	–3.68195200	0.02874200	0.01595400
C	–2.90444700	1.17382000	–0.01297300
H	–3.38966600	2.15246300	0.00938600
C	–1.47281000	1.19107200	–0.02383300
C	–0.77459500	2.42225600	–0.02507200
H	–1.35192500	3.34619000	–0.02628600
C	0.61069100	2.47044600	–0.02538600
H	1.11730300	3.43250000	–0.02890500

C	1.39630500	1.29342200	–0.01976000
C	0.71792600	0.03529800	–0.02108400
O	–3.58375600	–2.56825700	–0.07398200
H	–4.54210500	–2.47223200	–0.12572400
B	2.93652700	1.32669900	–0.01272700
C	5.95456400	0.65881300	0.86464400
H	5.46553500	1.34395500	1.55264300
C	7.34779000	0.55518200	0.87634100
H	7.92646700	1.18716000	1.54635700
C	7.99734200	–0.36433000	0.04731900
H	9.08106800	–0.44584200	0.05465900
C	7.22821700	–1.17912200	–0.79184600
H	7.71650800	–1.89649900	–1.44781200
C	5.83742500	–1.06945700	–0.80684900
H	5.25615400	–1.68975600	–1.48331800
C	5.15663700	–0.15026800	0.02320200
C	3.68195200	–0.02874500	0.01592000
C	2.90444700	–1.17382200	–0.01304200
H	3.38966700	–2.15246600	0.00927400
C	1.47281000	–1.19107400	–0.02388900
C	0.77459500	–2.42225800	–0.02516900
H	1.35192500	–3.34619200	–0.02642500
C	–0.61069100	–2.47044900	–0.02547500
H	–1.11730300	–3.43250200	–0.02902800
C	–1.39630500	–1.29342500	–0.01979800
C	–0.71792600	–0.03530100	–0.02108000
O	3.58375700	2.56825600	–0.07390500
H	4.54210500	2.47223200	–0.12565500

E = –1202.07784196 a.u.

Table S4. Cartesian coordinates and absolute energy of the geometry-optimized structure (B3LYP/6-31++G**) of compound **3**.

	x	y	z
C	2.88325200	1.24554500	0.14396500
C	5.96058200	–0.53829000	0.87399900
H	5.47837800	–1.26708800	1.52105800
C	7.35118700	–0.40694800	0.90755600
H	7.93678900	–1.05585700	1.55282000
C	7.98580900	0.56012900	0.12403100
H	9.06695100	0.65998300	0.14612800
C	7.21657200	1.39737700	–0.68985700
H	7.70025700	2.14830200	–1.30843700

C	5.82740800	1.26681900	–0.72237900
H	5.24057000	1.90573500	–1.37622200
C	5.16934600	0.30045300	0.06273000
C	3.69237100	0.15339400	0.03541800
B	2.98957700	–1.22720800	–0.17181700
C	1.42842100	–1.25771600	–0.17573500
C	0.70329100	–2.43885700	–0.32580700
H	1.24157100	–3.37522800	–0.44520400
C	–0.70335100	–2.43882000	–0.32596200
H	–1.24166800	–3.37515600	–0.44547900
C	–1.42842800	–1.25764700	–0.17602600
C	–0.71327900	–0.03228900	–0.02574100
B	–2.98964100	–1.22694000	–0.17237600
C	–5.96039800	–0.53865900	0.87377700
H	–5.47809300	–1.26784300	1.52031900
C	–7.35102700	–0.40746100	0.90755800
H	–7.93646900	–1.05679300	1.55253800
C	–7.98582800	0.55992300	0.12457400
H	–9.06697000	0.65973100	0.14686200
C	–7.21675600	1.39761900	–0.68901700
H	–7.70059400	2.14881900	–1.30714700
C	–5.82759300	1.26720300	–0.72177900
H	–5.24091900	1.90650200	–1.37539100
C	–5.16933900	0.30052900	0.06280000
C	–3.69235300	0.15348900	0.03518800
C	–2.88321800	1.24564300	0.14369000
H	–3.32241400	2.23470700	0.28230300
C	–1.42777000	1.20587000	0.12368600
C	–0.70267400	2.38588100	0.26573500
H	–1.23514200	3.32656300	0.38126700
C	0.70271900	2.38586600	0.26582300
H	1.23518100	3.32654300	0.38139000
C	1.42780400	1.20582200	0.12387000
C	0.71329200	–0.03231500	–0.02561300
O	–3.66651900	–2.39947000	–0.38603900
H	–4.62721200	–2.29170200	–0.40347900
O	3.66654000	–2.39981600	–0.38425900
H	4.62723700	–2.29215900	–0.40146200
H	3.32246400	2.23461600	0.28257100

E = –1202.00985560 a.u.

Table S5. Cartesian coordinates and absolute energy of the geometry-optimized structure (B3LYP/6-31++G**) of compound **4a**.

	x	y	z
C	–0.13695700	–3.74463100	–0.00286700
C	–1.51248200	–3.42531400	–0.00989300
C	–1.94459700	–2.10942000	–0.00718400
C	–0.97364000	–1.04562000	–0.00253400
C	0.43330200	–1.35831600	0.00023400
C	0.80188400	–2.74015900	0.00231800
C	–1.40890500	0.31014200	–0.00213400
C	–0.43330300	1.35831100	0.00033300
C	0.97364000	1.04561500	–0.00244000
C	1.40890400	–0.31014700	–0.00213500
C	–0.80188600	2.74015300	0.00252900
C	0.13695500	3.74462600	–0.00256600
C	1.51248000	3.42531000	–0.00960800
C	1.94459600	2.10941600	–0.00699700
B	3.46216700	1.77949300	–0.01119400
C	3.85369800	0.27843700	0.02247500
C	2.82922100	–0.62586000	0.00567600
B	–3.46216900	–1.77949600	–0.01137600
C	–3.85370000	–0.27844300	0.02239300
C	–2.82922100	0.62585400	0.00567300
C	–5.26253900	0.18706600	0.01872000
C	5.26253900	–0.18706700	0.01879000
C	6.20401300	0.36546500	0.91120900
C	7.53364600	–0.06333700	0.91450500
C	7.95794200	–1.04830600	0.01892400
C	7.03881000	–1.60366200	–0.87646400
C	5.71009300	–1.17664500	–0.87829200
C	–5.71007300	1.17672100	–0.87828900
C	–7.03878800	1.60374500	–0.87644700
C	–7.95793800	1.04832100	0.01888100
C	–7.53366100	0.06327600	0.91438800
C	–6.20403100	–0.36553300	0.91107900
H	0.18238400	–4.78287400	–0.00172600
H	–2.25099500	–4.22200800	–0.01688200
H	1.84630800	–3.02228400	0.00847000
H	–1.84630900	3.02227600	0.00870200
H	–0.18238700	4.78286900	–0.00134200
H	2.25099300	4.22200500	–0.01653000
H	3.09683800	–1.67703600	0.02265300
H	–3.09683800	1.67702900	0.02271200
H	5.87970300	1.10234000	1.64208800
H	8.23537600	0.36774400	1.62313200
H	8.99243800	–1.37866500	0.01752500

H	7.35951700	–2.36467500	–1.58252500
H	5.01056100	–1.59552900	–1.59625200
H	–5.01052800	1.59566000	–1.59620300
H	–7.35948000	2.36481700	–1.58245000
H	–8.99243200	1.37868600	0.01749300
H	–8.23540500	–0.36785900	1.62297000
H	–5.87973600	–1.10246800	1.64190500
O	–4.36527400	–2.81285500	–0.07954500
H	–5.28407600	–2.51564900	–0.11612600
O	4.36527500	2.81285500	–0.07927600
H	5.28407700	2.51565000	–0.11585900

E = –1355.64780994 a.u.

Table S6. Cartesian coordinates and absolute energy of the geometry-optimized structure (B3LYP/6-31++G**) of the anion of compound **4a**.

	x	y	z
C	0.15757900	–3.76216000	–0.04048200
C	1.51941700	–3.44961700	–0.02747600
C	1.95399800	–2.11796900	–0.02219500
C	0.98170200	–1.05875800	–0.02250700
C	–0.42400200	–1.37387500	–0.02801400
C	–0.78716100	–2.74294000	–0.04192300
C	1.41628800	0.31088800	–0.01595500
C	0.42400200	1.37387400	–0.02810800
C	–0.98170200	1.05875700	–0.02260700
C	–1.41628900	–0.31088800	–0.01595900
C	0.78716200	2.74293800	–0.04211000
C	–0.15757900	3.76215800	–0.04076600
C	–1.51941700	3.44961600	–0.02776500
C	–1.95399800	2.11796800	–0.02239300
B	–3.46437900	1.78955000	–0.01331600
C	–3.85211200	0.30589800	–0.02814900
C	–2.80930300	–0.61196800	–0.00813700
B	3.46437800	–1.78955000	–0.01311000
C	3.85211200	–0.30590000	–0.02805500
C	2.80930200	0.61196900	–0.00813300
C	5.24768400	0.18120900	–0.00071000
C	–5.24768400	–0.18120900	–0.00078200
C	–6.24578800	0.40803500	–0.81127400
C	–7.57011100	–0.03600300	–0.78456500
C	–7.94775400	–1.09032900	0.05237700
C	–6.97639800	–1.69334900	0.86006600

C	–5.65610700	–1.24359900	0.83792300
C	5.65609600	1.24366900	0.83791100
C	6.97638800	1.69342100	0.86003400
C	7.94775400	1.09033100	0.05241000
C	7.57012200	0.03593300	–0.78444700
C	6.24579900	–0.40810600	–0.81113600
H	–0.17143800	–4.79918800	–0.04993100
H	2.26321800	–4.24209200	–0.02299500
H	–1.83328300	–3.02416100	–0.05565300
H	1.83328300	3.02415800	–0.05583900
H	0.17143800	4.79918500	–0.05028500
H	–2.26321900	4.24209100	–0.02336000
H	–3.08513900	–1.66281100	–0.01690800
H	3.08513800	1.66281000	–0.01698200
H	–5.96218800	1.19236600	–1.50882700
H	–8.30630900	0.43553900	–1.43169800
H	–8.97749500	–1.43688700	0.07461600
H	–7.25254800	–2.51134200	1.52172000
H	–4.92204400	–1.70284500	1.49407100
H	4.92202500	1.70297100	1.49401000
H	7.25252900	2.51147000	1.52162100
H	8.97749500	1.43689000	0.07463300
H	8.30632900	–0.43566600	–1.43152900
H	5.96220900	–1.19249800	–1.50862400
O	4.37717900	–2.84661500	0.05401100
H	5.28617300	–2.53043600	0.12008100
O	–4.37718000	2.84662000	0.05371100
H	–5.28617600	2.53044700	0.11979100

E = –1355.72454051 a.u.

Table S7. Cartesian coordinates and absolute energy of the geometry-optimized structure (B3LYP/6-31++G**) of compound **4b**.

	x	y	z
B	3.33148500	–2.02181900	–0.04119500
F	5.67876700	–1.47822400	1.95602900
F	8.28620900	–0.79576100	1.99148400
F	9.29473000	0.90639400	0.09993800
F	7.64598600	1.91186700	–1.83538300
F	5.04588500	1.23581500	–1.89938100
O	4.14153800	–3.12591800	–0.10302800
H	5.08740800	–2.94800200	–0.04989700
C	3.81614600	–0.54741800	0.00762500

C	2.85939300	0.42724500	–0.01788300
H	3.19322800	1.45754800	0.00615500
C	1.42251400	0.21045800	–0.05245600
C	0.89758500	–1.11216600	–0.06131900
C	–1.79314000	2.23808200	–0.06405500
C	–1.27067400	3.52085700	–0.08583500
H	–1.95223000	4.36643000	–0.08945600
C	0.12344000	3.74471300	–0.10708300
H	0.51220400	4.75840300	–0.13183200
C	0.99171400	2.67912900	–0.09870400
H	2.05259400	2.88933100	–0.12294500
C	0.52713600	1.32701000	–0.07000900
C	5.24834900	–0.15083400	0.02989100
C	6.13702200	–0.64763900	0.99533900
C	7.48583600	–0.30372000	1.03482400
C	8.00051600	0.56624400	0.07707500
C	7.15580000	1.08115100	–0.90373200
C	5.81022200	0.72262200	–0.91587900
B	–3.33147400	2.02174000	–0.04134500
F	–5.04604000	–1.23568300	–1.89951700
F	–7.64621400	–1.91160000	–1.83541900
F	–9.29475700	–0.90621900	0.10005100
F	–8.28604400	0.79573500	1.99171200
F	–5.67854900	1.47805100	1.95615700
O	–4.14156700	3.12580900	–0.10333800
H	–5.08743000	2.94783000	–0.05023900
C	–3.81612200	0.54734000	0.00755500
C	–2.85937600	–0.42732800	–0.01790200
H	–3.19321800	–1.45763500	0.00623500
C	–1.42250500	–0.21052600	–0.05250700
C	–0.89757600	1.11210600	–0.06131300
C	1.79314700	–2.23814500	–0.06403500
C	1.27067400	–3.52091600	–0.08593000
H	1.95223100	–4.36649100	–0.08951700
C	–0.12343800	–3.74476800	–0.10735600
H	–0.51220100	–4.75845300	–0.13225000
C	–0.99170900	–2.67918200	–0.09897900
H	–2.05259100	–2.88936400	–0.12338600
C	–0.52712600	–1.32707100	–0.07010800
C	–5.24834000	0.15081000	0.02987600
C	–5.81030400	–0.72253900	–0.91594900
C	–7.15589700	–1.08098600	–0.90374000
C	–8.00053100	–0.56611900	0.07716700
C	–7.48576200	0.30373700	1.03496400
C	–6.13692600	0.64757000	0.99541400

E = –2347.97054139 a.u.

Table S8. Cartesian coordinates and absolute energy of the geometry-optimized structure (B3LYP/6-31++G**) of compound **5**.

	x	y	z
H	2.80681600	–3.65278500	0.00465000
C	2.14346200	–2.79150100	0.00310900
C	2.70824700	–1.49869100	0.00227000
C	–0.11010500	–1.88182600	0.00117700
C	1.84914900	–0.36713200	0.00304600
C	0.76993400	–2.98424100	0.00107500
C	0.43884700	–0.56221800	0.00407500
C	2.39777200	0.96762200	–0.00049900
H	0.35915900	–3.99024300	–0.00065200
C	1.53060800	2.03971700	–0.00334800
H	1.93618600	3.04893100	–0.00917000
C	0.11010500	1.88182400	0.00107700
C	–0.76993400	2.98423900	0.00092100
C	–0.43884800	0.56221600	0.00404700
C	–2.14346200	2.79150000	0.00296900
H	–0.35915800	3.99024100	–0.00086100
H	–2.80681500	3.65278400	0.00446600
C	–2.70824700	1.49869000	0.00219900
C	–1.84914900	0.36713000	0.00303300
C	–2.39777200	–0.96762400	–0.00043800
C	–1.53060800	–2.03971900	–0.00323400
H	–1.93618600	–3.04893300	–0.00900200
C	–4.15537800	1.34738200	0.01040800
C	–4.81805700	0.15364500	0.02527800
C	–6.30207600	0.11769100	0.01757900
C	–9.13044100	0.02840300	0.00798400
C	–7.05185100	0.90568900	–0.87734200
C	–7.00759500	–0.72200000	0.90354500
C	–8.40423500	–0.76292000	0.90148800
C	–8.44676000	0.86428100	–0.88021500
H	–6.53017400	1.53968700	–1.58872700
H	–6.45846000	–1.31125100	1.63403800
H	–8.92379000	–1.40776600	1.60480900
H	–9.00098800	1.47930000	–1.58386800
H	–10.21586800	–0.00597200	0.00287500
C	4.15537700	–1.34738300	0.01046400
C	4.81805800	–0.15364400	0.02526500
C	6.30207600	–0.11769200	0.01755700
C	9.13044100	–0.02839900	0.00794400

C	7.00759700	0.72208000	0.90344500
C	7.05185000	–0.90576300	–0.87730100
C	8.44675800	–0.86435400	–0.88018100
C	8.40423600	0.76300200	0.90138000
H	6.45846300	1.31139800	1.63388500
H	6.53017300	–1.53982000	–1.58863300
H	9.00098600	–1.47943200	–1.58378300
H	8.92379300	1.40791300	1.60464100
H	10.21586800	0.00597900	0.00282700
H	4.72310800	–2.27891600	0.02717600
H	–4.72310800	2.27891600	0.02707200
B	–3.94601100	–1.14235800	–0.00810800
B	3.94601200	1.14235500	–0.00818200
O	4.46584400	2.41072700	–0.08095100
H	5.43144800	2.42852300	–0.11943600
O	–4.46584600	–2.41073200	–0.08082500
H	–5.43144900	–2.42852800	–0.11930600

E = –1431.89943858 a.u.

Table S9. Cartesian coordinates and absolute energy of the geometry-optimized structure (B3LYP/6-31++G**) of the anion of compound **5**.

	x	y	z
H	–2.81565500	3.66383200	0.00383500
C	–2.14794800	2.80363500	0.00487300
C	–2.72572400	1.50283100	0.00268100
C	0.11097800	1.88640600	0.00818200
C	–1.85643700	0.36204300	0.00899700
C	–0.78582000	2.99685000	0.00631700
C	–0.44155300	0.56097900	0.01051600
C	–2.40047500	–0.96639400	0.01025300
H	–0.37129600	4.00242700	0.00536500
C	–1.51278600	–2.04546900	0.00713000
H	–1.91867900	–3.05524600	0.00322800
C	–0.11097800	–1.88640600	0.00806300
C	0.78582000	–2.99684900	0.00613200
C	0.44155200	–0.56097800	0.01048300
C	2.14794700	–2.80363500	0.00470800
H	0.37129600	–4.00242700	0.00511500
H	2.81565500	–3.66383100	0.00361900
C	2.72572400	–1.50283000	0.00260100
C	1.85643700	–0.36204300	0.00898300
C	2.40047500	0.96639400	0.01032500

C	1.51278600	2.04546900	0.00726600
H	1.91867900	3.05524700	0.00342800
C	4.14493400	–1.34411800	0.00453200
C	4.80836300	–0.12703800	0.02873700
C	6.28779100	–0.10548000	0.01319200
C	9.13516100	–0.04305000	–0.01624100
C	7.03864700	–0.95397400	–0.83155500
C	7.01857100	0.77639700	0.84199200
C	8.41531400	0.80847600	0.82707900
C	8.43340100	–0.92816300	–0.84280700
H	6.50864400	–1.62665600	–1.50011500
H	6.47942000	1.41018600	1.54173300
H	8.94234300	1.49322100	1.48759300
H	8.97642400	–1.59389800	–1.50993600
H	10.22149600	–0.01876900	–0.02937500
C	–4.14493400	1.34411900	0.00459600
C	–4.80836300	0.12703700	0.02872300
C	–6.28779100	0.10547900	0.01317000
C	–9.13516100	0.04304800	–0.01627900
C	–7.01857300	–0.77644100	0.84192200
C	–7.03864400	0.95401500	–0.83153800
C	–8.43339800	0.92820300	–0.84279800
C	–8.41531700	–0.80852000	0.82700100
H	–6.47942500	–1.41026600	1.54163300
H	–6.50863800	1.62673100	–1.50006100
H	–8.97641800	1.59397100	–1.50989600
H	–8.94234900	–1.49329800	1.48747800
H	–10.22149500	0.01876700	–0.02942000
H	–4.72588900	2.26913900	0.01959500
H	4.72588800	–2.26913900	0.01947800
B	3.93675700	1.14986300	0.00860800
B	–3.93675700	–1.14986300	0.00852000
O	–4.45468100	–2.44543000	–0.05625600
H	–5.41745200	–2.44837800	–0.11688100
O	4.45468100	2.44543400	–0.05608900
H	5.41745200	2.44838600	–0.11671200

E = –1431.97337020 a.u.

Table S10. Cartesian coordinates and absolute energy of the geometry-optimized structure (B3LYP/6-31++G**) of compound **6**.

	x	y	z
H	–2.81565500	3.66383200	0.00383500
C	–2.14794800	2.80363500	0.00487300

C	–2.72572400	1.50283100	0.00268100
C	0.11097800	1.88640600	0.00818200
C	–1.85643700	0.36204300	0.00899700
C	–0.78582000	2.99685000	0.00631700
C	–0.44155300	0.56097900	0.01051600
C	–2.40047500	–0.96639400	0.01025300
H	–0.37129600	4.00242700	0.00536500
C	–1.51278600	–2.04546900	0.00713000
H	–1.91867900	–3.05524600	0.00322800
C	–0.11097800	–1.88640600	0.00806300
C	0.78582000	–2.99684900	0.00613200
C	0.44155200	–0.56097800	0.01048300
C	2.14794700	–2.80363500	0.00470800
H	0.37129600	–4.00242700	0.00511500
H	2.81565500	–3.66383100	0.00361900
C	2.72572400	–1.50283000	0.00260100
C	1.85643700	–0.36204300	0.00898300
C	2.40047500	0.96639400	0.01032500
C	1.51278600	2.04546900	0.00726600
H	1.91867900	3.05524700	0.00342800
C	4.14493400	–1.34411800	0.00453200
C	4.80836300	–0.12703800	0.02873700
C	6.28779100	–0.10548000	0.01319200
C	9.13516100	–0.04305000	–0.01624100
C	7.03864700	–0.95397400	–0.83155500
C	7.01857100	0.77639700	0.84199200
C	8.41531400	0.80847600	0.82707900
C	8.43340100	–0.92816300	–0.84280700
H	6.50864400	–1.62665600	–1.50011500
H	6.47942000	1.41018600	1.54173300
H	8.94234300	1.49322100	1.48759300
H	8.97642400	–1.59389800	–1.50993600
H	10.22149600	–0.01876900	–0.02937500
C	–4.14493400	1.34411900	0.00459600
C	–4.80836300	0.12703700	0.02872300
C	–6.28779100	0.10547900	0.01317000
C	–9.13516100	0.04304800	–0.01627900
C	–7.01857300	–0.77644100	0.84192200
C	–7.03864400	0.95401500	–0.83153800
C	–8.43339800	0.92820300	–0.84279800
C	–8.41531700	–0.80852000	0.82700100
H	–6.47942500	–1.41026600	1.54163300
H	–6.50863800	1.62673100	–1.50006100
H	–8.97641800	1.59397100	–1.50989600
H	–8.94234900	–1.49329800	1.48747800
H	–10.22149500	0.01876700	–0.02942000
H	–4.72588900	2.26913900	0.01959500

H	4.72588800	–2.26913900	0.01947800
B	3.93675700	1.14986300	0.00860800
B	–3.93675700	–1.14986300	0.00852000
O	–4.45468100	–2.44543000	–0.05625600
H	–5.41745200	–2.44837800	–0.11688100
O	4.45468100	2.44543400	–0.05608900
H	5.41745200	2.44838600	–0.11671200

E = –1589.16864211 a.u.

Table S11. Cartesian coordinates and absolute energy of the geometry-optimized structure (B3LYP/6-31++G**) of compound **7**.

	x	y	z
C	0.24691800	2.51307300	–0.04632600
C	1.55171300	1.99303800	–0.02476300
C	1.79795500	0.61744300	–0.01034100
C	0.66563200	–0.25480600	–0.02654600
C	–0.66564100	0.25482600	–0.02651200
C	–0.86606200	1.67182000	–0.04566000
C	0.86604900	–1.67180300	–0.04565400
C	–0.24693100	–2.51305400	–0.04621000
C	–1.55172600	–1.99301700	–0.02457900
C	–1.79796400	–0.61742200	–0.01020200
B	–3.25020200	–0.03597500	0.01318400
C	–3.36822600	1.52346800	–0.08394900
C	–2.20304700	2.24078900	–0.08215600
C	2.20303200	–2.24077400	–0.08221000
B	3.25019400	0.03599700	0.01298100
C	3.36820900	–1.52345200	–0.08409400
C	–4.48706200	–1.01302200	0.12155800
C	–5.25366700	–1.33665700	–1.02349700
C	–6.33110600	–2.22397700	–0.91713900
C	–6.69049700	–2.80624300	0.30338000
C	–5.93472700	–2.47411500	1.43261600
C	–4.84251900	–1.59983600	1.35960600
C	–4.07056700	–1.27507000	2.62407000
C	–4.91731200	–0.73243200	–2.37132900
C	–7.84195400	–3.78150800	0.39259600
C	–4.65290100	2.26832800	–0.18947800
C	–4.78500800	3.34173100	–1.09353200
C	–5.97354100	4.06727100	–1.18840000
C	–7.06454800	3.73704000	–0.37976500
C	–6.95407700	2.67090300	0.51705300
C	–5.76723800	1.94146600	0.60588100

C	4.48706700	1.01303200	0.12132700
C	4.84250300	1.59990800	1.35939800
C	5.93472100	2.47411400	1.43242000
C	6.69057300	2.80616300	0.30317300
C	6.33122300	2.22386500	–0.91730300
C	5.25371500	1.33657200	–1.02367800
C	4.91744600	0.73228500	–2.37150400
C	4.07047400	1.27520400	2.62382900
C	7.84196000	3.78149700	0.39254800
C	4.65287800	–2.26831500	–0.18968000
C	4.78493500	–3.34173100	–1.09372400
C	5.97346300	–4.06727200	–1.18864700
C	7.06451300	–3.73702900	–0.38007600
C	6.95409100	–2.67087800	0.51673300
C	5.76725700	–1.94143900	0.60561400
H	0.09783100	3.59003200	–0.06473100
H	2.39322000	2.68053300	–0.02213400
H	–0.09784700	–3.59001400	–0.06457600
H	–2.39323200	–2.68051300	–0.02186300
H	–2.24108400	3.33066800	–0.09756900
H	2.24106800	–3.33065400	–0.09759000
H	–6.90745200	–2.46141800	–1.80963000
H	–6.20210900	–2.90411700	2.39626600
H	–4.54475900	–1.72404200	3.50169500
H	–3.03996100	–1.64511900	2.57670900
H	–4.00923500	–0.19350600	2.79841300
H	–3.88699300	–0.95866400	–2.67189700
H	–5.58077800	–1.11433500	–3.15278800
H	–5.01780600	0.35908300	–2.35339400
H	–8.64305600	–3.51980200	–0.30636200
H	–7.51729100	–4.80123200	0.14824300
H	–8.26669200	–3.80705900	1.40100600
H	–3.95296200	3.59276000	–1.74561200
H	–6.04950000	4.88457000	–1.90038400
H	–7.99125100	4.29889500	–0.45274400
H	–7.79505500	2.40260200	1.15035500
H	–5.70241900	1.11650400	1.30578200
H	6.20210200	2.90412500	2.39607300
H	6.90762700	2.46123100	–1.80977100
H	5.58093500	1.11418000	–3.15294600
H	5.01798500	–0.35922700	–2.35351700
H	3.88713500	0.95846100	–2.67213600
H	4.00895900	0.19364300	2.79812500
H	4.54471400	1.72406400	3.50148400
H	3.03992900	1.64542100	2.57645200
H	7.51550300	4.80254200	0.15621400
H	8.27179800	3.80112400	1.39895000

H	8.63962500	3.52452300	–0.31203400
H	3.95285200	–3.59276700	–1.74575400
H	6.04938300	–4.88458100	–1.90062400
H	7.99121300	–4.29888500	–0.45309600
H	7.79510400	–2.40256900	1.14998400
H	5.70247900	–1.11646300	1.30550200

E = –1749.48735162 a.u.

Table S12. Cartesian coordinates and absolute energy of the geometry-optimized structure (B3LYP/6-31++G**) of compound **8**.

	x	y	z
C	1.61049000	3.37829300	0.07857500
C	2.74381500	2.53780300	0.07755100
C	2.62917900	1.15245400	0.05560300
C	1.30984200	0.57356200	0.02329300
C	0.14393100	1.41648700	0.02023700
C	0.34923700	2.83022400	0.05247600
C	1.16947200	–0.84108500	–0.00869600
C	–0.14392500	–1.41627100	0.02200100
C	–1.30984600	–0.57333700	0.02408400
C	–1.16946400	0.84126200	–0.00968500
C	–0.34923800	–2.82997100	0.05584600
C	–1.61048400	–3.37801800	0.08261800
C	–2.74381700	–2.53753800	0.08077500
C	–2.62917800	–1.15220600	0.05718900
B	–3.90834100	–0.26268200	0.04990700
C	–3.65123200	1.26163900	–0.09297800
C	–2.34396500	1.68315300	–0.08678000
B	3.90835600	0.26293000	0.04902600
C	3.65125800	–1.26160600	–0.09225400
C	2.34396800	–1.68306200	–0.08493100
C	4.71302800	–2.29099500	–0.25653400
C	–4.71313300	2.29078200	–0.25778200
C	–4.57031600	3.32416800	–1.20625900
C	–5.54771900	4.30896900	–1.35846900
C	–6.69727100	4.28630700	–0.56406500
C	–6.85988700	3.26463700	0.37572500
C	–5.88562700	2.27575200	0.52126800
C	4.56862600	–3.32643100	–1.20258100
C	5.54597600	–4.31126500	–1.35471700
C	6.69718200	–4.28656100	–0.56275300
C	6.86143000	–3.26286600	0.37451900
C	5.88712600	–2.27401100	0.52007900

C	–5.34191700	–0.92277900	0.15793600
C	–6.12960300	–1.12272600	–1.00141100
C	–7.38571300	–1.73208300	–0.89949900
C	–7.90692900	–2.14783700	0.33083900
C	–7.12480700	–1.94577700	1.47234400
C	–5.85857100	–1.34893900	1.40439500
C	–5.06502100	–1.15505500	2.68216900
C	–5.62205300	–0.68889200	–2.36142300
C	–9.28130200	–2.77075800	0.42325500
C	5.34174600	0.92337200	0.15716800
C	6.13350100	1.11615000	–1.00046600
C	7.39294300	1.71848800	–0.89651900
C	7.91110000	2.13881200	0.33340400
C	7.12750000	1.93804700	1.47430200
C	5.85835000	1.34794800	1.40438700
C	5.06465600	1.15184100	2.68175100
C	5.63061800	0.67505300	–2.35986500
C	9.26266600	2.81042000	0.42021600
H	1.73209800	4.45726900	0.10425500
H	3.73464000	2.98308800	0.09807100
H	–0.49955600	3.50107900	0.06785900
H	0.49954900	–3.50081400	0.07194700
H	–1.73211300	–4.45696000	0.10949500
H	–3.73460600	–2.98289300	0.10181600
H	–2.17192500	2.75262000	–0.14260200
H	2.17186700	–2.75258700	–0.13919700
H	–3.69479100	3.33814500	–1.84977200
H	–5.41512000	5.08793100	–2.10437400
H	–7.46029400	5.05040300	–0.68133800
H	–7.74991400	3.23405400	0.99805400
H	–6.03073600	1.48973400	1.25323600
H	3.69191300	–3.34193300	–1.84443300
H	5.41209400	–5.09179100	–2.09875800
H	7.46024900	–5.05060600	–0.68007500
H	7.75282800	–3.23049800	0.99477600
H	6.03375900	–1.48643100	1.25003900
H	–7.97194600	–1.88487700	–1.80405700
H	–7.50702700	–2.26270000	2.44110000
H	–5.64593400	–1.46077000	3.55731900
H	–4.13705300	–1.73842700	2.67788700
H	–4.77598400	–0.10643100	2.82644000
H	–4.65424500	–1.14705100	–2.59829200
H	–6.32382100	–0.96732000	–3.15318100
H	–5.48429700	0.39795100	–2.40612200
H	–9.48477900	–3.42006600	–0.43480900
H	–9.38879700	–3.36870300	1.33361300
H	–10.06463700	–2.00209900	0.44118900

H	7.98589700	1.85858300	–1.79870700
H	7.51265300	2.24664500	2.44458800
H	4.77591500	0.10296400	2.82486000
H	5.64510300	1.45702700	3.55739200
H	4.13650600	1.73490700	2.67768700
H	4.66354400	1.13199900	–2.60195700
H	6.33477900	0.94994000	–3.15073900
H	5.49318000	–0.41201000	–2.39975800
H	9.18562100	3.88540500	0.21188000
H	9.69979600	2.70169000	1.41775100
H	9.96577100	2.38898400	–0.30575400

E = –1903.12841168 a.u.

Table S13. Cartesian coordinates and absolute energy of the geometry-optimized structure (B3LYP/6-31++G**) of compound **9**.

	x	y	z
C	0.21100800	3.07383400	–0.00061900
C	0.69690700	1.74773800	0.00566100
C	–0.24063500	0.67085600	0.00927300
C	–1.63918100	0.92981000	0.00961200
C	–2.09563800	2.27233500	–0.00575500
C	–1.15207800	3.32427900	–0.00653100
C	2.09336600	1.44827300	0.01241100
C	2.58959100	0.15583400	0.02217700
C	1.63924800	–0.92985700	0.00971800
C	0.24070200	–0.67090300	0.00934000
C	–0.69683900	–1.74778600	0.00580900
C	–2.09329800	–1.44832200	0.01251300
C	–2.58952300	–0.15588100	0.02216600
C	2.09570700	–2.27238200	–0.00551200
C	1.15214700	–3.32432600	–0.00620200
C	–0.21094000	–3.07388200	–0.00033700
B	4.12246700	–0.13837100	0.03395900
C	4.52498900	–1.64727600	–0.04030000
C	3.51277200	–2.57380600	–0.03368600
B	–4.12239700	0.13832600	0.03396200
C	–4.52491300	1.64722100	–0.04044100
C	–3.51270200	2.57375600	–0.03396300
C	–5.15578400	–1.05688900	0.10034200
C	–5.81144000	–1.50580400	–1.07274400
C	–6.70907700	–2.57663300	–1.00767200
C	–6.99457300	–3.22934000	0.19792000
C	–6.34601400	–2.78023600	1.35147500

C	–5.43252700	–1.71649300	1.32012300
C	–4.76575000	–1.28121800	2.61124100
C	–5.54332900	–0.84009900	–2.40702200
C	–7.97446100	–4.37979100	0.24264800
C	–5.92583600	2.14104300	–0.13993600
C	–6.25836800	3.18322600	–1.02892700
C	–7.56245200	3.67293300	–1.11694800
C	–8.57190600	3.13111300	–0.31650900
C	–8.26241600	2.09155300	0.56475300
C	–6.95940600	1.59787000	0.64637300
C	5.15580000	1.05688900	0.10034000
C	5.81156400	1.50576500	–1.07267600
C	6.70944900	2.57640300	–1.00748100
C	6.99482400	3.22912600	0.19810800
C	6.34650200	2.77974300	1.35170700
C	5.43278300	1.71622800	1.32023500
C	4.76637500	1.28051500	2.61139400
C	5.54364400	0.83999900	–2.40696000
C	7.97184400	4.38203200	0.24235500
H	0.91945500	3.89773700	–0.00227400
H	–1.51157700	4.35006600	–0.01552900
H	2.79235100	2.28200600	0.01076200
H	–2.79228000	–2.28205800	0.01093000
H	1.51164700	–4.35011400	–0.01509700
H	–0.91938700	–3.89778500	–0.00192800
H	3.76058900	–3.63600100	–0.04019300
H	–3.76052800	3.63594900	–0.04060400
H	–7.20152800	–2.90710600	–1.92077300
H	–6.55540700	–3.26716100	2.30220300
H	–4.86066200	–0.20107500	2.77710900
H	–5.20841500	–1.78838700	3.47360400
H	–3.69257500	–1.50531800	2.60971400
H	–4.48281700	–0.89696400	–2.68119400
H	–6.11795400	–1.31447300	–3.20799600
H	–5.81536200	0.22169000	–2.38617200
H	–8.96427100	–4.07481500	–0.11719300
H	–7.64333800	–5.21119100	–0.39117900
H	–8.09251400	–4.76302700	1.26055300
H	–5.48896200	3.59624800	–1.67547200
H	–7.79108300	4.47118100	–1.81781100
H	–9.58804800	3.50879000	–0.38442000
H	–9.03800400	1.65951900	1.19100900
H	–6.73997000	0.78943400	1.33388400
H	7.20234800	2.90654800	–1.92045300
H	6.55644900	3.26614400	2.30258100
H	5.20882800	1.78790100	3.47373800
H	3.69307900	1.50403100	2.60995200

H	4.86188400	0.20041500	2.77721900
H	4.48331100	0.89766100	–2.68166800
H	6.11902700	1.31379500	–3.20773200
H	5.81482500	–0.22199800	–2.38580000
H	7.61764900	5.22850600	–0.35845700
H	8.12013100	4.73934100	1.26572500
H	8.95070800	4.09120700	–0.15656200
C	5.92590800	–2.14111700	–0.13979300
C	6.95956000	–1.59773900	0.64626700
C	6.25836000	–3.18351700	–1.02856200
C	8.26256600	–2.09143200	0.56463300
H	6.74021000	–0.78912300	1.33359100
C	7.56243500	–3.67324100	–1.11659300
H	5.48889800	–3.59669800	–1.67493800
C	8.57197000	–3.13121500	–0.31639400
H	9.03821700	–1.65921700	1.19068500
H	7.79099800	–4.47166100	–1.81728400
H	9.58810800	–3.50889900	–0.38431900

E = –1979.37960129 a.u.

Table S14. Cartesian coordinates and absolute energy of the geometry-optimized structure (B3LYP/6-31++G**) of compound **10**.

	x	y	z
C	1.24185200	–2.01852100	0.11094800
C	1.24831700	–0.60040800	0.04870300
C	0.00585100	0.09374700	0.01028300
C	–1.23390100	–0.60551500	0.05078800
C	–1.22189400	–2.02275400	0.11197300
C	0.01162800	–2.69282200	0.14335300
C	0.00323900	1.51220100	–0.07698600
C	–1.22744700	2.22747500	–0.12298300
C	–2.45163500	1.48826000	–0.06561400
C	–2.48913900	0.10783500	0.02554700
C	1.22845400	2.23210800	–0.12759200
C	1.19774300	3.63910700	–0.22966000
C	–0.00103100	4.36139600	–0.28163300
C	–1.19950700	3.62981400	–0.22317700
C	2.49927300	0.11797400	0.02084000
C	2.45482800	1.49917500	–0.07255800
B	–3.83999200	–0.67838300	0.08133800
C	–3.72282200	–2.23071000	0.08216600
C	–2.46145700	–2.77226000	0.11872900
C	2.48440100	–2.76273800	0.11821400

C	3.74316900	–2.21520400	0.08156700
B	3.85321700	–0.66215600	0.07761300
C	–4.88236500	–3.16505100	0.02194300
C	4.90704400	–3.14437500	0.02481900
C	–0.04700600	5.89758800	–0.39848200
C	1.36033600	6.52256800	–0.46283400
C	–0.80918900	6.29172800	–1.68744800
C	–0.78065100	6.48504000	0.83192800
C	–4.85548500	–4.28687800	–0.83061300
C	–5.92294000	–5.18518500	–0.88257400
C	–7.05085200	–4.98285400	–0.08279300
C	–7.09903900	–3.87064000	0.76213600
C	–6.03285900	–2.97083600	0.80895800
C	6.05560000	–2.94302000	0.81291500
C	7.12563000	–3.83846700	0.77034800
C	7.08333400	–4.95338300	–0.07132600
C	5.95747800	–5.16277500	–0.87219700
C	4.88618200	–4.26880100	–0.82451300
C	–5.20900400	0.11419300	0.11660800
C	–5.68812200	0.68943100	1.31779100
C	–6.90257600	1.38827900	1.32625600
C	–7.66519300	1.55490600	0.16532900
C	–7.18213300	0.98916200	–1.01936900
C	–5.97798400	0.27535000	–1.06029400
C	–5.51359200	–0.32380700	–2.37213600
C	–4.91144200	0.54495900	2.61261000
C	–8.95604200	2.34174800	0.18504300
C	5.21900300	0.13606900	0.11206100
C	5.69472600	0.71577200	1.31246200
C	6.90648800	1.41925600	1.32063800
C	7.66962600	1.58629800	0.16011500
C	7.18991300	1.01616700	–1.02382900
C	5.98855300	0.29763600	–1.06436500
C	5.52792100	–0.30637400	–2.37530700
C	4.91724700	0.57127400	2.60679600
C	8.95733900	2.37827800	0.17945900
H	0.01354500	–3.78037500	0.18543100
H	–3.38748200	2.04224600	–0.09656500
H	2.14938100	4.15773100	–0.26981300
H	–2.15241900	4.15075400	–0.25738000
H	3.38826300	2.05706500	–0.10621300
H	–2.34771700	–3.85636400	0.16412300
H	2.37546200	–3.84725700	0.16515700
H	1.27212600	7.61058400	–0.54665000
H	1.94615700	6.30991100	0.43800600
H	1.92526100	6.17072100	–1.33282400
H	–0.84991800	7.38254900	–1.78347800

H	–1.83880000	5.92081200	–1.68425200
H	–0.31087500	5.89017000	–2.57628100
H	–0.25915000	6.22708200	1.75990900
H	–0.82513400	7.57758600	0.75907600
H	–1.80774700	6.11570300	0.91054000
H	–3.99567400	–4.44206500	–1.47672000
H	–5.87637700	–6.03733100	–1.55526500
H	–7.88402300	–5.67862700	–0.12257900
H	–7.97043600	–3.70018500	1.38837800
H	–6.09053400	–2.11358500	1.46972300
H	6.10878000	–2.08358300	1.47120600
H	7.99536500	–3.66246100	1.39736800
H	7.91943600	–5.64581800	–0.10779500
H	5.91549800	–6.01710900	–1.54241200
H	4.02794400	–4.42962600	–1.47133100
H	–7.26232100	1.80909000	2.26373300
H	–7.76056800	1.09933600	–1.93500400
H	–6.18375400	–0.04882300	–3.19203000
H	–4.50539200	0.01572400	–2.63836600
H	–5.48187900	–1.41864200	–2.32112000
H	–3.96787000	1.10269600	2.58382200
H	–5.49028900	0.91649100	3.46338800
H	–4.65072800	–0.50031500	2.81913200
H	–9.65902200	1.97520500	–0.56988800
H	–9.44609200	2.28140600	1.16209900
H	–8.77706000	3.40431600	–0.02496100
H	7.26368700	1.84348800	2.25755400
H	7.76880200	1.12666100	–1.93914300
H	6.19640200	–0.02850300	–3.19561000
H	5.50305800	–1.40132000	–2.32261300
H	4.51762400	0.02640900	–2.64207000
H	4.65926800	–0.47436800	2.81486500
H	5.49425200	0.94591400	3.45747500
H	3.97215000	1.12633200	2.57611300
H	9.44726400	2.32089400	1.15676500
H	9.66206300	2.01378100	–0.57483600
H	8.77415600	3.43990900	–0.03166500

E = –2136.64846616 a.u.

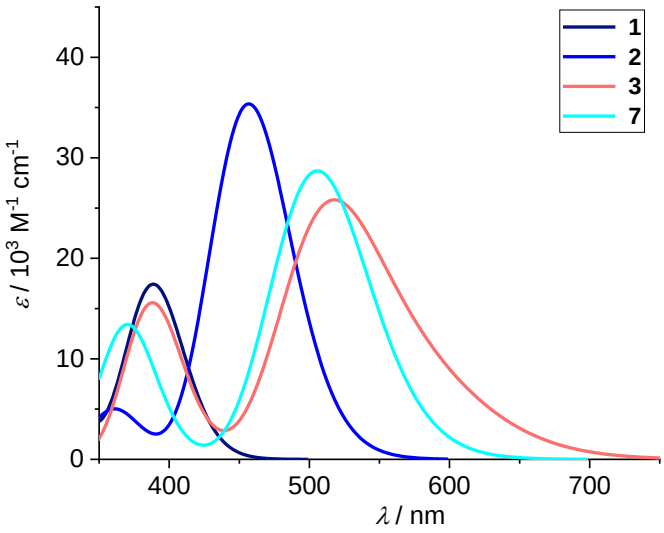

Figure S112. Simulated absorption spectra of compounds **1–3** and **7** based on the results obtained from TDDFT calculations (B3LYP/6-31++G**). A half-width at half height of 0.20 eV was used for the simulations.

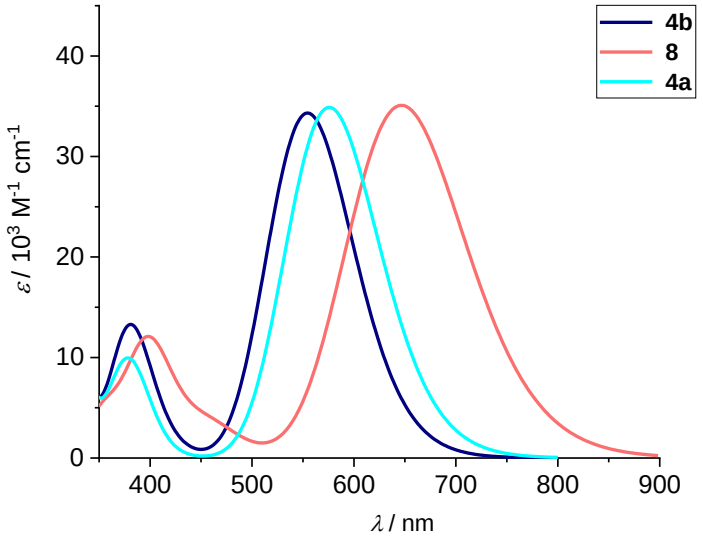

Figure S113. Simulated absorption spectra of compounds **4a,b** and **8** based on the results obtained from TDDFT calculations (B3LYP/6-31++G**). A half-width at half height of 0.20 eV was used for the simulations.

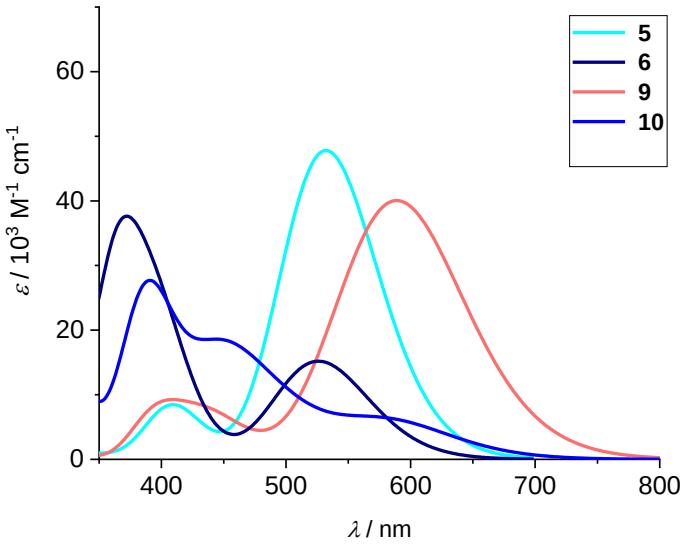

Figure S114. Simulated absorption spectra of compounds **5, 6, 9** and **10** based on the results obtained from TDDFT calculations (B3LYP/6-31++G**). A half-width at half height of 0.20 eV was used for the simulations.

Table S15. Absorption properties of compounds **1-10** as obtained from TDDFT calculations (B3LYP/6-31++G**). The relevant transitions are listed with the respective wavelengths and oscillator strengths as well as the orbitals that are mainly involved in the transitions (H indicates the highest occupied molecular orbital and L stands for the lowest unoccupied molecular orbital, respectively).

Compound	Wavelength [nm]	Oscillator strength	Character
1	328	0.0643	H–1 → L (70%)
	389	0.2583	H → L (92%)
2	361	0.0714	H–2 → L (82%)
	457	0.5244	H → L (96%)
3	387	0.2033	H–8 → L (47%)
			H–9 → L (45%)
	514	0.3505	H–3 → L (80%)
	584	0.0945	H → L (82%)
4a	379	0.1462	H–3 → L (78%)
	576	0.5173	H → L (99%)
4b	380	0.1915	H–2 → L (88%)
	555	0.5090	H → L (99%)

5	409	0.1250	H–3 → L (86%)
	532	0.7088	H → L (100%)
6	368	0.3622	H–2 → L (36%)
			H → L+1 (34%)
	399	0.2759	H–2 → L (23%)
			H → L+1 (40%)
	526	0.2251	H → L (98%)
7	373	0.1646	H–2 → L (92%)
	506	0.4257	H → L (95%)
8	399	0.1691	H–9 → L (82%)
	648	0.5141	H → L (96%)
9	397	0.0993	H–9 → L (88%)
	442	0.0917	H–6 → L (91%)
	549	0.1162	H–2 → L (89%)
	595	0.5208	H → L (89%)
10	388	0.1786	H–6 → L (51%)
			H–7 → L (40%)
	391	0.2050	H–6 → L (51%)
			H–7 → L (26%)
	444	0.2044	H → L+1 (83%)
	482	0.0877	H–3 → L (86%)
	584	0.0847	H → L (98%)

9. Organic Thin-Film Transistors and Organic Solar Cells

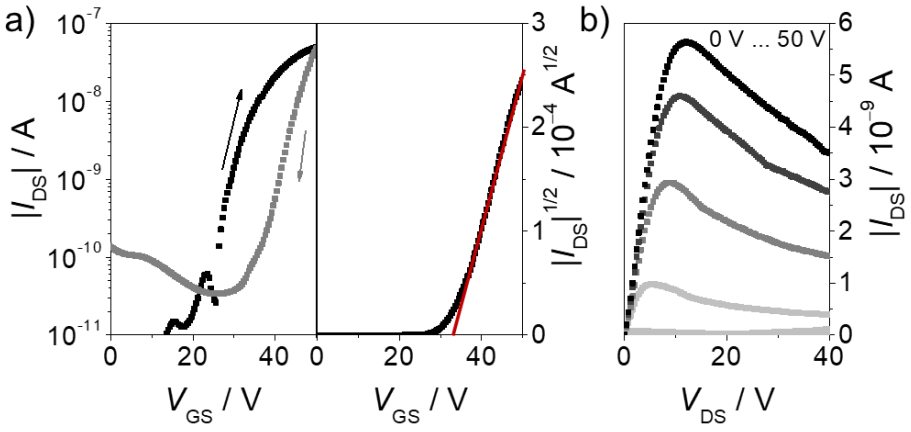

Figure S115. (a) Transfer and (b) output characteristics of a vacuum-processed OTFT of **8** on $Si/SiO_2/AlO_x$/TPA substrate measured under inert conditions.

Table S16. n-channel mobility (μ_n), threshold voltage (V_T) and current on/off ratio (I_{on}/I_{off}) of vacuum-processed OTFTs of **8** on $Si/SiO_2/AlO_x$/TPA substrate.[a]

Compound	T_{sub} [°C]	μ_n [cm^2 V^{-1} s^{-1}]	V_T [V]	I_{on}/I_{off} [1]
8	190	0.0031 ± 0.0002	26	10^4

[a] Statistical data taken from 20 independent devices.

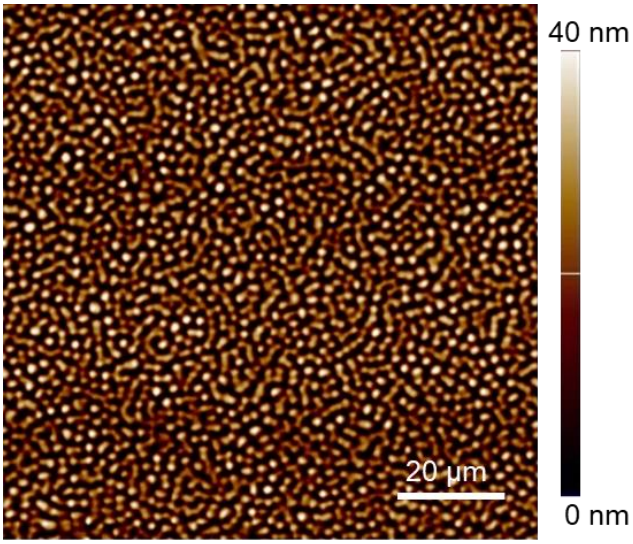

Figure S116. AFM height images of a 30 nm vacuum-deposited thin film of **8** on $Si/SiO_2/AlO_x$/TPA substrate.

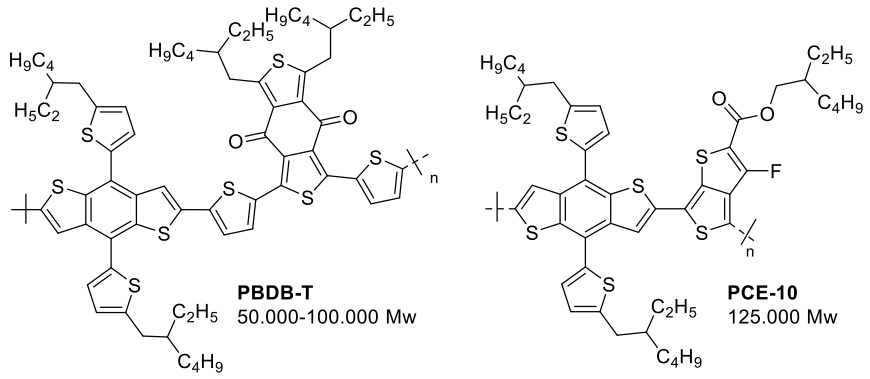

Figure S117. Donor polymers PBDB-T and PCE10 used in solar cell fabrication with **8**.

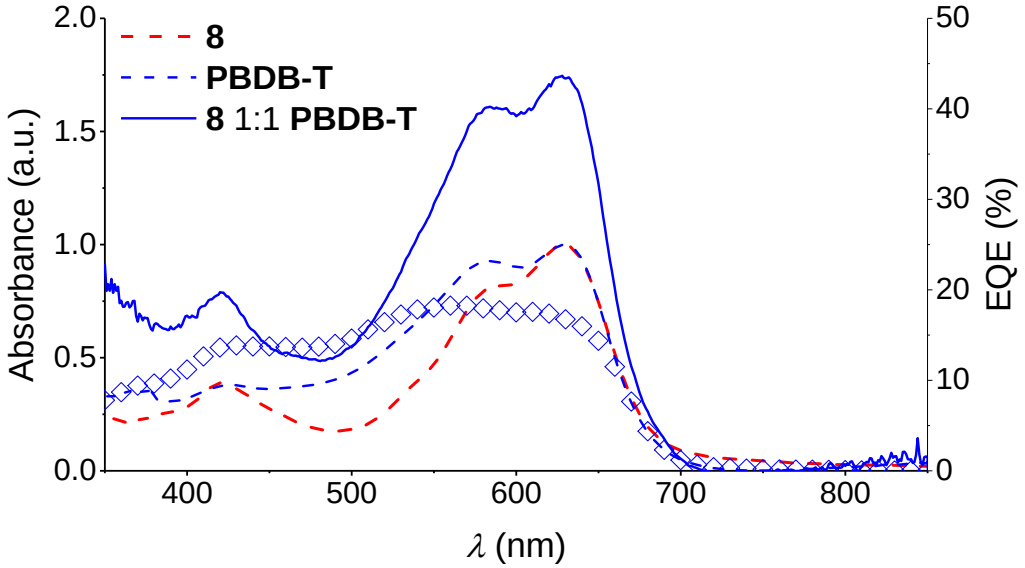

Figure S118. UV-Vis absorption (thin film on ITO/ZnO) spectra of **8** (dashed red line), donor polymer PBDB-T (dashed blue line) and the active layer (solid blue line; 1:1 mixing ratio) as well as the respective EQE curve (open blue symbol) of the BHJ organic solar cell.

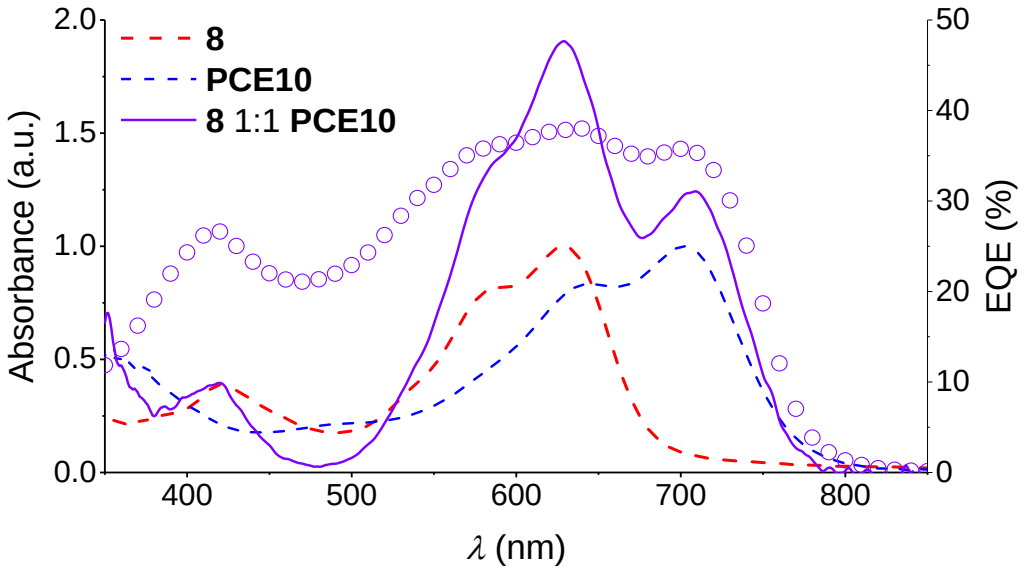

Figure S119. UV-Vis absorption (thin film on ITO/ZnO) spectra of **8** (dashed red line), donor polymer PCE10 (dashed blue line) and the active layer (solid violet line; 1:1 mixing ratio) as well as the respective EQE curve (open violet symbol) of the BHJ organic solar cell.

10. References

[S1] Brahmi, M. M.; Monot, J.; Desage-El Murr, M.; Curran, D. P.; Fensterbank, L.; Lacôte, E.; Malacria, M. *J. Org. Chem.* **2010,** *75*, 6983-6985.

[S2] Andrus, M. B.; Song, C.; Zhang, J. *Org. Lett.* **2002,** *4*, 2079-2082.

[S3] Meier, H.; Praß, E.; Zertani, R.; Eckes, H.-L. *Chem. Ber.* **1989,** *122*, 2139-2146.

[S4] Liu, Q.-X.; Zhang, W.; Zhao, X.-J.; Zhao, Z.-X.; Shi, M.-C.; Wang, X.-G. *Eur. J. Org. Chem.* **2013,** *2013*, 1253-1261.

[S5] Ju, H.; Wang, K.; Zhang, J.; Geng, H.; Liu, Z.; Zhang, G.; Zhao, Y.; Zhang, D. *Chem. Mater.* **2017,** *29*, 3580-3588.

[S6] Berlman, I. B., *Handbook of Fluorescence Spectra of Aromatic Molecules*; Academic Press: London, 1971.

[S7] Seybold, G.; Wagenblast, G. *Dyes Pigm.* **1989,** *11*, 303-317.

[S8] Würth, C.; Grabolle, M.; Pauli, J.; Spieles, M.; Resch-Genger, U. *Nat. Protoc.* **2013,** *8*, 1535-1550.

[S9] Fry, A. J. *Laboratory Techniques in Electroanalytical Chemistry*; 2nd ed.; Marcel Dekker Ltd: New York, 1996.

[S10] Sheldrick, G. *Acta Cryst. A* **2008,** *64*, 112-122.

[S11] Becke, A. D. *Phys. Rev. A* **1988**, *38*, 3098-3100.

[S12] Lee, C.; Yang, W.; Parr, R. G. *Phys. Rev. B* **1988**, *37*, 785-789.

[S13] Becke, A. D. *J. Chem. Phys.* **1993**, *98*, 5648-5652.

[S14] Krishnan, R.; Binkley, J. S.; Seeger, R.; Pople, J. A. *J. Chem. Phys.* **1980**, *72*, 650-654.

[S15] Clark, T.; Chandrasekhar, J.; Spitznagel, G. W.; Schleyer, P. v. R. *J. Comput. Chem.* **1983**, *4*, 294–301.

[S16] Frisch, M. J.; Pople, J. A.; Binkley, J. S. *J. Chem. Phys.* **1984**, *80*, 3265-3269.

[S17] Gaussian 09, Revision D.01, Frisch, M. J.; Trucks, G. W.; Schlegel, H. B.; Scuseria, G. E.; Robb, M. A.; Cheeseman, J. R.; Scalmani, G.; Barone, V.; Mennucci, B.; Petersson, G. A.; Nakatsuji, H.; Caricato, M.; Li, X.; Hratchian, H. P.; Izmaylov, A. F.; Bloino, J.; Zheng, G.; Sonnenberg, J. L.; Hada, M.; Ehara, M.; Toyota, K.; Fukuda, R.; Hasegawa, J.; Ishida, M.; Nakajima, T.; Honda, Y.; Kitao, O.; Nakai, H.; Vreven, T.; Montgomery, J. A.; Peralta, J. E.; Ogliaro, F.; Bearpark, M.; Heyd, J. J.; Brothers, E.; Kudin, K. N.; Staroverov, V. N.; Keith, T.; Kobayashi, R.; Normand, J.; Raghavachari, K.; Rendell, A.; Burant, J. C.; Iyengar, S. S.; Tomasi, J.; Cossi, M.; Rega, N.; Millam, J. M.; Klene, M.; Knox, J. E.; Cross, J. B.; Bakken, V.; Adamo, C.; Jaramillo, J.; Gomperts, R.; Stratmann, R. E.; Yazyev, O.; Austin, A. J.; Cammi, R.; Pomelli, C.; Ochterski, J. W.; Martin, R. L.; Morokuma, K.; Zakrzewski, V. G.; Voth, G. A.; Salvador, P.; Dannenberg, J. J.; Dapprich, S.; Daniels, A. D.; Farkas, O.; Foresman, J. B.; Ortiz, J. V.; Cioslowski, J.; Fox, D. J. Gaussian, Inc., Wallingford CT, 2013.

[S18] Filippetti, A. *Phys. Rev. A* **1998,** *57*, 914-919.

[S19] Dennington, R. K., T.; Millam, J. *GaussView, Version 5*, Semichem Inc.: 2009.

[S20] Sun, Y.; Seo, J. H.; Takacs, C. J.; Seifter, J.; Heeger A. J. *Adv. Mater.* **2011**, *23*, 1679-1683.